AD_____

Award Number: DAMD17-01-1-0450

TITLE: MCAK and Stathmin Upregulation in Breast Cancer Cells: Etiology and Response to Pharmacologic Reagents

PRINCIPAL INVESTIGATOR: Linda Wordeman, Ph.D.

CONTRACTING ORGANIZATION: University of Washington
Seattle, Washington 98105-6692

REPORT DATE: July 2004

TYPE OF REPORT: Final

PREPARED FOR: U.S. Army Medical Research and Materiel Command
Fort Detrick, Maryland 21702-5012

DISTRIBUTION STATEMENT: Approved for Public Release;
Distribution Unlimited

The views, opinions and/or findings contained in this report are those of the author(s) and should not be construed as an official Department of the Army position, policy or decision unless so designated by other documentation.

REPORT DOCUMENTATION PAGE

Form Approved
OMB No. 074-0188

Public reporting burden for this collection of information is estimated to average 1 hour per response, including the time for reviewing instructions, searching existing data sources, gathering and maintaining the data needed, and completing and reviewing this collection of information. Send comments regarding this burden estimate or any other aspect of this collection of information, including suggestions for reducing this burden to Washington Headquarters Services, Directorate for Information Operations and Reports, 1215 Jefferson Davis Highway, Suite 1204, Arlington, VA 22202-4302, and to the Office of Management and Budget, Paperwork Reduction Project (0704-0188), Washington, DC 20503

1. AGENCY USE ONLY (Leave blank)	2. REPORT DATE	3. REPORT TYPE AND DATES COVERED
	July 2004	Final (1 Jul 2001 - 30 Jun 2004)

4. TITLE AND SUBTITLE
MCAK and Stathmin Upregulation in Breast Cancer Cells: Etiology and Response to Pharmacologic Reagents

5. FUNDING NUMBERS
DAMD17-01-1-0450

6. AUTHOR(S)
Linda Wordeman, Ph.D.

7. PERFORMING ORGANIZATION NAME(S) AND ADDRESS(ES)
University of Washington
Seattle, Washington 98105-6692

E-Mail: worde@u.washington.edu

8. PERFORMING ORGANIZATION REPORT NUMBER

9. SPONSORING / MONITORING AGENCY NAME(S) AND ADDRESS(ES)
U.S. Army Medical Research and Materiel Command
Fort Detrick, Maryland 21702-5012

10. SPONSORING / MONITORING AGENCY REPORT NUMBER

11. SUPPLEMENTARY NOTES
Original contains color plates: All DTIC reproductions will be in black and white.

12a. DISTRIBUTION / AVAILABILITY STATEMENT
Approved for Public Release; Distribution Unlimited

12b. DISTRIBUTION CODE

13. ABSTRACT (Maximum 200 Words)

The goal of this study is to assay the role that two modulators of microtubule dynamics, Mitotic centromere-associated Kinesin (MCAK) and Op18/stathmin (stathmin) play in the development of cancer. These proteins are elevated in aggressive breast cancer tumors and changes in the levels and activity of these proteins are correlated with aneuploidy and invasiveness. In addition to our previously discovered C-terminal regulation, we have uncovered another major regulatory mechanism to control microtubule dynamics through MCAK activity. Phosphorylation of conserved serine residues in the neck and N-terminus of MCAK by Aurora B kinase inhibits its activity. It is likely that phosphorylation and dephosphorylation controls MCAK's activity during mitosis and also, via other kinases, during interphase. We have also identified two other Kin I kinesins which regulate microtubule dynamics in cultured cells and are likely to be regulated by kinases and phosphatases. These regulatory kinases also control stathmin activity in cells. Regulation of these proteins via cascades of kinase and phosphatase activities opens up a major new area for the application of therapeutics to control microtubule dynamics and augment existing cancer therapies that target microtubules. These data, which were reported as preliminary in Annual Report 2003 are now published or close to submission.

14. SUBJECT TERMS
Mitosis, centromere, microtubule, mitotic spindle, stathmin, cancer MCAK, immortalization, transformation, aneuploidy

15. NUMBER OF PAGES
104

16. PRICE CODE

17. SECURITY CLASSIFICATION OF REPORT	18. SECURITY CLASSIFICATION OF THIS PAGE	19. SECURITY CLASSIFICATION OF ABSTRACT	20. LIMITATION OF ABSTRACT
Unclassified	Unclassified	Unclassified	Unlimited

Table of Contents

Introduction

The purpose of this study is to determine the role that two modulators of microtubule dynamics, mitotic centromere-associated kinesin (MCAK) (*1*) and op18/stathmin (stathmin) (*2*), play in the development of cancer. Alterations in the levels of these modulators of microtubule dynamics can lead to aneuploidy (chromosome gain or loss) and also to changes in the metastatic potential of cancer cells. Specifically, we plan to correlate elevated levels or decreased levels of MCAK or Stathmin with immortalization, aneuploidy and proliferative potential. Specifically, we plan to correlate elevated levels or decreased levels of MCAK or Stathmin with immortalization, aneuploidy and proliferative potential. Previously, the most potent anti-cancer drugs have targeted microtubule polymer dynamics making the regulation of microtubule polymer levels by depolymerizing proteins such as MCAK and stathmin a key focal point in the development and treatment of cancer (*3, 4*). Most of the key research accomplishments for the full support period are now published and are included as appendix material. For this reason, a detailed description of new research accomplishments is provided below for the period of July 1, 2003 to June 30, 2004 with reference to the influence of these data on the direction of the entire project.

Research Accomplishments

Two unexpected and key discoveries altered the direction of the project:

(1) In the second year of funding we determined that MCAK is regulated by Aurora B kinase. Aurora B kinase is upregulated in many cancers and is a key second messenger in the regulation of cell division and microtubule dynamics (*5-7*). This was published in the highly respected journal, Developmental Cell ((*8*) also see Appendix) and is the subject of speculative a review due to its importance in the field (*9*). Furthermore, in the third year of funding we have determined that MCAK interacts with the tips of microtubules in a phosphorylation dependent manner. The promising anti-cancer drug, Roscovitine, increases this interaction by promoting the interaction of MCAK with tubulin dimers (see appendix). This would stimulate the tubulin autoregulatory system in cells in a manner similar to the effects of the anticancer drug paclitaxel. Hence, kinase inhibitors may be a potent combination therapy to use with paclitaxel-based chemotherapies.

(2) In the third year of funding we discovered another class of microtubule depolymerizing kinesins (Kif2A) is present in dividing cells and involved in regulating microtubule polymer levels and mitotic spindle assembly. Kif2A was previously thought to be predominantly neuronal. It turns out that two isoforms of Kif2A exist: Kif2Aa, which is present in neuronal tissue; Kif2Ab, which is present in dividing tissue (*10*). We determined that Kif2Ab was indeed present in CHO and HeLa cells in our lab. Simultaneously, another group reported the interplay between MCAK and Kif2A in mammalian cells(*11*). We have determined that the regulation of

Kif2A and MCAK, and the interaction with tubulin dimers is distinctly different (see appendix) despite both being regulated by Aurora kinases. In the case of Kif2A, its centrosomal localization puts it under the control of Aurora A, a key player in cancer progression (*12, 13*). The discovery that MCAK and Kif2A cooperate to regulate microtubule polymer is a key discovery because if anti-cancer reagents could be developed that distinguish between Kif2Aa and Kif2Ab, then proliferative tissue could be selectively targeted without the problem of peripheral neuropathies that limit present chemotheraputic regimes.

Research on these key points prevented us from following up on stathmin regulation and also on model breast cancer cell lines to the extent that we planned in our original proposal. However, in total, we have established a more promising research foundation on the role of MCAK in cancer progression by establishing a solid link between the MCAK family of microtubule depolymerizing kinases and the Aurora family of kinases. This provides us with a foundation from which to establish a model system for the effects of microtubule dynamics regulators and transformation.

Work during the course of the grant is briefly summarized here, details are present in the papers and manuscripts provided in the Appendix.
We established that MCAK is a highly potent depolymerizer of microtubules and its substrate, unlike other kinesins, is the end of the microtubule(*14*). Also supplied in Appendix. We determined that a domain of MCAK ("neck") outside of the motor domain is essential for depolymerizing activity (*15, 16*). This is provided in the Appendix. The neck domain is phosphorylated by Aurora B kinase which regulates its activity and localization (*8*). Appendix of paper is provided. The C-terminus of MCAK regulates the association of MCAK with microtubule lattice. Lattice association, which is also seen in the presence of paclitaxel, may be another method to regulate MCAK's activity in cells (*17*). Paper provided in Appendix. MCAK and a related microtubule depolymerizing kinesin, Kif2Ab, cooperate to assemble mitotic spindles and segregate chromosomes. Cooperation is achieved by the respective localization of the two kinesins at either end of the chromosome. MCAK is associated with the centromere which Kif2Ab is associated with the centrosome and spindle poles (Figure 1). MCAK but not Kif2 or stathmin is part of the tip complex of polymerizing microtubules. The association of MCAK with tips is dependent on Aurora B phoshorylation

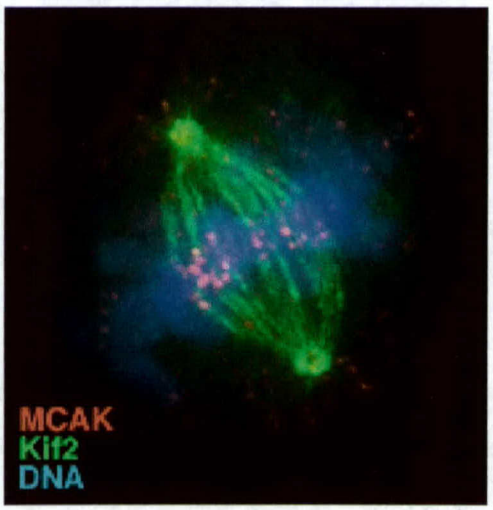

Figure 1: A CHO cell labeled for endogenous MCAK (red) and Kif2Aβ (green). DNA is shown in blue. MCAK is associated with the plus ends of microtubules at the centromere whereas Kif2Aβ is primarily associated with the centrosome at the minus ends of the microtubules and along the microtubule lattice.

and is promoted by the kinase inhibitor Roscovitine. Manuscript to be submitted to JCB 9/2004 is provided in the Appendix. We have shown, in collaboration with Les Wilson (UCSB) that MCAK promotes catastrophes (rapid episodes of microtubule depolymerization) in unstabilized (live) human microtubules (*18*). The paper also illustrates that MCAK has tubulin sequestration activity. This study is provided in the Appendix. Finally, we have determined that kinase and phosphatase regulation of MCAK at the centromere controls chromosome movement and error correction during cell division. To be presented at the Aneuploidy 2004 Meeting in Cortona, Italy, Sept. 17-22, 2004. Abstract is included.

Key Research Accomplishments for the entire support period:

- Identification of feedback regulation between MCAK and Op18/stathmin. This suggests that the transformation potential of MCAK and Op18/stathmin are undoubtedly linked.
- Identification of feedback regulation between MCAK and tubulin. This supports our hypothesis in Statement of Work (III) that the tubulin autoregulatory system responds to changes in the levels of MCAK protein and therefore, must, be considered in evaluating the transformation potential of MCAK.
- Demonstration that MCAK is capable of depolymerizing paclitaxel-stabilized microtubules in cells. This suggests that elevated levels of MCAK protein could antagonize certain anti-cancer drugs which target microtubules.
- Development of a method for consistent quantitation of microtubule-depolymerizing activity at the level of the light microscope.
- Design of a biomolecular screen which will identify cancer-related genes which respond to changes in MCAK and Op18/stathmin protein levels.
- Determination that the electrostatic potential of the neck of MCAK is essential for depolymerization activity. These data serve as the basis for the inactivation of MCAK by kinases and the reactivation by phosphatase activity. Published in the Journal of Cell Biology and cited by Faculty of 1000. Reprint included (Ovechkina et al.).
- Modulation of MCAK activity by RNAi.
- Preparation of cell line for a biomolecular screen which will identify cancer-related genes that respond to changes in MCAK and Op18/stathmin protein levels.
- Discovery that increased phosphatase activity results in a decrease in microtubule polymer in interphase cells.
- MCAK increases the number of catastrophes in live human microtubules. MCAK also affects overall microtubule polymer level in an ATP-independent manner. Reprint included.
- Established that MCAK is a substrate of Aurora B kinase. Aurora kinases are key players in the development of cancer. Reprint included.
- Determination that MCAK is part of the microtubule tip tracking complex and that phosphorylation of MCAK by Aurora B kinase prevents the interaction of MCAK with microtubule tips. Neither stathmin or Kif2Aα/β are part of this tip complex suggesting that global regulation of microtubule dynamics in cells results from a competition between MCAK and EB1 with other depolymerizers playing a minor role. Manuscript included.
- Determination that MCAK's C-terminal tail interferes with lattice ATPase activity and that this activity can enhance MCAK's depolymerization potential. Reprint included.
- Identified that Aurora B regulation of MCAK activity at the centromere affects chromosome movement and direction. Invited Abstract included.

Reportable Outcomes for the entire Support period:

- Abstract: American Association for Cell Biology Annual Meeting. Regulation of Mitotic Centromere-associated Kinesin (MCAK). A. T. Moore and L. Wordeman. Mol. Biol. Cell 2001. 12:437a.
- Abstract: American Association for Cell Biology Annual Meeting. The role of the neck domain in the microtubule depolymerization activity of MCAK. Mol. Biol. Cell 2001 12:436a.
- Presentation: Chromosome Segregation: the Role of Microtubule Motors. L. Wordeman. Current Concepts in Oral Biology. University of Washington School of Dentistry.
- Abstract: Era of Hope Meeting: Regulation of Mitotic Centromere-associated Kinesin (MCAK). A. T. Moore and L. Wordeman.
- Abstract: American Association for Cell Biology Annual Meeting. K-loop insertion restores microtubule depolymerizing activity of a "neckless" MCAK mutant. Mol. Biol. Cell 2002 13:322a.
- Presentation:Science in Medicine Lecture: Order from Chaos: Microtubule dynamics and Chromosome Segregation.
- Publication: K-loop insertion rescues depolymerizing activity of a "neckless" MCAK mutant. 2002. Y. Ovechkina, M. Wagenbach and L. Wordeman. J. Cell Biol. 159:557-562.
- Publication: Unconventional Motoring: An overview of the Kin C and Kin I kinesins. 2003. Traffic 4:367-375.
- Publication: Wordeman, L. (2003) Breathing down the neck of Unc104. JCB, 163:693-695.
- Abstract: American Association for Cell Biology Annual Meeting. Aurora B regulates MCAK activity at the mitotic centromere. Andrews et al. Mol. Biol. Cell 2003.
- Abstract: American Association for Cell Biology Annual Meeting. Mitotic centromere-associated kinesin (MCAK) dramatically increases the catastrophe frequency of HeLa Cell microtubules. Newton et al. Mol. Biol. Cell 2003.
- Abstract: American Association for Cell Biology Annual Meeting. MCAK's C-terminus inhibits its lattice stimulated ATPase activity. Moore and Wordeman. Mol. Biol. Cell 2003.
- Abstract: American Association for Cell Biology Annual Meeting. Dosplaced MCAK activity opposes microtubule capture at the kinetochore. Feinstein and Wordeman. Mol. Biol. Cell 2003.
- Publication: Andrews et al, (2004) Aurora B regulates MCAK activity at the mitotic centromere. Dev. Cell 6:253-268.
- Publication: Newton et al. (2004) MCAK, a Kin I kinesin, increases the catastrophe frequency of steady-state HeLa cell microtubules in an ATP-dependent manner in vitro. FEBS Lett. 572:80-84.
- Publication: Moore and Wordeman (2004)The Carboxyl-terminus of Mitotic Centromere-associated kinesin (MCAK) inhibits its lattice stimulated ATPase activity. Biochem. J. 2004: In press.
- Publication: Moore and Wordeman (2004) The mechanism, dunction and regulation of depolymerizing kinesins during mitosis. Trends in Cell Biol. In press.
- Invited Abstract: 6th International workshop on Chromosome Segregation and Aneuploidy, Cortona, Italy. The Influence of Aurora B-regulated MCAK on Oscillatory Chromosome Movement.

Supported Personnel

Linda Wordeman, Principal Investigator
Ayana T. Moore, Research Assistant
Michael Wagenbach, Research Technologist III
Marla Feinstein, Research Assistant

Conclusions

We have developed the most detailed mechanistic model for MCAK and Kif2A function in cells. Detailed mechanistic analyses are critical in order to understand regulation, as our studies of the neck, which lead to a mechanism for regulation by Aurora B, illustrate. Furthermore, our live human microtubule and tip studies show that MCAK interacts with tubulin dimers in a phosphorylation-dependent manner. In total this supports our hypothesis for the DOD Idea grant that MCAK influences the tubulin autoregulatory system, which by extension, has the potential to affect the levels of other microtubule modulating proteins such as Kif2Aβ and stathmin. While this is an impressive foundation for further studies we have not realized our goal in developing a model cell culture system to test the effects of changing the levels of these proteins on transformation and tumor progression. Since the start of this funding period, great technical advances have been made with respect to the ease and cost of screening transcriptional and proteomic response to alterations in cellular protein levels. If we can obtain further funding we will continue this line of investigation using a proteomic approach. MCAK levels are upregulated in both breast cancer (*19*) and prostate cancers (SAGE analysis). We have access to normal and tumorigenic prostate samples (coutesy of Tom Takayama, Dept. of Urology, University of Washington School of Medicine) that we can assay for MCAK, Kif2Aβ and Aurora B levels. In this way, we hope to extend these studies to precisely define the clinically relevant link between MCAK family proteins, stathmin and tumor progression.

References

1. L. Wordeman, T. J. Mitchison, *J Cell Biol* **128**, 95 (Jan, 1995).
2. L. D. Belmont, T. J. Mitchison, *Cell* **84**, 623 (Feb 23, 1996).
3. M. A. Jordan, L. Wilson, *Nat Rev Cancer* **4**, 253 (Apr, 2004).
4. J. A. Hadfield, S. Ducki, N. Hirst, A. T. McGown, *Prog Cell Cycle Res* **5**, 309 (2003).
5. P. Chieffi *et al.*, *J Endocrinol* **181**, 263 (May, 2004).
6. H. Katayama, W. R. Brinkley, S. Sen, *Cancer Metastasis Rev* **22**, 451 (Dec, 2003).
7. P. Meraldi, R. Honda, E. A. Nigg, *Curr Opin Genet Dev* **14**, 29 (Feb, 2004).
8. P. D. Andrews *et al.*, *Dev Cell* **6**, 253 (Feb, 2004).
9. G. J. Gorbsky, *Curr Biol* **14**, R346 (May 4, 2004).
10. N. Santama *et al.*, *Embo J* **17**, 5855 (Oct 15, 1998).
11. N. J. Ganem, D. A. Compton, *J Cell Biol* **166**, 473 (Aug 16, 2004).
12. A. Hoque *et al.*, *Cancer Epidemiol Biomarkers Prev* **12**, 1518 (Dec, 2003).
13. K. Kamada *et al.*, *Oncol Rep* **12**, 593 (Sep, 2004).
14. A. W. Hunter *et al.*, *Mol Cell* **11**, 445 (Feb, 2003).
15. T. Maney, M. Wagenbach, L. Wordeman, *J Biol Chem* **276**, 34753 (Sep 14, 2001).
16. Y. Ovechkina, M. Wagenbach, L. Wordeman, *J Cell Biol* **159**, 557 (Nov 25, 2002).
17. A. T. Moore, L. Wordeman, *Biochem J* **Pt** (Jul 13, 2004).
18. C. N. Newton, M. Wagenbach, Y. Ovechkina, L. Wordeman, L. Wilson, *FEBS Lett* **572**, 80 (Aug 13, 2004).
19. C. M. Perou *et al.*, *Proc Natl Acad Sci U S A* **96**, 9212 (Aug 3, 1999).

Appendix

1-Ovechkina et al paper. K-loop is essential.
2-Ovechkina and Wordeman. Unconvential motoring review.
3-Andrews et al paper. Aurora B regulates MCAK.
4-Newton et al. paper. MCAK's affect on live human microtubules.
5-Moore and Wordeman paper. C-terminus regulates MCAK activity.
6-Moore and Wordeman review. Final page proofs.
7-Moore et al. manuscript. MCAK is on microtubule tips.
8-6th International workshop on Chromosome Segregation and Aneuploidy, Cortona Italy. Meeting Abstract.

K-loop insertion restores microtubule depolymerizing activity of a "neckless" MCAK mutant

Yulia Ovechkina, Michael Wagenbach, and Linda Wordeman

Department of Physiology and Biophysics, University of Washington School of Medicine, Seattle, WA 98195

Unlike most kinesins, mitotic centromere–associated kinesin (MCAK) does not translocate along the surface of microtubules (MTs), but instead depolymerizes them. Among the motile kinesins, refinements that are unique for specific cellular functions, such as directionality and processivity, are under the control of a "neck" domain adjacent to the ATP-hydrolyzing motor domain. Despite its apparent lack of motility, MCAK also contains a neck domain. We found that deletions and alanine substitutions of highly conserved positively charged residues in the MCAK neck domain significantly reduced MT depolymerization activity. Furthermore, substitution of MCAK's neck domain with either the positively charged KIF1A K-loop or poly-lysine rescues the loss of MT-depolymerizing activity observed in the neckless MCAK mutant. We propose that the neck, analogously to the K-loop, interacts electrostatically with the tubulin COOH terminus to permit diffusional translocation of MCAK along the surface of MTs. This weak-binding interaction may also play an important role in processivity of MCAK-induced MT depolymerization.

Introduction

Members of the kinesin superfamily transport cargo along the surface of microtubules (MTs)* using the power of an ATP-hydrolyzing motor domain (Goldstein and Philp, 1999; Woehlke and Schliwa, 2000). Mitotic centromere–associated kinesin (MCAK) is a member of the Kin I subfamily of kinesin-related proteins that shares high homology within the motor domain with other members of the kinesin superfamily (Wordeman and Mitchison, 1995; Vale and Fletterick, 1997). However, although most kinesins translocate along the surface of MTs, MCAK and its homologues depolymerize MTs from either end (Walczak et al., 1996; Desai et al., 1999; Hunter and Wordeman, 2000; Kinoshita et al., 2001; Maney et al., 2001). Kinetic analysis suggests that processivity and diffusional motility may contribute to MCAK's rapid rate of MT depolymerization (unpublished data). The novel ability to modulate MT dynamics suggests that these kinesins may be important contributors to cell cycle progression (Zhai et al., 1996) and tumorgenesis (Lakshmi et al., 1993).

The direction of transport and the affinity for MTs are molecular refinements that adapt motile kinesins for specific cellular functions within the realm of intracellular transport, cell division, and MT dynamics (Goldstein and Philp, 1999; Woehlke and Schliwa, 2000). The "neck" domain, a region adjacent to the motor domain (head), is responsible for conferring directionality and processivity to the core motor domain (Case et al., 1997; Henningsen and Schliwa, 1997; Endow and Waligora, 1998; Romberg et al., 1998). MCAK's neck domain is highly conserved within the Kin I subfamily, but is very divergent from other kinesin-related proteins (Vale and Fletterick, 1997; Maney et al., 2001). A truncated MCAK protein, consisting of the neck domain (A182-D246) plus the core motor domain (P247-E581), shows MT depolymerization activity similar to that of the full-length (FL) MCAK (Maney et al., 2001). However, the neck itself does not possess depolymerizing activity (Maney et al., 1998), nor does it confer depolymerization activity to a motile kinesin because a chimera consisting of the MCAK neck fused to the motor domain of a conventional kinesin (KIF5B) exhibits no MT depolymerization activity when expressed in cultured cells (Maney et al., 2001). Finally, the neck domain is not involved in dimerization because the A182-E581 fragment of MCAK, which includes the neck, is a monomer (Maney et al., 2001). What, then, is the role of the neck domain in the MT depolymerization activity of MCAK?

The electrostatic interactions between a positively charged neck domain and the negatively charged COOH terminus of tubulin have been shown to be important for the processivity of conventional kinesins. The addition of positive charges to the neck of a conventional kinesin increases its processivity by perhaps tethering the kinesin near the MT surface

Address correspondence to Linda Wordeman, Dept. of Physiology and Biophysics, University of Washington, 1959 NE Pacific St., Box 357290, Seattle, WA 98195-7290. Tel.: (206) 543-4135. Fax: (206) 685-0619. E-mail: worde@u.washington.edu

*Abbreviations used in this paper: FL, full-length; MCAK, mitotic centromere–associated kinesin; MT, microtubule.

Key words: Kin I; XKCM1; kinesins; processivity; diffusional motility

© The Rockefeller University Press, 0021-9525/2002/11/557/6 $5.00
The Journal of Cell Biology, Volume 159, Number 4, November 25, 2002 557–562
http://www.jcb.org/cgi/doi/10.1083/jcb.200205089

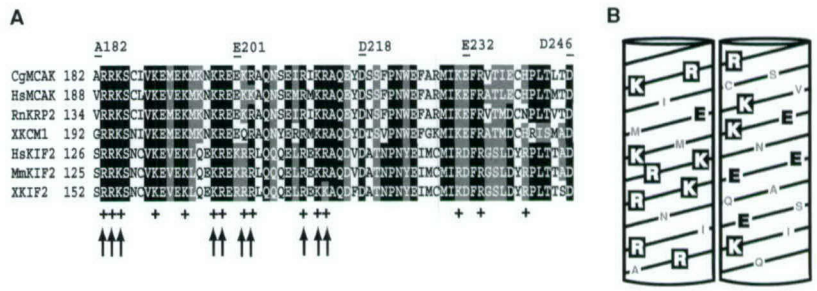

Figure 1. **The structural analysis of the MCAK neck.** (A) Sequence alignment of the neck domain of seven Kin I kinesins: CgMCAK, *C. griseus* (residues A182-D246; GenBank/EMBL/DDBJ accession no. U11790); HsMCAK, *Homo sapiens* (GenBank/EMBL/DDBJ accession no. U63743); RnKRP2, *Rattus norvegicus* (GenBank/EMBL/DDBJ accession no. U44979); XKCM1, *Xenopus laevis* (GenBank/EMBL/DDBJ accession no. U36485); HsKIF2, *Homo sapiens* (GenBank/EMBL/DDBJ accession no. CAA69621); MmKIF2, *Mus musculus* (GenBank/EMBL/DDBJ accession no. D12644); XKIF2, *X. laevis* (GenBank/EMBL/DDBJ accession no. U36486). Identical residues are shaded in black, similar ones are shaded in gray. The 64-amino acid neck domain sequences are 50% identical and 75% similar. The + symbols indicate highly conserved positively charged amino acids in the neck domain. The arrows show residues that were substituted for alanine. The borders of deletions in the neck domain are indicated by flanking residue numbers above the neck alignment. (B) Two sides of a helical diagram of a highly charged hydrophilic helix (residues R183–Q215) found in the CgMCAK neck. Positively charged amino acids are white, negatively charged residues are black, and the other residues are gray.

(Thorn et al., 2000). Similarly, the positively charged K-loop in the motor domain of the KIF1 single-headed kinesin provides a flexible attachment site for binding to MTs in the weakly bound state (Okada and Hirokawa, 2000; Rogers et al., 2001). Given the high percentage of positively charged amino acids in the MCAK neck region and their strong conservation among Kin I kinesins (Fig. 1 A), it is reasonable to suggest that the neck might be anchoring MCAK to MTs. Here, we used mutational analysis and chimeras to test whether the MCAK neck functions as an electrostatic tether. We found that although the removal of positive charges from the neck region significantly diminished the MT depolymerization activity of MCAK, the insertion of the positively charged K-loop into "neckless" MCAK completely restored its MT depolymerization activity. We propose that the neck, analogous to the K-loop, may interact electrostatically with the negatively charged MT lattice. This interaction may serve to target MCAK to MT ends by diffusional motility. The weak electrostatic interaction between MCAK's neck and MT ends may also play an important role in processivity of MCAK-induced MT depolymerization.

Results and discussion

Quantitation of MT depolymerization activity in vivo

To estimate the effect of the deletions in the MCAK neck domain on the MT depolymerization activity, we devised a quantitative in vivo MT depolymerization assay. In brief, EGFP–MCAK fusion constructs were transfected into cultured cells, fixed, and stained for tubulin (Fig. 2). Digital images were acquired using a cooled CCD camera. The transfected cells chosen for quantitation displayed similar EGFP–MCAK fusion protein expression levels (Figs. 3 and 4). The average pixel intensity (the mean gray value) over the entire cellular area was measured and corrected for noncellular background. Cells transfected with a control EGFP construct showed normal levels of MT polymer and were assigned an MT polymer value of 100%. EGFP-transfected cells displayed a mean tubulin fluorescence value of 1,902 gray-scale units, which represented the sum of free tubulin and MT polymer fluorescence (Fig. 3 A). Expression of FL MCAK resulted in the loss of all MTs at the analyzed level of expression with only a lightly stained background of unpolymerized tubulin remaining (Fig. 2 D, arrow). Such cells showed a mean tubulin fluorescence value of 734 gray-scale units, which was designated as 0% of the MT polymer (Fig. 3 A). Consequently, the mean intensity of tubulin fluorescence in the FL MCAK–transfected cells was less than half of that in the EGFP-transfected cells.

The low level of free (unpolymerized) tubulin seen in cells transfected with FL MCAK might be a result of a tubulin autoregulation mechanism. Increasing the concentration of free tubulin by depolymerizing MTs with MT-destabilizing drugs, e.g., nocodazole, leads to a rapid decrease in the level of tubulin mRNAs and an eventual decrease in the unassembled tubulin level (Cleveland et al., 1981; Gonzalez-Garay and Cabral, 1996). Similar to MCAK-mediated MT depolymerization, we found that treatment with a low concentration of nocodazole (1 μM) for 12 h produced cells with a low

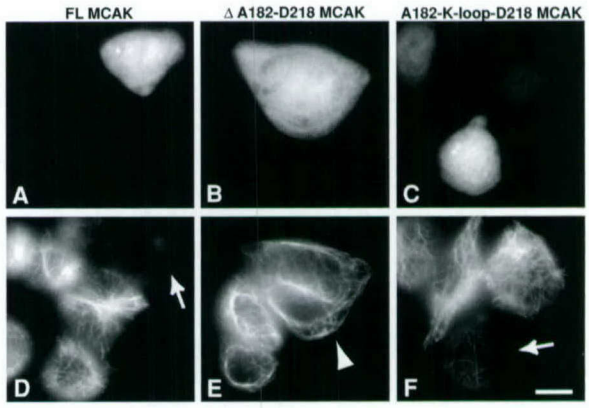

Figure 2. **Depolymerization of MTs by MCAK and MCAK mutants.** (A–C) EGFP fluorescence, (D–F) tubulin staining of the same cells. A cell transfected with full-length (FL) MCAK (A and D) displays a loss of MT polymer and low intensity unpolymerized tubulin staining (arrow). A cell transfected with the neckless MCAK mutant (B and E; Δ A182-D218 MCAK) exhibits a normal network of cytoplasmic MTs (arrowhead) as a consequence of the significantly decreased MT depolymerization activity of neckless MCAK. (C and F) Cells transfected with the A182-K-loop-D218 MCAK construct, the K-loop insertion into the neckless Δ A182-D218 MCAK mutant. The insertion of the KIF1A K-loop (NKNKKKKK) into the neckless MCAK restores the MT depolymerization activity to the level of FL MCAK. Arrow in F illustrates a cell with MT polymer loss similar to that in FL MCAK–transfected cells (D, arrow). All panels are the same magnification. Bar, 10 μm.

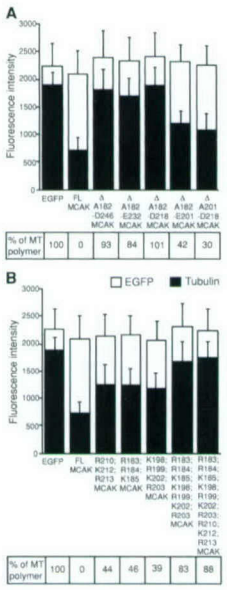

Figure 3. **Removal of positive charges in the neck domain significantly reduced MT depolymerization activity of MCAK.** (A) The effect of deletions in the neck region. Each Δ symbol represents a deletion of the MCAK neck region with borders indicated by flanking amino acid numbers. (B) The effect of alanine substitutions in the neck region. The residues changed to alanine are shown for each MCAK mutant. The average pixel intensity over the cell area is plotted on the y axis in gray-scale units. White bars show the mean EGFP fluorescence. Black bars represent the mean tubulin fluorescence. Error bars are SDs. EGFP indicates cells transfected with the EGFP control; FL MCAK designates cells transfected with FL wild-type MCAK. The percentage of MT polymer left in the transfected cells is shown.

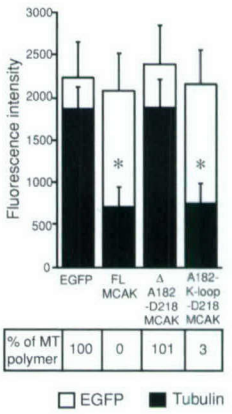

Figure 4. **Insertion of KIF1A K-loop into the neckless MCAK fully restores MT depolymerization activity.** y and x axis categories are the same as described in Fig. 3 legend. Error bars are SDs. A182-K-loop-D218 MCAK represents cells transfected with the KIF1A K-loop insertion into the neckless MCAK mutant, A182-NKNKKKKK-D218 MCAK. Asterisks label two samples, FL MCAK and A182-K-loop-D218 MCAK, whose means are statistically similar ($P = 0.92$) to each other as determined using the *t* test. The percentage of MT polymer left in the transfected cells is indicated.

intensity free-tubulin background and no MTs. The mean tubulin fluorescence intensity of these cells was 798 ± 169 gray-scale units ($n = 88$) as determined by the in vivo depolymerization assay described in this report. The mean tubulin intensity of cells treated with 1 μM nocodazole for 15 min was 1,645 ± 189 ($n = 41$). These cells displayed almost no MT polymer and bright free-tubulin staining due to the fact that 15 min was not long enough for autoregulation to take place and decrease the level of free tubulin. Nontreated cells with a normal network of cytoplasmic MTs showed the mean tubulin intensity equal to 1,870 ± 301 ($n = 77$).

The removal of positive charges from the neck domain dramatically reduced MT depolymerization activity of MCAK

As expected from previous studies (Maney et al., 2001), cells transfected with neckless MCAK (Δ A182-D246) displayed a normal MT network. The mean tubulin fluorescence of the Δ A182-D246 MCAK mutant was similar to that of the EGFP control and equaled 1,825 gray-scale units (Fig. 3 A). Cells transfected with MCAK mutants containing progressively smaller deletions in the neck domain, Δ A182-E232 and Δ A182-D218 (Fig. 2 E, arrowhead), also showed normal levels of MT polymer that were similar to that of the EGFP-transfected cells (Fig. 3 A). Hence, these neckless MCAK mutants exhibited severely impaired MT depolymerization activity. Smaller deletions in the neck region (Δ A182-E201 and Δ E201-D218) diminished MT depolymerization activity to a lesser degree. (Fig. 3 A). Next, we performed alanine substitutions of the highly conserved positively charged residues in the neck domain (Fig. 1, arrows) to test whether the loss of positive charges in this region affects the depolymerization activity of MCAK. Alanine substitutions of 3–4 positively charged amino acids resulted in some reduction of MT depolymerization activity (more than 50% of MTs were depolymerized in the transfected cells). Substitutions of 7 to 10 amino acids resulted in much greater inhibition of the depolymerization activity (<20% of MTs were depolymerized; Fig. 3 B). Therefore, the total sum of removed positive charges was of greater importance than the positions of the substituted residues.

In summary, we identified Δ A182-D218 as the smallest neck deletion that would reduce MT depolymerizing activity to the level of the EGFP control (Fig. 3 A). This region contains 13 (36%) positively charged residues and 7 (19%) negatively charged residues (Fig. 1). The net charge of A182-D218 region is positive and equals +6. Alanine substitutions of only 7 positive residues rendered the net charge of A182-D218 segment negative and resulted in greatly diminished MT depolymerization activity (Fig. 3 B). The A182-D218 region contains a highly charged hydrophilic helix (residues R183-Q215) as predicted by SSpro2 server (http://promoter.ics.uci.edu/BRNN-PRED [Baldi et al., 1999]). The helical wheel representation of this helix shows that the positively charged residues lie mostly on one side of the helix, whereas the opposite side contains most of the negatively charged residues found in this neck region (Fig. 1 B).

KIF1A K-loop insertion into neckless MCAK rescues MT depolymerization activity

We have shown that elimination of the positive charges in the MCAK neck region, A182-D218, either by deletions or alanine substitutions inhibits MT depolymerization activity of MCAK. Conversely, Niederstrasser et al. (2002) showed that the interaction between the COOH terminus of tubulin (C-hook) and MCAK is required for MT depolymerization because subtilisin cleavage of the C-hook abolishes depolymerization of MTs by the MCAK homologue, XKCM1. Furthermore, Okada and Hirokawa (2000) have shown that the positively charged K-loop of KIF1A interacts with the negatively charged C-hook and serves as an electrostatic tether to support the diffusion of KIF1A along MT protofilament. The positively charged neck of MCAK might interact with the negatively charged C-hook of tubulin analogously to the KIF1A K-loop. We tested this hypothesis by inserting the K-loop of KIF1A into the MT depolymerization deficient neckless MCAK. We found that MCAK with the A182-D218 neck segment replaced by the KIF1A K-loop, NKNKKKKK, (abbreviated as A182-K-loop-D218 MCAK) depolymerized MTs with the same efficiency as FL MCAK (Figs. 2 F and 4). Moreover, mitotic cells transfected with the A182-NKNKKKKK-D218 MCAK mutant displayed the same mitotic defects (unpublished data) described for overexpression of FL MCAK, namely bundling

and depolymerization of spindle MTs, which in turn resulted in prometaphase arrest and an elevated mitotic index in transfected cells (Maney et al., 1998).

None of the MCAK mutations described in this report interfered with centromere or centrosome binding. The nuclear/cytoplasmic localization of the mutants was identical to that of wild-type FL MCAK (unpublished data). All MCAK mutants showed the ability to bind MTs in vivo when cells were extracted before fixation in the absence of nucleotide (unpublished data) in a manner identical to FL MCAK (Maney et al., 1998). This implies that all mutated MCAKs were functional proteins with motor domains able to bind MT lattice in the nucleotide-free state, similar to conventional kinesins.

In vitro MT depolymerization activity of MCAK neck mutants

The rescue of the MT depolymerization–deficient neckless MCAK by K-loop insertion suggests that the MCAK neck is affecting the interactions between motor and MTs rather than regulating the depolymerization activity. To test this hypothesis further, we replicated our depolymerization assays in vitro. We expressed and purified the following proteins: core motor plus neck (A182-S583); core motor plus alanine-substituted neck (A182-Ala-S583 with substituted residues indicated by arrows in Fig. 1 A); core motor plus truncated neck (D218-S583); core motor plus K-loop in substitution for the neck (A182-K-loop-D218-S583); core motor plus poly-lysine (5K) in substitution for the neck (A182–5K-D218-S583); and core motor domain of MCAK (I253-S583; Fig. 5 A). The purified proteins were added to the taxol-stabilized MTs and were incubated at 24 ± 1°C for 10 min in the presence of 1 mM ATP. The depolymerization of tubulin polymer was measured as the percentage of tubulin released in the supernatant after subtraction of tubulin in supernatant of the no-motor control reaction and normalizing the supernatant and pellet fractions. Fig. 5 B shows the supernatants and pellets of the in vitro depolymerization reactions containing 100 nM active motor proteins and 1,500 nM taxol MTs. Although the core motor plus neck (A182-S583) depolymerizes 92 ± 4% of tubulin polymer, the core motor plus alanine-substituted neck, A182-Ala-S583 depolymerized only 10 ± 4% of tubulin polymer (Fig. 5 B). The truncated neck plus core motor (D218-S583) lacks the positively charged helix found in the FL neck (Fig. 1 B). This protein depolymerized only 13 ± 5% of tubulin polymer. Therefore, removal of positive charges from the neck either by alanine substitutions or deletions dramatically suppresses the MT depolymerization activity of this kinesin, but does not eliminate it completely in vitro. Although analogous neckless MCAK mutants (Δ A182-D246, Δ A182-E232, and Δ A182-D218) expressed to high levels in vivo displayed no detectable depolymerization activity (Fig. 2 E, 3A), in corroboration with our in vitro data, extremely high levels of expression showed a slightly disassembled MT network (unpublished data).

Also, we substituted the positively charged helix found in the A182-D218 region of CgMCAK neck (Fig. 1 B) with the positively charged K-loop of KIF1A by linking the K-loop to the NH_2 terminus of truncated neck plus core motor construct, D218-S583. This construct exhibited five-fold-increased depolymerization activity over D218-S583 (Fig. 5 B). However, although the K-loop rescues the depolymerization activity of the neckless mutant 100% in vivo

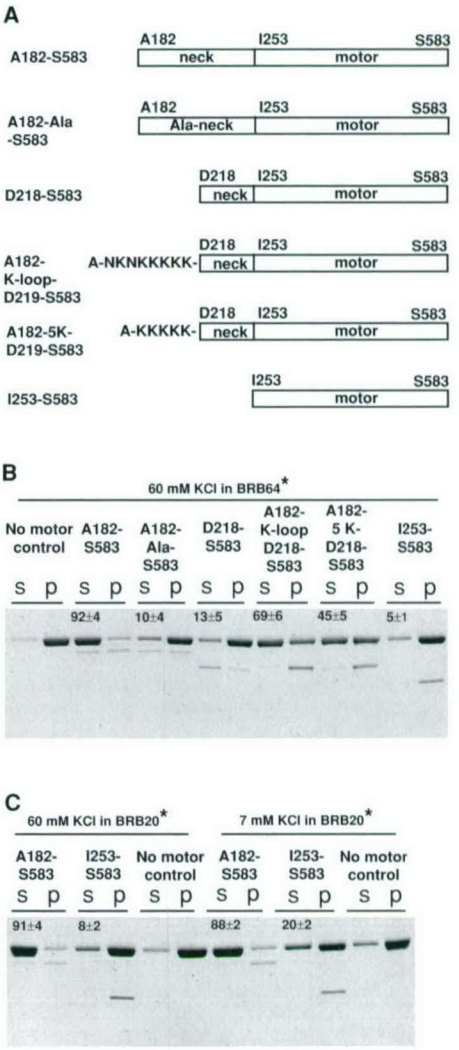

Figure 5. **Depolymerization activity of MCAK mutants in vitro.** (A) Diagram illustrating the truncated MCAK mutants used for in vitro depolymerization assays: core motor plus neck (A182-S583); core motor plus alanine-substituted neck (A182-Ala-S583 with R183, R184, K185, K198, R199, K202, R203, R210, K212, and R213 substituted to alanine); core motor plus truncated neck (D218-S583); core motor plus K-loop (NKNKKKKK) in substitution for the neck (A182-K-loop-D218-S583); core motor plus poly-L-lysine (KKKKK) in substitution for the neck (A182–5K-D218-S583); and core motor (I253-S583). B compares the depolymerization activity of the truncated MCAK mutants described above. C compares the depolymerization activity of the core motor plus neck (A182-S583) and the core motor domain of MCAK (I253-S583) in 60 mM KCl, BRB20 versus 7 mM KCl, BRB20. For both B and C, the percentage of tubulin in the supernatant of no-motor control reactions was subtracted from the percentage of tubulin in supernatant of the motor-containing reactions. The numbers are percentages of tubulin released in supernatant of the motor-containing reactions. The average of at least three experiments ± SD is shown for each supernatant fraction. In each case, the top band on the gel is tubulin and the bottom band is the added motor. In all assays, 100 nM of active motor protein was added to 1,500 nM taxol-stabilized MTs in the presence of 1 mM ATP. *Refer to Materials and methods for exact buffer composition.

(Fig. 4), it rescues only 75% of the depolymerization activity of D218-A182 construct in vitro (Fig. 5 B). Therefore, the MCAK neck plus motor (A182-S583) is still the most optimal construct for MT depolymerization, which might be one of the reasons why it is so highly conserved. It is likely that the K-loop rescues the depolymerization activity because it contains positively charged residues. We have further confirmed that charge is an important functional property of the neck by constructing the poly-lysine mutant, A182-KKKKK-D218-S583 (abbreviated as A182–5K-D218-S583), which contains poly-lysine peptide instead of K-loop in place of A182-D218 neck region. Fig. 5 B shows that the poly-lysine peptide substitution rescues the depolymerization activity of D218-S583, but to a lesser degree than the K-loop substitution, perhaps due to fewer positive charges found in the poly-lysine peptide (+5) than in K-loop (+6).

The rescue of the MT depolymerization–deficient neckless MCAK by K-loop insertion suggests that the MCAK neck might function analogously to the K-loop. The K-loop of KIF1A mediates diffusional motility (Okada and Hirokawa, 2000; Rogers et al., 2001). Similarly, we propose that the neck of MCAK may support diffusional motility to transport MCAK along the MT protofilament toward MT ends where Kin I–mediated MT depolymerization occurs (Desai et al., 1999). The neck of MCAK may also use diffusional motility to confer accelerated kinetics or processivity to the core motor domain (unpublished data).

Moores et al. (2002) have clearly shown that a conserved core motor domain of a *Plasmodium falciparum* Kin I kinesin (pKinI) can disassemble MTs. However, the assay conditions (extremely low ionic strength) were chosen to maximize electrostatic interactions. Maximizing the electrostatic interactions and raising the stoichiometry of Kin I/tubulin ($\geq$1:10) obviates the need for processivity or diffusional motility despite the fact that it is essential for depolymerization under physiological conditions. We have duplicated the low ionic strength conditions used by Moores et al. (2002). The decrease in salt concentration from 60 to 7 mM KCl in BRB20 buffer produced a twofold increase of tubulin polymer depolymerized by the core motor (Fig. 5 C). This shows that the core motor of MCAK (I253-S583) is also a definite but enfeebled depolymerizer. Direct comparison of the neck plus motor (A182-S583) with the conserved core motor (I253-S583) shows that the neck plus motor is a tremendously more effective depolymerizer than the core motor (Fig. 5, B and C).

In summary, we demonstrated that deletions or alanine substitutions of positively charged residues of A182-D218 neck region drastically reduced the MT depolymerization activity. Insertion of the positively charged KIF1A K-loop or poly-lysine rescued the neckless MCAK mutants. We propose that the neck acts as an electrostatic tether. This electrostatic tether may increase the rate of MT depolymerization by either increasing the on-rate of MCAK to MT ends (perhaps by mediating diffusional motility) or decreasing the off-rate of MCAK from MTs (perhaps by conferring processivity to the core motor domain; unpublished data). The data presented here do not allow us to distinguish between diffusional targeting and processivity. Mediation of diffusional targeting and processivity are two distinct and not mutually exclusive hypotheses for the contribution of the neck to the MT depolymerization activity of MCAK.

Materials and methods

Constructs

pTRE2-EGFP-CgMCAK was made by the subcloning of NheI-BspEI EGFP cDNA fragment (from pEGFP-C1; CLONTECH Laboratories, Inc.) and the BspEI-NotI *Cricetulus griseus* MCAK cDNA fragment (from pOPRSVICAT-GFP-MCAK; Maney et al., 1998) into the pTRE2 vector (CLONTECH Laboratories, Inc.) digested with NheI and NotI. The gene expression level controlled by TRE promoter is similar to the high expression levels in the traditional CMV promoter–driven systems (Yin et al., 1996). The deletion, alanine substitution, and K-loop insertion constructs were prepared by overlap PCR using specially designed mutagenic primers and PfuTurbo® DNA polymerase (Stratagene). The mutations were confirmed by DNA sequencing. Constructs for bacterially expressed proteins were made by amplifying the coding sequences of MCAK mutants from the constructs in pTRE2 vector with PfuTurbo® DNA polymerase (Stratagene), and then subcloning the resulting fragments into pET-28a+ (Novagen) digested with Nco1 and Not1.

Cell transfection and immunofluorescence

CHO AA8 Tet-Off™ cells (CLONTECH Laboratories, Inc.) were grown in 90% αMEM, 10% FBS, and 100 μg/ml G418 at 37°C, 5% CO_2. 1 d before transfection, cells were plated onto 12-mm coverslips at low density (2×10^4 cells/cm^2). Transfections were done with ExGen 500 transfection reagent (MBI Fermentas). Cells were cultured for 24 h after transfection and fixed with 1% PFA in precooled methanol for 10 min. The cells were then incubated with mouse anti–tubulin DM1α (Sigma-Aldrich) at 1:50 dilution for 1 h and Texas red anti–mouse antibodies (Jackson ImmunoResearch Laboratories) at 1:100 dilution in PBS plus 0.1% Triton X-100 and 1% BSA for 1 h. Cells were washed with PBS, stained with DAPI, and mounted in Vectashield® mounting medium (Vector Laboratories). Analysis was done with a microscope (model FX-A; Nikon) equipped with 60×/1.4 NA Plan Apo oil objective. The digital images were acquired with a cooled CCD camera (SenSys; Photometrics) controlled by QED camera software (QED Imaging, Inc.).

Quantitation of MT depolymerization activity in vivo

To quantify the microtubule (MT) depolymerization activity, we collected digital images of the transfected cells at the same exposure for each set of GFP and MT images and below saturation level of the camera (the 4,096 gray-value maximum). All images were saved as 12-bit TIFF images for quantification by NIH Image 1.62 software and Microsoft Excel. Mean EGFP or tubulin fluorescence intensities over the entire cellular area were measured as the average gray value within the area. Mean fluorescence over the cell-free area in each image was subtracted from mean fluorescence over the cellular area to correct for background fluorescence. All analyzed cells were in interphase and were free of aggregates of overexpressed protein. 20–90 transfected cells were measured for each construct with >500 cells quantified overall. To quantify the MT polymer left in the transfected cells, we assigned an MT polymer value of 0% to the cells transfected with full-length (FL) MCAK, which displayed no MTs and a mean tubulin fluorescence intensity equal to 734 gray-scale units. Similar to nontransfected cells, EGFP-transfected cells showed normal levels of MT polymer, which was given a 100% value. The mean tubulin fluorescence of EGFP-transfected cells was equal to 1,902 gray-scale units. To quantify the percentage of MT polymer left in the cells transfected with mutant MCAK constructs, we used the following formula: {[(the mean tubulin fluorescence intensity of mutant-transfected cells − 734)/1,168] × 100%} where 1168 is the difference between EGFP control and FL MCAK mean gray values.

In vitro MT depolymerization assays

The bacterially expressed COOH-terminally 6his-tagged proteins were purified as described in Maney et al. (2001). The active motor concentration was determined as the concentration of nucleotide-binding sites because there is one ATP-binding site per each monomeric motor protein analyzed in this study in vitro. The concentration of nucleotide-binding sites was measured radiometrically as described by Coy et al. (1999). The depolymerization of taxol-stabilized MTs, polymerized from bovine tubulin (Cytoskeleton, Inc.), was performed as described in Maney et al. (2001). In brief, for the assay shown in Fig. 5 A, 100 nM of the active motor proteins in 20 μl of the elution buffer (250 mM imidazole, pH 7.0, 300 mM KCl,

0.2 mM $MgCl_2$, 0.01 mM Mg-ATP, 1 mM DTT, and 20% glycerol) was mixed with 1,500 nM taxol-stabilized MTs in 80 μl of BRB80 (80 mM Pipes, pH 6.8, 1 mM EGTA, and 1 mM $MgCl_2$), 12.5 μM taxol, 1 mM DTT, and 1.25 mM Mg-ATP incubated at 24 ± 1°C for 10 min, and then centrifuged at 30 psi for 10 min. For the assay shown in Fig. 5 B, 100 nM of the active motor proteins in 2.3 μl of the elution buffer was mixed with 1,500 nM taxol-stabilized MTs in 97.7 μl of BRB20 (20 mM Pipes, pH 6.8, 1 mM EGTA, and 1mM $MgCl_2$), 10.2 μM taxol, 1 mM DTT, 10 μg/ml BSA, and 1.02 mM Mg-ATP with or without addition of KCl up to 60 mM, incubated at 24 ± 1°C for 10 min, and then centrifuged at 30 psi for 10 min. Supernatants and pellets were assayed for the presence of tubulin on Coomassie-stained SDS-polyacrylamide gels (Novex). Gels were calibrated and quantified using NIH Image 1.62 software. The percentage of tubulin in the supernatant of no-motor control reactions was subtracted from the percentage of tubulin in supernatant of the motor-containing reactions. The percentages of tubulin released in supernatant of the motor-containing reactions were then normalized with the percentages of tubulin in the corresponding pellet fractions.

We thank Andy Hunter, Ayana Moore, and Kathleen Rankin for many discussions and comments on the manuscript. We also thank Ayana Moore (University of Washington School of Medicine, Seattle, WA) for the pTRE2-GreenLantern-CgMCAK plasmid.

This work was supported by the National Institutes of Health grant (GM53654A) and the Department of Defense grant (DAMD17-01-1-0450) to L. Wordeman.

Submitted: 17 May 2002
Revised: 16 October 2002
Accepted: 17 October 2002

References

Baldi, P., S. Brunak, P. Frasconi, G. Soda, and G. Pollastri. 1999. Exploiting the past and the future in protein secondary structure prediction. *Bioinformatics.* 15:937–946.

Case, R.B., D.W. Pierce, N. Hom-Booher, C.L. Hart, and R.D. Vale. 1997. The directional preference of kinesin motors is specified by an element outside of the motor catalytic domain. *Cell.* 90:959–966.

Cleveland, D.W., M.A. Lopata, P. Sherline, and M.W. Kirschner. 1981. Unpolymerized tubulin modulates the level of tubulin mRNAs. *Cell.* 25:537–546.

Coy, D.L., M. Wagenbach, and J. Howard. 1999. Kinesin takes one 8-nm step for each ATP that it hydrolyzes. *J. Biol. Chem.* 274:3667–3671.

Desai, A., S. Verma, T.J. Mitchison, and C.E. Walczak. 1999. Kin I kinesins are microtubule-destabilizing enzymes. *Cell.* 96:69–78.

Endow, S.A., and K.W. Waligora. 1998. Determinants of kinesin motor polarity. *Science.* 281:1200–1202.

Goldstein, L.S., and A.V. Philp. 1999. The road less traveled: emerging principles of kinesin motor utilization. *Annu. Rev. Cell Dev. Biol.* 15:141–183.

Gonzalez-Garay, M.L., and F. Cabral. 1996. alpha-Tubulin limits its own synthesis: evidence for a mechanism involving translational repression. *J. Cell Biol.* 135:1525–1534.

Henningsen, U., and M. Schliwa. 1997. Reversal in the direction of movement of a molecular motor. *Nature.* 389:93–96.

Hunter, A.W., and L. Wordeman. 2000. How motor proteins influence microtubule polymerization dynamics. *J. Cell Sci.* 113:4379–4389.

Kinoshita, K., I. Arnal, A. Desai, D.N. Drechsel, and A.A. Hyman. 2001. Reconstitution of physiological microtubule dynamics using purified components. *Science.* 294:1340–1343.

Lakshmi, M.S., C. Parker, and G.V. Sherbet. 1993. Metastasis associated MTS1 and NM23 genes affect tubulin polymerisation in B16 melanomas: a possible mechanism of their regulation of metastatic behaviour of tumours. *Anticancer Res.* 13:299–303.

Maney, T., A.W. Hunter, M. Wagenbach, and L. Wordeman. 1998. Mitotic centromere-associated kinesin is important for anaphase chromosome segregation. *J. Cell Biol.* 142:787–801.

Maney, T., M. Wagenbach, and L. Wordeman. 2001. Molecular dissection of the microtubule depolymerizing activity of mitotic centromere-associated kinesin. *J. Biol. Chem.* 276:34753–34758.

Moores, C.A., M. Yu, J. Guo, C. Beraud, R. Sakowicz, and R.A. Milligan. 2002. A mechanism for microtubule depolymerization by KinI kinesins. *Mol. Cell.* 9:903–909.

Niederstrasser, H., H. Salehi-Had, E.C. Gan, C. Walczak, and E. Nogales. 2002. XKCM1 acts on a single protofilament and requires the C terminus of tubulin. *J. Mol. Biol.* 316:817–828.

Okada, Y., and N. Hirokawa. 2000. Mechanism of the single-headed processivity: diffusional anchoring between the K-loop of kinesin and the C terminus of tubulin. *Proc. Natl. Acad. Sci. USA.* 97:640–645.

Rogers, K.R., S. Weiss, I. Crevel, P.J. Brophy, M. Geeves, and R. Cross. 2001. KIF1D is a fast non-processive kinesin that demonstrates novel K-loop-dependent mechanochemistry. *EMBO J.* 20:5101–5113.

Romberg, L., D.W. Pierce, and R.D. Vale. 1998. Role of the kinesin neck region in processive microtubule-based motility. *J. Cell Biol.* 140:1407–1416.

Thorn, K.S., J.A. Ubersax, and R.D. Vale. 2000. Engineering the processive run length of the kinesin motor. *J. Cell Biol.* 151:1093–1100.

Vale, R.D., and R.J. Fletterick. 1997. The design plan of kinesin motors. *Annu. Rev. Cell Dev. Biol.* 13:745–777.

Walczak, C.E., T.J. Mitchison, and A. Desai. 1996. XKCM1: a *Xenopus* kinesin-related protein that regulates microtubule dynamics during mitotic spindle assembly. *Cell.* 84:37–47.

Woehlke, G., and M. Schliwa. 2000. Walking on two heads: the many talents of kinesin. *Nat. Rev. Mol. Cell Biol.* 1:50–58.

Wordeman, L., and T.J. Mitchison. 1995. Identification and partial characterization of mitotic centromere-associated kinesin, a kinesin-related protein that associates with centromeres during mitosis. *J. Cell Biol.* 128:95–104.

Yin, D.X., L. Zhu, and R.T. Schimke. 1996. Tetracycline-controlled gene expression system achieves high-level and quantitative control of gene expression. *Anal. Biochem.* 235:195–201.

Zhai, Y., P.J. Kronebusch, P.M. Simon, and G.G. Borisy. 1996. Microtubule dynamics at the G2/M transition: abrupt breakdown of cytoplasmic microtubules at nuclear envelope breakdown and implications for spindle morphogenesis. *J. Cell Biol.* 135:201–214.

Traffic 2003; 4: 367–375
Blackwell Munksgaard

Copyright © Blackwell Munksgaard 2003
ISSN 1398-9219

Review

Appendix 2

Unconventional Motoring: An Overview of the Kin C and Kin I Kinesins

Yulia Ovechkina and Linda Wordeman*

University of Washington School of Medicine, Department of Physiology and Biophysics, Seattle, WA 98195, USA
** Corresponding author: Linda Wordeman, worde@u.washington.edu*

All kinesins share a conserved core motor domain implying a common mechanism for generating force from ATP hydrolysis. How is it then that kinesins exhibit such divergent activities: motility, microtubule cross-linking and microtubule depolymerization? Although conventional motile kinesins have served as the paradigm for understanding kinesin function, the unconventional kinesins exploit variations on the motile theme to perform unexpected tasks. This review summarizes the biological functions and examines the possible molecular mechanisms of Kin C and Kin I unconventional kinesins. We also discuss the possible differences between the microtubule destabilization models proposed for Kar3 and Kin I kinesins.

Key words: depolymerization, Kar3, KIF2, kinesin, Kip3, Klp5/6, MCAK, microtubule dynamics, motor, XKCM1

Received 2 March 2003, revised and accepted for publication 26 March 2003

Kinesins are a large superfamily of microtubule motor proteins that use the energy of ATP hydrolysis to produce force. They are defined by the presence of a catalytic core motor domain (historically known as the 'head' domain), which hydrolyzes ATP and binds to microtubules (MTs). Kinesins are classified into three subfamilies based on the position of their motor domain within the primary sequence of the protein. The Kin C subfamily comprises kinesins with a C-terminally located core motor domain; Kin N kinesins have an N-terminally located core motor domain; and Kin I kinesins possess an internally located core motor domain (Figure 1). All kinesins share a high degree of sequence identity within the core motor domain. The crystal structures of the Kin N and Kin C core motor domains are clearly similar to each other (1,2). The first kinesin to be identified was purified from the giant axon of the squid (3). This extensively studied member of the Kin N family of kinesins serves as the prototype for all other kinesin-related proteins by virtue of its relative abundance and ubiquitous tissue distribution. As a result, Kin N kinesins that are structurally related to squid axonal kinesin have earned the designation 'conventional kinesins'. By default, the Kin C and Kin I kinesins have been labeled 'unconventional kinesins'.

Functionally, the position of a kinesin's motor domain within the polypeptide chain usually predicts its directionality. Kin N kinesins walk toward the plus ends of MTs, whereas Kin C kinesins translocate toward the minus ends of MTs. Unexpectedly, the Kin I kinesins are not able to translocate along MTs in the conventional sense but, instead, depolymerize MT filaments from both ends (4,5). It is important to note, however, that the directionality of motile kinesins is not directly controlled by the position of the motor domain in the polypeptide chain but rather by the conserved region immediately outside the motor core domain, called the 'neck' domain [reviewed in (6,7)]. Vale and Fletterick (8) have defined the neck domain as 'the most class-specific region' within the kinesin primary sequence. This region is highly conserved within each respective kinesin subfamily but extremely variable across subfamilies (8). It is thought that the conserved core motor domains of both Kin N and Kin C subfamilies possess intrinsic slow plus-end directed motile activity. The Kin N-type neck may act to amplify this activity, while the presence of a Kin C-type neck is sufficient to direct the motor toward MT minus-ends [reviewed in (6,9)]. The neck domains of the Kin C and Kin I kinesins are located N-terminally to the core motor domain, while the neck of the Kin N kinesins is C-terminal to the core motor (Figure 1). Many kinesins contain an α-helical coiled-coil stalk domain through which they dimerize (Figure 1). In addition, kinesins typically have a globular tail domain capable of carrying out a wide variety of functions, such as interacting with cargo or kinesin-associated proteins (10); regulating the core motor ATPase activity (11); providing non-ATP dependent MT binding sites (12); and targeting kinesins to different locations in cells (13).

All conventional kinesins (Kin N subfamily members) characterized so far are processive, meaning they are able to take hundreds of steps before dissociating from an MT filament [reviewed in (14,15)]. Processivity requires that the motor be continuously attached to the MT during successive steps in the cycle of translocation. In the case of conventional kinesin, conformational changes in the dimerized heads are coupled intermolecularly to the ATP hydrolysis cycle, so that one head is always strongly bound

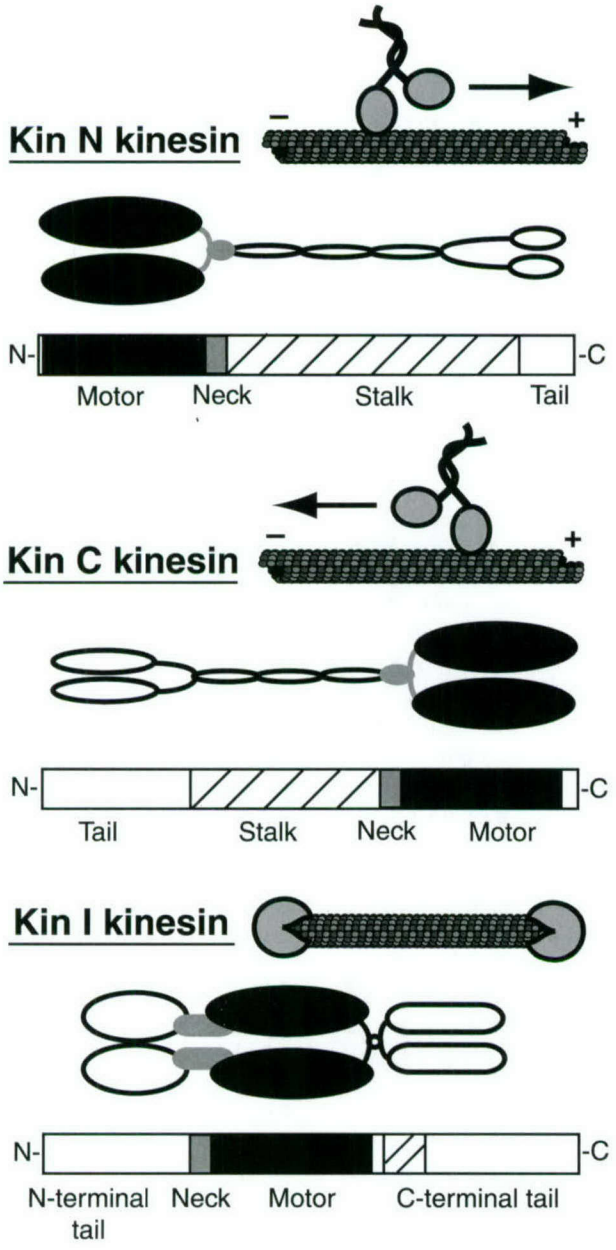

Figure 1: Schematic representations of kinesin structure. Members of Kin N, Kin C, and Kin I kinesin subfamilies are shown. Kin N kinesins move toward the plus ends of MTs, Kin C kinesins translocate toward the minus ends of MTs, whereas the Kin I kinesins depolymerize MTs from both ends. The conserved core motor domain is shaded in black; the neck is in gray; tail domains are in white; and coiled-coil regions are striped.

to MTs while the motor domains translocate in a hand-over-hand manner along the surface of the microtubule lattice. In contrast, the Kin C dimeric kinesins are nonprocessive motors. They lack the ability to take even a few successive steps along a MT filament [reviewed in (6,15)]. However, when multiple nonprocessive motors work together, for example by attaching to a surface of a vesicle, they can processively transport it along MTs. A recent study by Hunter et al. (4) has demonstrated that the Kin I kinesin, CgMCAK, is a processive depolymerase. A single CgMCAK dimer will remove multiple tubulin dimers while maintaining an attachment to MT ends (4).

All in all, the unconventional kinesins are important for numerous biological processes and their malfunctions have been implicated in human diseases [reviewed in (16,17)]. Mutations in the Kin C kinesin, DmNCD, cause chromosome nondisjunction during female meiosis in *Drosophila* (18). Related Kin C kinesins also operate during vertebrate meiosis and mitosis to insure accurate chromosome segregation (19,20). Chromosome nondisjunction during meiosis is the most common cause of mental retardation and conceptus wastage in humans (21), making this class of kinesins of fundamental importance for genomic stability and human health.

In addition, the ability of Kin I kinesins to modulate microtubule dynamics has major implications for both chromosome segregation and malignancy. A member of the Kin I subfamily, HsMCAK (KNSL6), is overexpressed in human cancers (22,23). The hamster homolog of HsMCAK can depolymerize paclitaxel-stabilized MTs in cells (24). Significantly, the other major MT depolymerizing nonmotor protein, stathmin, is incapable of destabilizing cellular MTs in the presence of comparable levels of paclitaxel (24,25). Therefore, HsMCAK overexpression, in particular, may be responsible for decreased sensitivity to the microtubule-stabilizing anticancer drug paclitaxel (Taxol, registered trademark of Bristol Myers Squibb) in some cancers (26). HsMCAK may antagonize the effect of paclitaxel by promoting MT dynamics. Targeting cancer cells with MCAK inhibitors alone or together with paclitaxel may present a potential strategy in treatment of paclitaxel-resistant tumors.

The functional contribution of the unconventional kinesins to cell division and other cellular processes is mechanistically linked with their activities at a molecular level. Here, we will review the molecular mechanisms and cellular functions of the Kin C and Kin I unconventional kinesins.

Kin C Kinesins are Minus-End Directed Motor Proteins

Kin C kinesins are minus-end directed motor proteins that have been implicated in the organization of bipolar spindles, retrograde transport, and Golgi apparatus positioning (summarized in Table 1). Kin Cs contain ATP-independent MT binding sites outside of the core motor domain (12). The ability of these kinesins to bundle MTs suggests that they possess MT cross-linking activity (12,19). Combining MT cross-linking activity with motile activity would enable these molecules to slide one MT with respect to another. Hence, it was proposed that Kin C kinesins cross-link spindle MTs and move toward the minus ends to promote

Table 1: Diverse functions of Kin C kinesins. Representative members of Kin C subfamily are shown. The first two letters of the motor name refer to the species name: Dm, *Drosophila melanogaster*; Xl, *Xenopus laevus*; Hs, *Homo sapiens*; Sc, *Saccharomyces cerevisiae*; Mm, *Mus musculus*

Kin C kinesins	Subcellular localization	Mutant (deficient) phenotype	Functions
DmNCD	spindles and spindle poles (18)	spindles with splayed poles and chromosome nondisjunction during female meiosis (18)	organizing ends of oocyte spindle MTs into poles; and spindle integrity (18,27,28)
XlCTK2	spindles and spindle poles (19)	inhibition of bipolar spindle assembly in *Xenopus* egg extracts (19)	promoting bipolar spindle assembly in *Xenopus* egg extracts (19)
HsHSET	spindles and spindle poles (20)	splayed spindle poles and loss of spindle bipolarity in murine oocytes (20)	establishing spindle poles during meiosis (20)
ScKAR3	spindles and spindle pole bodies (39,42)	failure in nuclear fusion during mating (35); aberrant MT arrays and prophase arrest during meiosis (75); short mitotic spindles and increased number and length of cytoplasmic MTs (35,39)	cross-bridging MTs between fusing nuclei to draw them together during mating (35); nuclear and spindle positioning (76); and spindle integrity (39,76)
MmKIFC2	neural cell bodies, dendrites, and axons (77)	Homozygous KifC2 mouse mutants were viable and reproduced normally (78)	retrograde transport (77)
MmKIFC3	perinuclear regions in the adrenocortical cells (79); apical plasma membrane in epithelial cells (80)	fragmentation of the Golgi apparatus under the cholesterol-depleted condition (79)	Golgi positioning and integration (79); apical transport in epithelial cells (80)

focused association of the MT minus ends at the spindle poles (18,27,28). The minus-end directed activity of Kin C kinesins appears to act antagonistically to the plus-end directed activity of BimC kinesins (Kin N type) (20,28–30). Kin C kinesins produce forces which pull spindle poles together, while BimC kinesins produce forces which separate spindle poles. Deficiency in BimC activity results in centrosome separation defects and failure of bipolar spindle formation, whereas removal of Kin C activity in BimC mutants rescues these defects (20,29,30). Thus, opposing motors generate counteracting forces to establish and maintain bipolar spindle structure [reviewed in (31)]. The contribution of Kin C kinesin activity to the establishment of spindle poles is most essential during meiosis or in the absence of centrosomes (18,27,28). Kin C function is thought to be supplemented to a greater degree by centrosomes and also the minus-end directed motor, dynein, in somatic cells (20,28).

Interestingly, ScKar3 stands out from the Kin C subfamily because of its ability to destabilize MTs *in vitro* specifically from minus ends (32). MT destabilizing activity has not yet been reported for any other Kin C kinesin tested *in vitro* (33,34). As expected, a truncated ScKar3 protein [lacking N-terminal nonmotor MT binding domain (35), 1–276 residues] fused to GST tag exhibited minus-end directed motility *in vitro* (32). However, while observing minus-end directed motility of GST-ScKar3, Endow et al. noted that MT lengths were reducing, giving the appearance that minus ends of MTs was moving faster than plus ends (32). This suggested that ScKar3 might be directly destabilizing MTs, preferably from the minus ends. The MTs used in this assay were weakly stabilized by paclitaxel (1 paclitaxel molecule per 5 tubulin dimers). Increasing the paclitaxel concentration inhibited the ScKar3-mediated MT minus-end destabilization (32). It was suggested that ScKar3 causes MT minus-end instability by binding between two adjacent protofilaments, which results in weakening MT protofilament lateral connections at the MT minus ends (36). The inhibition of ScKar3-mediated MT destabilization by paclitaxel is consistent with this idea, since paclitaxel stabilizes MTs by strengthening lateral interactions between MT protofilaments (37). Comparison of the crystal structure of the ScKar3 motor domain with those of both conventional Kin N kinesin and also the Kin C kinesin, DmNCD, revealed that ScKar3 has a significantly shorter L11 loop within the core motor domain (36). The L11 loop is thought to bind in the groove between MT protofilaments (38). The shorter L11 loop may force the Kar3 motor to bind deeper into the groove, triggering the lateral separation of protofilaments at the MT ends and thus initiating an MT catastrophe event (36).

The microtubule destabilizing activity of ScKar3 kinesin has also been documented *in vivo*. Mutations of ScKar3 resulted in both increased number and length of cytoplasmic MTs in budding yeast (39). Experiments *in vivo* implicate only

one other member of the Kin C subfamily, the fission yeast SpKlp2 kinesin, as an MT destabilizer (40). Further analysis of MT destabilizing activity of ScKar3 and SpKlp2 could provide important information regarding the molecular basis of this activity. Combining motility and MT depolymerizing activity may be unique to these two yeast Kin C motors. This could be one mechanism by which yeast make do with fewer kinesins than other eukaryotic cells.

While conventional Kin N kinesins and the well-characterized minus-end directed motor, DmNCD (Kin C), operate as homodimers, ScKar3 functions as a monomeric motor *in vivo* (41,42). The monomeric ScKar3 motor domain has recently been shown to associate as a heterodimer with one of two nonmotor polypeptides (Cik1 or Vik1) through corresponding coiled-coil domains. The two ScKar3 heterodimers have different cellular localizations and possibly functions. The ScKar3/Cik1 heterodimer localizes along cytoplasmic MTs during mating and along spindle MTs during mitosis, where it acts as an MT cross-linking and sliding motor (41,42). In contrast, the ScKar3/Vik1 heterodimer localizes to the mitotic spindle poles, where it organizes MT ends into spindle poles and may also destabilize cytoplasmic MTs (39,42).

These data suggest several important questions: Do any other Kin C kinesins form single motor heterodimers? How are the activities of ScKar3 heterodimeric complexes regulated? Is the MT destabilization activity of ScKar3 unique among Kin C kinesins? An *in vitro* analysis of MT motile, cross-linking and destabilizing activities of ScKar3/Vik1 and ScKar3/Cik1 heterodimers would help to elucidate the molecular mechanism of these activities.

Kin I Kinesins are MT Depolymerases

Despite the presence of the conserved core motor domain, Kin Is do not generate movement but function as MT depolymerases that disassemble MTs in an ATP-dependent fashion *in vitro* or *in vivo* (4,5). Kin Is have a unique ability to target primarily MT ends, while Kin N and Kin C kinesins have a higher affinity for the MT lattice. Likewise, while the MT lattice is known to maximally stimulate the ATPase activity of Kin N and Kin C kinesins, Kin Is have a substantial MT-end stimulated ATPase activity. Non-polymeric tubulin dimers and MT lattice also stimulate the Kin I's ATPase but to a much lesser extent (4). Kin Is efficiently depolymerize both paclitaxel and GMP-CPP stabilized MTs *in vitro* (4,5,24). Kin Is accumulate predominantly at both ends of MTs in the presence of AMP-PNP (a nonhydrolyzable ATP analogue) *in vitro*. Electron microscopic analysis of MT ends after incubation with Kin I kinesins revealed curled protofilaments (5,43). Furthermore, Niederstrasser et al. demonstrated that Kin Is are capable of depolymerizing zinc-induced tubulin polymers, characterized by an antiparallel MT protofilament arrangement unlike the parallel arrangement of protofilaments in cellular MTs (44). These data indicate that, unlike the proposed model for Kar3, Kin Is do not bind two adjacent protofilaments to force them apart to induce depolymerization. Instead, Kin Is induce protofilament curling by acting on a single MT protofilament. Three-dimensional EM reconstruction of a *Plasmodium* Kin I, pKinI, bound to single protofilament curls showed that the core motor domain binds both α and β tubulin subunits (43). It is thought that the binding of Kin Is either directly induces or stabilizes a conformational change in a GTP-tubulin dimer at the MT ends that reflects the GDP-tubulin state of depolymerizing microtubules without stimulating GTP hydrolysis on tubulin subunits (4,5). The stabilization of the curved GDP-like conformation of the terminal GTP-tubulin dimer results in destabilization of the lateral interactions between tubulin subunits in the MT lattice and loss of tubulin dimers from MT ends (45). The C-terminus of β-tubulin is required for the tubulin conformational change induced by Kin I kinesin binding (43,44).

Kinetic analysis suggests that CgMCAK, a hamster Kin I, is a processive MT depolymerase. One MCAK molecule is capable of removing approximately 20 tubulin dimers from the end of MT protofilament before it dissociates (4). Another important kinetic feature of CgMCAK-mediated MT depolymerization is the exceptionally rapid targeting of CgMCAK to MT ends: the on-rate of CgMCAK to MT ends exceeds by 100 times the rate at which tubulin dimers bind to MT ends during polymerization. These data led Hunter et al. to suggest that CgMCAK targets MT ends by diffusion along the MT lattice (4). MT-end targeting through one-dimensional diffusion along the MT protofilament is much faster than targeting through three-dimensional diffusion and is compatible with the on-rate for CgMCAK to MT ends.

The conserved core motor domain of Kin I kinesins is capable of stabilizing the curved protofilaments of depolymerizing microtubules (43). This is a key step in the mechanism of Kin I-induced MT depolymerization. However, under physiological conditions the core motor of CgMCAK (I253-S583) is unable to depolymerize MTs. The addition of the N-terminal neck domain (A182-R252) to the CgMCAK core motor domain restores MT depolymerizing activity to the level of the full-length CgMCAK both *in vivo* and *in vitro* (24,46). Hence, neck plus motor domain (A182-S583) constitutes the minimal MT depolymerase with MT depolymerizing activity similar to the full-length CgMCAK. The positively charged neck domain of CgMCAK may mediate diffusional motility through weak electrostatic interactions with the negatively charged MT lattice (46). These electrostatic interactions between the neck and the negatively charged tubulin C-terminus may also mediate processivity of CgMCAK-induced MT depolymerization. Thus, it is the catalytic processivity conferred by the neck domain that makes CgMCAK an active depolymerizer under physiological conditions.

Baculovirus-expressed Kin Is form homodimers (47–49). However, this dimerization is not essential for Kin I-mediated depolymerization activity since the minimal MT depolymerase, the neck plus motor, is a monomer (24). Kin Is lack an extended α-helical coiled-coil domain, which serves as a dimerization site for Kin N and Kin C kinesins. Only a small C-terminal domain of CgMCAK, ~40 C-terminal residues (A611-I648), is predicted to form a coiled-coil by the PairCoil program (50) and the prediction (< 50% probability coiled-coil) is relatively weak. Both the N-and C-terminal domains were shown to be necessary for CgMCAK kinetochore localization (13,48).

In contrast to the well-documented MT depolymerization activity of Kin I kinesins, Noda et al. reported that MmKIF2, a member of Kin I subfamily, generated plus-end directed motility (47). However, Desai et al. showed that XlKIF2 (which shares 80% identity with full-length MmKIF2 and 95% identity with the neck plus motor region of MmKIF2) is not able to move MTs but depolymerizes MTs similarly to the other Kin Is (5). Likewise, CgMCAK has not shown directed MT gliding motility in standard motility assays [our unpublished data,(4)]. The MmKif2 fraction, which was used for motility experiments by Noda et al. (47), was purified from Sf9 cells by incubating Sf9 cytoplasmic lysates with MTs in the absence of ATP and eluting MT-bound proteins with addition ATP – a process that could also extract endogenous kinesins from Sf9 cells. Thus, the possible contamination by endogenous plus-end directed kinesins cannot be excluded in the MmKIF2 motility assay by Noda et al. (47). By analogy to XlKIF2, we predict that MmKIF2 is an MT depolymerase.

The Kin I subfamily includes both MCAK-like and KIF2-like kinesin subclusters. The consensus protein sequences corresponding to either MCAK or KIF2 subclusters are highly similar but contain some differences, mostly in the N- and C-terminal tail domains (see online supplementary material for a protein sequence alignment of the Kin I subfamily kinesins). HsMCAK (accession #AAC27660) and HsKIF2 (accession #CAA69621) share 50% identity and 70% similarity within the full-length sequences and 70% identity and 90% similarity within the neck plus motor regions. In mammals, both MCAKs and KIF2s are expressed in the variety of tissues: hemopoietic cells, liver, kidney, spleen, lung, and brain tissues (22,47,49,51,52). MmKIF2 and its splice variant, MmKIF2β, are expressed at higher levels in developing brain and down-regulated in differentiated neurons and adult brain tissues (49,53). The expression of MmMCAK was detected in proliferating mouse myoblasts but was undetectable in differentiated myotubes as well as adult mouse skeletal muscles (54). Similarly, HsMCAK was found to decline to undetectable levels when proliferating monoblastoid cells were differentiated into monocytes (52). These data suggest that both mammalian KIF2s and MCAKs might be present at higher levels in proliferating tissues and at lower levels in differentiated tissues. In addition to the tissues above, mammalian MCAKs were also found to be expressed in: thymus, small intestine, colon, pancreas, ovary, testis, placenta, and mammary tissues as well as in tumor cell lines (22,23,52). HsMCAK (KNSL6) expression in colon cancer tissues and testis is at least 30–40 times the level detected in other tissues, which indicates a possible role of this kinesin in tumorgenesis and spermatogenesis (22). Testis-specific MCAK isoforms have been identified in humans and rats (55,56). Expression of the rat MCAK testis-specific isoform, KRP2, is restricted to a meiotically active region of the seminiferous epithelia in testis (56). While further experiments are needed to determine whether the testis-specific MCAK is present only in meiotic cells, the data above suggest that Kin Is may have important meiotic function(s) in addition to their role in mitosis.

It is unclear why cells require two highly similar depolymerizing kinesins: MCAKs and KIF2s. So far, both MCAK-like and KIF2-like proteins have been found in humans, rats, mice and frogs. MCAK is seen at kinetochores, centrosomes and midbodies in addition to a soluble pool present in nucleoplasm and cytoplasm. KIF2s appear not to localize to either kinetochores or centrosomes but are present in the cytoplasm (53,57). It is possible that KIF2 might primarily influence the dynamics of cytoplasmic MT ends, while MCAK influences both cytoplasmic MT ends and those that are embedded in centrosomes and kinetochores. MCAK and KIF2 tissue expression profiles largely overlap, but KIF2s are expressed at a higher level in developing brain tissues, where they are enriched in growth cones (49,57), while MCAKs are up-regulated in testis and proliferative cancer cells (22). It is not known whether MCAKs and KIF2s undergo cell-cycle specific regulation so that one is more active during mitosis while another is active during interphase.

Kin I Kinesins Regulate MT Dynamics Throughout the Cell Cycle

Kin Is play a major role in regulating MT dynamics *in vivo* [summarized in Table 2; reviewed in (58)]. Overexpression of CgMCAK in mammalian cells resulted in depolymerization of cytoplasmic and spindle MTs (24,48). *Xenopus* egg extracts depleted of XKCM1, a *Xenopus* Kin I, showed abnormally long MTs and 4-fold reduction in MT catastrophe frequency (59). In addition, a recent study demonstrated that physiological MT dynamics can be reconstituted by combination of purified MTs, XKCM1 and a MT-end stabilizing protein, XMAP215 (60). Maney et al. found that CgMCAK influences MT dynamics at mitotic kinetochores (48). CgMCAK localizes to the kinetochores in early prophase and remains there throughout mitosis. Depletion of CgMCAK from kinetochores either by antisense RNA or overexpression of a dominate-negative motorless mutant resulted in a lagging chromosome phenotype, which is likely to be the result of a deficiency in MT depolymerization activity at the lagging kinetochores during

Table 2: Diverse functions of Kin I kinesins. Representative members of Kin I subfamily are shown. The first two letters of the motor name refer to the species name: Cg, *Cricetulus griseus*; Xl, *Xenopus laevus*; Rn, *Rattus norvegicus*; Ce, *Caenorhabditis elegans*; Cf, *Cylindrotheca fusiformis*

Kin I kinesins	Subcellular localization	Mutant (deficient) phenotype	Functions
CgMCAK	spindle poles, kinetochores and mid-bodies (24,48)	lagging chromosomes during anaphase A in CHO cells (24,48)	regulation of MT dynamics throughout the cell cycle and depolymerization of kinetochore MTs during anaphase A in CHO cells(24,48)
XlKCM1	spindle poles and kinetochores (59)	abnormally long spindle MTs and metaphase chromosome misalignment in *Xenopus* egg extracts (59,61)	regulation of MT dynamics throughout the cell cycle and promoting metaphase chromosome alignment in *Xenopus* egg extracts (59,61,81)
CeMCAK	spindle poles and kinetochores (82)	loss of the spindle midzone during anaphase B in *C. elegans* embryos (83)	spindle midzone maintenance during anaphase B (83)
CfDSK1	spindles and spindle midzone (84)	inhibition of spindle elongation during anaphase B in the diatom *C. fusiformis* (84)	promoting spindle elongation during anaphase B (84)
RnKIF2	enriched in PC12 neurite growth cones and on nonsynaptic vesicle subtype(57)	retraction of NGF-induced PC12 neurites (57)	promoting growth cone extension (57)

anaphase (48). Displacement of XKCM1 from kinetochores by a dominant-negative mutant caused metaphase chromosome misalignment in the *Xenopus* egg extracts (61). In addition to kinetochore localization, CgMCAK also localizes to centrosomes and mid-bodies in cells (48). This localization pattern suggests that MCAK could also modulate MT dynamics at these locations as well. CgMCAK's centrosomal localization throughout the cell cycle suggests that it might be a candidate for a MT flux motor.

The importance of dynamic microtubules for proper spindle functioning is well established [reviewed in (31)]. However, the regulation of microtubule dynamics is likely to be essential for other motile processes such as growth cone extension. Exploration of the cytoplasm by dynamic microtubules followed by selective stabilization is an essential component of the motility mechanism of advancing growth cones [reviewed in (62)]. Drugs that inhibit MT dynamics have been shown to reduce neurite extension (63). Kin I kinesins would be hypothesized to increase microtubule dynamics in growing neurites. In agreement with this hypothesis, RnKIF2 appears to be important for PC12 neurite extension induced by NGF treatment (57). NGF significantly up-regulates the expression of RnKIF2 in PC12 cells where RnKIF2 becomes enriched in growth cones of NGF-induced neurites. Moreover, RnKIF2 antisense oligonucleotides caused neurite retractions in NGF-treated PC12 cells (57). Interestingly, another MT destabilizing stathmin-like protein is also up-regulated in PC12 cells treated with NGF (64). Similarly to the RnKIF2 study, inhibition of stathmin expression by antisense oligonucleotides blocked the NGF-induced neurite outgrowth in PC12 cells (65). These data suggest that proteins that influence microtubule dynamics such as KIF2 and stathmin are important for neurite extension.

Kin I and Kip 3 Kinesins Constitute Closely Related but Different Subfamilies

The *Schizosaccharomyces pombe* SpKlp5/6 kinesins were recently found to have similar properties to the Kin I subfamily kinesins (66–69). However, differences in primary sequence structure, activity and function have prompted researchers to give them their own closely related but distinct subfamily: the Kip 3 subfamily (70,71). SpKlp5/6 were found to localize to kinetochores and also have some features in common with CENP-E, a plus-end directed kinesin (66). Depletion of the Kip 3 subfamily kinesins from yeast cells showed MT-depolymerization deficient phenotypes (67–69,71,72). Kip 3 kinesins have N-terminally located motor and C-terminally located neck domains. The Kip 3 related kinesin from *Drosophila*, DmKlp67A, was shown to move MTs in the plus-end direction in an *in vitro* motility assay (73). Mutations in the same kinesin, DmKlp67A, were reported to produce abnormally elongated spindles, a phenotype which is consistent with the loss of MT destabilization activity (74). Therefore, it is possible that members of the Kip 3 subfamily of kinesins are capable of both motile and depolymerizing activities, as is Kar3. The weak structural and sequence correspondence between the Kin I and Kip 3 kinesin subfamilies suggests that the mechanism of MT destabilization by Kip 3 kinesins may be different from that of Kin Is. Detailed

analysis of the MT destabilizing activities of Kip 3 kinesins *in vitro* are required to elucidate the molecular mechanism of Kip 3-mediated MT depolymerization.

Conclusions

While significant progress has been made recently in elucidating Kin C and Kin I kinesin mechanism and functions in cells, many important questions remain to be answered: What are the structural differences between kinesins that translocate along MTs and kinesins that depolymerize them? What are the differences and similarities between molecular mechanisms of MT depolymerizing activities of Kar3, Kin I and Kip 3 kinesins? What are the functional differences between MCAK-like and KIF2-like kinesins? How are Kin Is regulated in cells? The answers to these questions will help us understand how the unconventional kinesins were specialized during evolution for their fundamental cellular roles.

Acknowledgments

We thank Jeremy Cooper, Marla Feinstein, Ayana Moore, Kathleen Rankin and Mike Wagenbach for valuable comments on the manuscript. L. Wordeman is supported by a National Institutes of Health grant (GM53654A) and a Department of Defense grant (DAMD17-01-1-0450).

Online supplemental material shows a protein sequence alignment of the Kin I subfamily kinesins.

References

1. Kull FJ, Sablin EP, Lau R, Fletterick RJ, Vale RD. Crystal structure of the kinesin motor domain reveals a structural similarity to myosin. Nature 1996;380:550–555.
2. Sablin EP, Kull FJ, Cooke R, Vale RD, Fletterick RJ. Crystal structure of the motor domain of the kinesin-related motor ncd. Nature 1996;380:555–559.
3. Vale RD, Reese TS, Sheetz MP. Identification of a novel force-generating protein, kinesin, involved in microtubule-based motility. Cell 1985;42: 39–50.
4. Hunter AW, Caplow M, Coy DL, Hancock WO, Diez S, Wordeman L, Howard J. The kinesin-related protein MCAK is a microtubule depolymerase that forms an ATP-hydrolyzing complex at microtubule ends. Mol Cell 2003;11:445–457.
5. Desai A, Verma S, Mitchison TJ, Walczak CE. Kin I kinesins are microtubule-destabilizing enzymes. Cell 1999;96:69–78.
6. Higuchi H, Endow SA. Directionality and processivity of molecular motors. Curr Opin Cell Biol 2002;14:50–57.
7. Endow SA. Determinants of molecular motor directionality. Nat Cell Biol 1999;1:E163–E167.
8. Vale RD, Fletterick RJ. The design plan of kinesin motors. Annu Rev Cell Dev Biol 1997;13:745–777.
9. Vale RD, Milligan RA. The way things move. looking under the hood of molecular motor proteins. Science 2000;288:88–95.
10. Kamal A, Goldstein LS. Principles of cargo attachment to cytoplasmic motor proteins. Curr Opin Cell Biol 2002;14:63–68.
11. Hackney DD, Stock MF. Kinesin's IAK tail domain inhibits initial microtubule-stimulated ADP release. Nat Cell Biol 2000;2:257–260.
12. Karabay A, Walker RA. Identification of microtubule binding sites in the Ncd tail domain. Biochemistry 1999;38:1838–1849.
13. Wordeman L, Wagenbach M, Maney T. Mutations in the ATP-binding domain affect the subcellular distribution of mitotic centromere-associated kinesin (MCAK). Cell Biol Int 1999;23:275–286.
14. Schief WR, Howard J. Conformational changes during kinesin motility. Curr Opin Cell Biol 2001;13:19–28.
15. Endow SA, Barker DS. Processive and nonprocessive models of kinesin movement. Annu Rev Physiol 2003;65:161–175.
16. Goldstein LS, Philp AV. The road less traveled. emerging principles of kinesin motor utilization. Annu Rev Cell Dev Biol 1999;15:141–183.
17. Mandelkow E, Mandelkow EM. Kinesin motors and disease. Trends Cell Biol 2002;12:585–591.
18. Hatsumi M, Endow SA. Mutants of the microtubule motor protein, nonclaret disjunctional, affect spindle structure and chromosome movement in meiosis and mitosis. J Cell Sci 1992;101:547–559.
19. Walczak CE, Verma S, Mitchison TJ. XCTK2: a kinesin-related protein that promotes mitotic spindle assembly in *Xenopus laevis* egg extracts. J Cell Biol 1997;136:859–870.
20. Mountain V, Simerly C, Howard L, Ando A, Schatten G, Compton DA. The kinesin-related protein, HSET, opposes the activity of Eg5 and cross-links microtubules in the mammalian mitotic spindle. J Cell Biol 1999;147:351–366.
21. Hassold T, Hunt P. To err (meiotically) is human: the genesis of human aneuploidy. Nat Rev Genet 2001;2:280–291.
22. Scanlan MJ, Welt S, Gordon CM, Chen YT, Gure AO, Stockert E, Jungbluth AA, Ritter G, Jager D, Jager E, Knuth A, Old LJ. Cancer-related serological recognition of human colon cancer: identification of potential diagnostic and immunotherapeutic targets. Cancer Res 2002;62:4041–4047.
23. Perou CM, Jeffrey SS, van de Rijn M, Rees CA, Eisen MB, Ross DT, Pergamenschikov A, Williams CF, Zhu SX, Lee JC, Lashkari D, Shalon D, Brown PO, Botstein D. Distinctive gene expression patterns in human mammary epithelial cells and breast cancers. Proc Natl Acad Sci USA 1999;96:9212–9217.
24. Maney T, Wagenbach M, Wordeman L. Molecular dissection of the microtubule depolymerizing activity of mitotic centromere-associated kinesin. J Biol Chem 2001;276:34753–34758.
25. Nishio K, Nakamura T, Koh Y, Kanzawa F, Tamura T, Saijo N. Oncoprotein 18 overexpression increases the sensitivity to vindesine in the human lung carcinoma cells. Cancer 2001;91:1494–1499.
26. Rowinsky EK. The development and clinical utility of the taxane class of antimicrotubule chemotherapy agents. Annu Rev Med 1997;48:353–374.
27. Matthies HJ, McDonald HB, Goldstein LS, Theurkauf WE. Anastral meiotic spindle morphogenesis: role of the non-claret disjunctional kinesin-like protein. J Cell Biol 1996;134:455–464.
28. Sharp DJ, Brown HM, Kwon M, Rogers GC, Holland G, Scholey JM. Functional coordination of three mitotic motors in *Drosophila* embryos. Mol Biol Cell 2000;11:241–253.
29. Pidoux AL, LeDizet M, Cande WZ. Fission yeast pkl1 is a kinesin-related protein involved in mitotic spindle function. Mol Biol Cell 1996;7:1639–1655.
30. Saunders WS, Hoyt MA. Kinesin-related proteins required for structural integrity of the mitotic spindle. Cell 1992;70:451–458.
31. Wittmann T, Hyman A, Desai A. The spindle: a dynamic assembly of microtubules and motors. Nat Cell Biol 2001;3:E28–E34.
32. Endow SA, Kang SJ, Satterwhite LL, Rose MD, Skeen VP, Salmon ED. Yeast Kar3 is a minus-end microtubule motor protein that destabilizes microtubules preferentially at the minus ends. EMBO J 1994;13: 2708–2713.
33. Prigozhina NL, Walker RA, Oakley CE, Oakley BR. Gamma-tubulin and the C-terminal motor domain kinesin-like protein, KLPA, function in the establishment of spindle bipolarity in *Aspergillus nidulans*. Mol Biol Cell 2001;12:3161–3174.

34. Walker RA, Salmon ED, Endow SA. The *Drosophila* claret segregation protein is a minus-end directed motor molecule. Nature 1990;347: 780–782.
35. Meluh PB, Rose MD. KAR3, a kinesin-related gene required for yeast nuclear fusion. Cell 1990;60:1029–1041.
36. Gulick AM, Song H, Endow SA, Rayment I. X-ray crystal structure of the yeast Kar3 motor domain complexed with Mg.ADP 2.3 A resolution. Biochemistry 1998;37:1769– 76.
37. Keskin O, Durell SR, Bahar I, Jernigan RL, Covell DG. Relating molecular flexibility to function: a case study of tubulin. Biophys J 2002;83: 663–680.
38. Sosa H, Dias DP, Hoenger A, Whittaker M, Wilson-Kubalek E, Sablin E, Fletterick RJ, Vale RD, Milligan RA. A model for the microtubule-Ncd motor protein complex obtained by cryo-electron microscopy and image analysis. Cell 1997;90:217–224.
39. Saunders W, Hornack D, Lengyel V, Deng C. The *Saccharomyces cerevisiae* kinesin-related motor Kar3p acts at preanaphase spindle poles to limit the number and length of cytoplasmic microtubules. J Cell Biol 1997;137:417–431.
40. Troxell CL, Sweezy MA, West RR, Reed KD, Carson BD, Pidoux AL, Cande WZ, McIntosh JR. pkl1 (+) and klp2 (+): two kinesins of the Kar3 subfamily in fission yeast perform different functions in both mitosis and meiosis. Mol Biol Cell 2001;12:3476–3488.
41. Barrett JG, Manning BD, Snyder M. The Kar3p kinesin-related protein forms a novel heterodimeric structure with its associated protein Cik1p. Mol Biol Cell 2000;11:2373–2385.
42. Manning BD, Barrett JG, Wallace JA, Granok H, Snyder M. Differential regulation of the Kar3p kinesin-related protein by two associated proteins, Cik1p and Vik1p. J Cell Biol 1999;144:1219–1233.
43. Moores CAYuM, Guo J, Beraud C, Sakowicz R, Milligan RA. A mechanism for microtubule depolymerization by Kinl kinesins. Mol Cell 2002;9:903–909.
44. Niederstrasser H, Salehi-Had H, Gan EC, Walczak C, Nogales E. XKCM1 acts on a single protofilament and requires the C terminus of tubulin. J Mol Biol 2002;316:817–828.
45. Muller-Reichert T, Chretien D, Severin F, Hyman AA. Structural changes at microtubule ends accompanying GTP hydrolysis: information from a slowly hydrolyzable analogue of GTP, guanylyl (alpha,beta) methylenediphosphonate. Proc Natl Acad Sci USA 1998;95: 3661–3666.
46. Ovechkina Y, Wagenbach M, Wordeman L. K-loop insertion restores microtubule depolymerizing activity of a 'neckless' MCAK mutant. J Cell Biol 2002;159:557–562.
47. Noda Y, Sato-Yoshitake R, Kondo S, Nangaku M, Hirokawa N. KIF2 is a new microtubule-based anterograde motor that transports membranous organelles distinct from those carried by kinesin heavy chain or KIF3A/B. J Cell Biol 1995;129:157–167.
48. Maney T, Hunter AW, Wagenbach M, Wordeman L. Mitotic centromere-associated kinesin is important for anaphase chromosome segregation. J Cell Biol 1998;142:787–801.
49. Aizawa H, Sekine Y, Takemura R, Zhang Z, Nangaku M, Hirokawa N. Kinesin family in murine central nervous system. J Cell Biol 1992;119:1287–1296.
50. Berger B, Wilson DB, Wolf E, Tonchev T, Milla M, Kim PS. Predicting coiled coils by use of pairwise residue correlations. Proc Natl Acad Sci USA 1995;92:8259–8263.
51. Debernardi S, Fontanella E, De Gregorio L, Pierotti MA, Delia D. Identification of a novel human kinesin-related gene (HK2) by the cDNA differential display technique. Genomics 1997;42:67–73.
52. Kim IG, June DY, Sohn U, Kim YH. Cloning and expression of human mitotic centromere-associated kinesin gene. Biochim Biophys Acta 1997;1359:181–186.
53. Santama N, Krijnse-Locker J, Griffiths G, Noda Y, Hirokawa N, Dotti CG. KIF2beta, a new kinesin superfamily protein in non-neuronal cells, is associated with lysosomes and may be implicated in their centrifugal translocation. EMBO J 1998;17:5855–5867.
54. Ginkel LM, Wordeman L. Expression and partial characterization of kinesin-related proteins in differentiating and adult skeletal muscle. Mol Biol Cell 2000;11:4143–4158.
55. Cheng LJ, Zhou ZM, Li JM, Zhu H, Zhou YD, Wang LR, Lin M, Sha JH. Expression of a novel HsMCAK mRNA splice variant, tsMCAK gene, in human testis. Life Sci 2002;71:2741–2757.
56. Sperry AO, Zhao LP. Kinesin-related proteins in the mammalian testes: candidate motors for meiosis and morphogenesis. Mol Biol Cell 1996;7:289–305.
57. Morfini G, Quiroga S, Rosa A, Kosik K, Caceres A. Suppression of KIF2 in PC12 cells alters the distribution of a growth cone nonsynaptic membrane receptor and inhibits neurite extension. J Cell Biol 1997;138:657–669.
58. Cassimeris L. Accessory protein regulation of microtubule dynamics throughout the cell cycle. Curr Opin Cell Biol 1999;11:134–141.
59. Walczak CE, Mitchison TJ, Desai A. XKCM1: a Xenopus kinesin-related protein that regulates microtubule dynamics during mitotic spindle assembly. Cell 1996;84:37–47.
60. Kinoshita K, Arnal I, Desai A, Drechsel DN, Hyman AA. Reconstitution of physiological microtubule dynamics using purified components. Science 2001;294:1340–1343.
61. Walczak CE, Gan EC, Desai A, Mitchison TJ, Kline-Smith SL. The microtubule-destabilizing kinesin XKCM1 is required for chromosome positioning during spindle assembly. Curr Biol 2002;12:1885–1889.
62. Suter DM, Forscher P. Substrate-cytoskeletal coupling as a mechanism for the regulation of growth cone motility and guidance. J Neurobiol 2000;44:97–113.
63. Tanaka E, Ho T, Kirschner MW. The role of microtubule dynamics in growth cone motility and axonal growth. J Cell Biol 1995;128:139–155.
64. Stein R, Orit S, Anderson DJ. The induction of a neural-specific gene, SCG10, by nerve growth factor in PC12 cells is transcriptional, protein synthesis dependent, and glucocorticoid inhibitable. Dev Biol 1988;127:316–325.
65. Di Paolo G, Pellier V, Catsicas M, Antonsson B, Catsicas S, Grenningloh G. The phosphoprotein stathmin is essential for nerve growth factor-stimulated differentiation. J Cell Biol 1996;133:1383–1390.
66. West RR, Malmstrom T, McIntosh JR. Kinesins klp5 (+) and klp6 (+) are required for normal chromosome movement in mitosis. J Cell Sci 2002;115:931–940.
67. West RR, Malmstrom T, Troxell CL, McIntosh JR. Two related kinesins, klp5+ and klp6+, foster microtubule disassembly and are required for meiosis in fission yeast. Mol Biol Cell 2001;12:3919–3932.
68. Garcia MA, Koonrugsa N, Toda T. Spindle-kinetochore attachment requires the combined action of Kin I-like Klp5/6 and Alp14/Dis1-MAPs in fission yeast. EMBO J 2002;21:6015–6024.
69. Garcia MA, Koonrugsa N, Toda T. Two kinesin-like Kin I family proteins in fission yeast regulate the establishment of metaphase and the onset of anaphase A. Curr Biol 2002;12:610–621.
70. Lawrence CJ, Malmberg RL, Muszynski MG, Dawe RK. Maximum likelihood methods reveal conservation of function among closely related kinesin families. J Mol Evol 2002;54:42–53.
71. Severin F, Habermann B, Huffaker T, Hyman T. Stu2 promotes mitotic spindle elongation in anaphase. J Cell Biol 2001;153 (2):435–442.
72. Straight AF, Sedat JW, Murray AW. Time-lapse microscopy reveals unique roles for kinesins during anaphase in budding yeast. J Cell Biol 1998;143:687–694.
73. Pereira AJ, Dalby B, Stewart RJ, Doxsey SJ, Goldstein LS. Mitochondrial association of a plus end-directed microtubule motor expressed during mitosis in *Drosophila*. J Cell Biol 1997;136:1081–1090.
74. Gandhi R, Bonaccorsi S, Wentworth DB, Gatti M, Pereira AJ. The KLP67A astral microtubule motor is required for proper spindle assembly during mitosis and male meiosis. Mol Biol Cell 2002;13 S(1815):322a.

75. Bascom-Slack CA, Dawson DS. The yeast motor protein, Kar3p, is essential for meiosis I. J Cell Biol 1997;139:459–467.
76. Cottingham FR, Gheber L, Miller DL, Hoyt MA. Novel roles for *Saccharomyces cerevisiae* mitotic spindle motors. J Cell Biol 1999;147: 335–350.
77. Hanlon DW, Yang Z, Goldstein LS. Characterization of KIFC2, a neuronal kinesin superfamily member in mouse. Neuron 1997;18: 439–451.
78. Yang Z, Roberts EA, Goldstein LS. Functional analysis of mouse C-terminal kinesin motor KifC2. Mol Cell Biol 2001;21:2463–2466.
79. Xu Y, Takeda S, Nakata T, Noda Y, Tanaka Y, Hirokawa N. Role of KIFC3 motor protein in Golgi positioning and integration. J Cell Biol 2002;158:293–303.
80. Noda Y, Okada Y, Saito N, Setou M, Xu Y, Zhang Z, Hirokawa N. KIFC3, a microtubule minus end-directed motor for the apical transport of annexin XIIIb-associated Triton-insoluble membranes. J Cell Biol 2001;155:77–88.
81. Kline-Smith SL, Walczak CE. The microtubule-destabilizing kinesin XKCM1 regulates microtubule dynamic instability in cells. Mol Biol Cell 2002;13:2718–2731.
82. Oegema K, Desai A, Rybina S, Kirkham M, Hyman AA. Functional analysis of kinetochore assembly in *Caenorhabditis elegans*. J Cell Biol 2001;153:1209–1226.
83. Grill SW, Gonczy P, Stelzer EH, Hyman AA. Polarity controls forces governing asymmetric spindle positioning in the *Caenorhabditis elegans* embryo. Nature 2001;409:630–633.
84. Wein H, Foss M, Brady B, Cande WZ. DSK1, a novel kinesin-related protein from the diatom *Cylindrotheca fusiformis* that is involved in anaphase spindle elongation. J Cell Biol 1996;133:595–604.

Developmental Cell, Vol. 6, 253–268, February, 2004, Copyright ©2004 by Cell Press

Aurora B Regulates MCAK at the Mitotic Centromere

Paul D. Andrews,[1,*] Yulia Ovechkina,[3] Nick Morrice,[2] Michael Wagenbach,[3] Karen Duncan,[1] Linda Wordeman,[3] and Jason R. Swedlow[1]
[1]Division of Gene Regulation and Expression
[2]MRC Protein Phosphorylation Unit
Wellcome Trust Biocentre
University of Dundee
Dow Street
Dundee DD1 5EH
United Kingdom
[3]Department of Physiology and Biophysics
University of Washington School of Medicine
1959 N.E. Pacific Street
Seattle, Washington 98195

Summary

Chromosome orientation and alignment within the mitotic spindle requires the Aurora B protein kinase and the mitotic centromere-associated kinesin (MCAK). Here, we report the regulation of MCAK by Aurora B. Aurora B inhibited MCAK's microtubule depolymerizing activity in vitro, and phospho-mimic (S/E) mutants of MCAK inhibited depolymerization in vivo. Expression of either MCAK (S/E) or MCAK (S/A) mutants increased the frequency of syntelic microtubule-kinetochore attachments and mono-oriented chromosomes. MCAK phosphorylation also regulates MCAK localization: the MCAK (S/E) mutant frequently localized to the inner centromere while the (S/A) mutant concentrated at kinetochores. We also detected two different binding sites for MCAK using FRAP analysis of the different MCAK mutants. Moreover, disruption of Aurora B function by expression of a kinase-dead mutant or RNAi prevented centromeric targeting of MCAK. These results link Aurora B activity to MCAK function, with Aurora B regulating MCAK's activity and its localization at the centromere and kinetochore.

Introduction

Accurate chromosome segregation requires the attachment of microtubules from opposing spindle poles to kinetochores formed on sister chromatids. The Aurora B kinase and its associated binding partners INCENP and survivin play a critical role in this process. Mutations in the yeast Aurora B homolog, Ipl1, generate stably mono-oriented chromosomes that fail to resolve (He et al., 2001; Tanaka et al., 2002). In *Drosophila* and *C. elegans*, Aurora B RNAi cells possess aberrant prometaphase-like mitotic spindles that fail to align their chromosomes on the metaphase plate and subsequently develop significant aneuploidy due to chromosome nondisjunction (Adams et al., 2001; Giet and Glover, 2001; Kaitna et al., 2000). Introduction of dominant-negative mutants of Aurora B or small molecule inhibitors into mammalian cells causes similar phenotypes (Ditchfield et al., 2003; Hauf et al., 2003; Murata-Hori and Wang, 2002). Together, these results suggest that the Aurora B complex plays a critical role in establishing bipolar chromosome attachment and that this function is highly conserved.

Aurora B, INCENP, and survivin all behave as chromosome passenger proteins, localizing between sister centromeres in the inner centromere from late G2 through to metaphase (Andrews et al., 2003; Carmena and Earnshaw, 2003). As chromosome segregation initiates, the complex leaves the inner centromere and concentrates on central spindle microtubules where it functions in cytokinesis. In yeast, the Aurora B/Ipl1p complex phosphorylates a number of inner and outer kinetochore proteins (Biggins et al., 1999; Cheeseman et al., 2002; Westermann et al., 2003). Aurora B also phosphorylates the centromere-specific histone H3 variant CENP-A (Zeitlin et al., 2001), as well as histone H3 localized throughout the chromosome (Hsu et al., 2000; Murnion et al., 2001). The concentration of the Aurora B complex at the inner centromere and its interaction with kinetochore components suggest that it may regulate the interactions between kinetochores and microtubule ends.

One possible substrate for the Aurora B complex is the Kinl kinesin MCAK. Unlike conventional kinesins, Kin I family members have their motor domains in the central portion of the molecule and use the hydrolysis of ATP to depolymerize microtubule ends (Desai et al., 1999; Hunter et al., 2003; Hunter and Wordeman, 2000). In *Xenopus* egg extracts, depletion of the *Xenopus* homolog XKCM1 decreases the catastrophe rate of microtubule ends and causes chromosomes to misalign on the mitotic spindle (Walczak et al., 2002, 1996). In mammalian cells, depletion of MCAK by antisense DNA inhibits anaphase A (Maney et al., 1998). MCAK/XKCM1 is localized to centromeres in early prophase and remains there throughout mitosis (Walczak et al., 1996; Wordeman et al., 1999).

A critical unanswered question is how MCAK/XKCM1 activity is regulated. As a regulator of microtubule end catastrophe, soluble MCAK/XKCM1 can affect the average length of spindle microtubules in *Xenopus* egg extracts (Walczak et al., 1996). However, MCAK/XKCM1 also functions during chromosome alignment (Walczak et al., 2002), suggesting that the activity of kinetochore-bound MCAK/XKCM1 might be regulated as chromosomes undergo saltatory motion in prometaphase and metaphase (Rieder and Salmon, 1994; Skibbens et al., 1993). We have examined the functional interactions between Aurora B and MCAK and found that the mitotic Aurora B complex is a critical regulator of MCAK function in vitro and in vivo.

Results

Spatial Distribution of Aurora B and MCAK in the Cell Cycle

Independent immunofluorescence studies have previously shown Aurora B and MCAK localized to centromeres of mammalian chromosomes from late prophase

*Correspondence: p.d.andrews@dundee.ac.uk

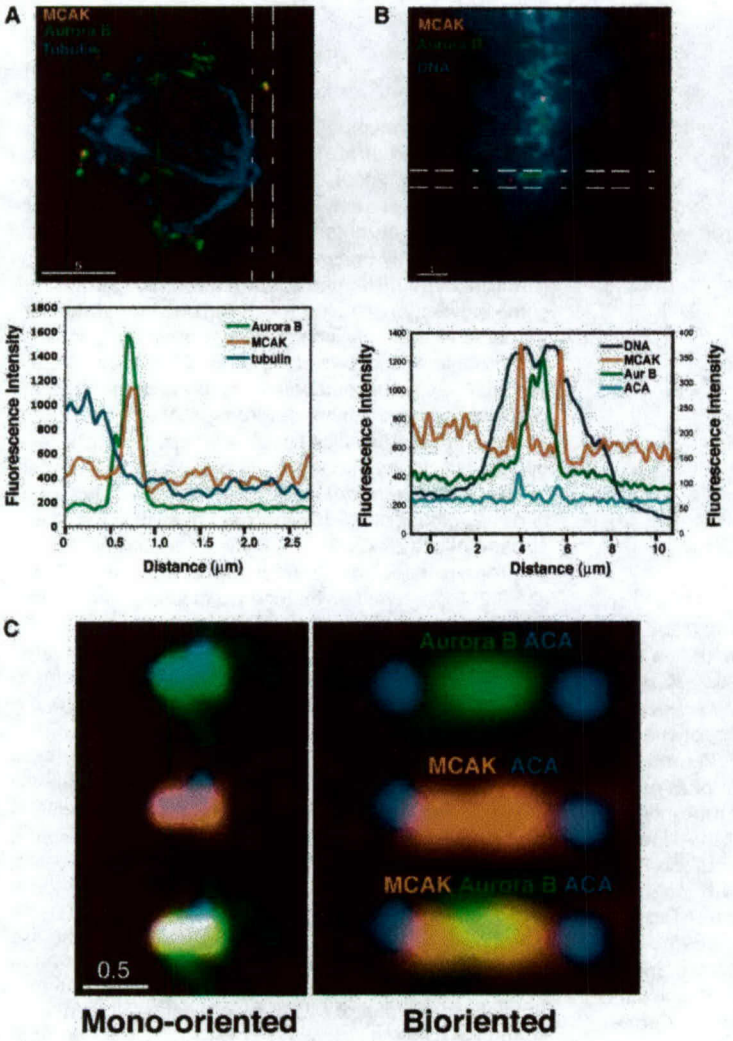

Figure 1. Aurora B and MCAK Localization in HeLa Cells

Prometaphase and metaphase HeLa cells stained for human MCAK, Aurora B, tubulin, and DNA. All images are single optical sections.

(A) In prometaphase mono-oriented chromosomes, Aurora B and MCAK show complete colocalization.

(B) In metaphase bioriented chromosomes under tension, MCAK and Aurora B are largely distinct, with MCAK close to ACA staining and Aurora B concentrated in the inner centromere. Line profiles (lower panel) show the spatial separation of the signals (lower panels).

(C) Differences in MCAK and Aurora B localization in prometaphase at high resolution. Images are from two different chromosomes from the same prometaphase cell. In mono-oriented chromosomes (left), sister centromeres are closely spaced, while in bioriented chromosomes (right) they are separated.

of the cell cycle to until the metaphase-anaphase transition (Andrews et al., 2003; Carmena and Earnshaw, 2003; Maney et al., 1998; Walczak et al., 1996). During anaphase and telophase, MCAK remains centromere-associated while Aurora B relocalizes to the spindle midzone. We re-examined the localization of Aurora B and MCAK during prometaphase and metaphase in mitotic HeLa cells. During prometaphase, Aurora B and MCAK colocalized in unattached or mono-oriented (i.e., attached to kinetochore fibers from one pole only) chromosomes (Figure 1A). The ACA antigen also localized with Aurora B and MCAK. By contrast, in chromosomes aligned along the metaphase plate, MCAK concentrated at two sites that partially colocalized with ACA staining but that were distinct from the strictly inner-centromeric localization of Aurora B (Figure 1B). MCAK and Aurora B also colocalized in cells treated with nocodozole and taxol (data not shown). To further define when the relative localization of Aurora B and MCAK changed, we examined prometaphase at high resolution (Figure 1C) and found two distinct types of Aurora B/MCAK colocalization. In centromeres under tension (as judged by the distance between ACA staining sites [Waters et al., 1996]), Aurora B and MCAK were only partially colocalized, whereas centromeres not under tension still showed significant colocalization. The localization of MCAK is therefore dynamic, initially colocalizing with Aurora B following assembly of mitotic chromosomes, but then becoming distinct from Aurora B as tension develops across sister kinetochores.

Aurora B Phosphorylates MCAK In Vitro

We next tested whether the Aurora B complex might phosphorylate MCAK in vitro. Recombinant full-length MCAK was incubated in the presence of ^{32}P-γ-ATP and mitotic Aurora B complex isolated from *Xenopus* chromosomes. We chose this strategy because we have failed to produce recombinant *Xenopus* Aurora B complex with the same activity and properties as the mitotic complex (Murnion et al., 2001; data not shown). Figure 2A shows that MCAK was phosphorylated in vitro by mitotic Aurora B complex. Kinase activity was not detected toward MCAK using interphase Aurora B or control IgG beads. To confirm this result, we incubated a

mixture of recombinant forms of Ipl1p and Sli15p, the budding yeast orthologs of Aurora B and INCENP, respectively, with recombinant MCAK. Mixing Sli15p and Ipl1p stimulates Ipl1p kinase activity (Kang et al., 2001). This mixture produced high levels of MCAK phosphorylation (Figure 2B). These results suggested MCAK is phosphorylated by Aurora B in vitro.

We next identified the sites in MCAK phosphorylated by the mitotic Aurora B complex. We incubated recombinant MCAK with interphase or mitotic Aurora B complex and ^{32}P-γ-ATP, or with recombinant yeast Ipl1p/Sli15p complex, and then analyzed ^{32}P-labeled tryptic peptides from MCAK by reverse-phase HPLC. The phosphopeptides generated with mitotic Aurora B were similar to those obtained with recombinant yeast Ipl1p/Sli15p (Supplemental Figure S1 [http://www.developmentalcell.com/cgi/content/full/6/2/253/DC1). As expected from MCAK's primary amino acid sequence, trypsin generated a significant number of very short MCAK peptides, many of which were radiolabeled. To simplify the profile, we used Lys-C for proteolytic cleavage. Analysis of Lys-C-digested MCAK phosphorylated by Aurora B produced three distinct peaks of radioactivity (Figure 2C), which were then characterized using a combination of Edman sequencing and MALDI-TOF (Figure 2D). Peak 1 corresponded to phosphorylation at Ser92, while Peak 2 corresponded to phosphorylation at Ser186. Peak 3 corresponded to phosphorylation at Ser106, Ser108, and Ser112, but MALDI-TOF analysis showed that all peptides in this fraction were monophosphorylated, indicating that only one of the three serines was phosphorylated in any single peptide. Comparison of the integrated peak heights from the HPLC analysis indicates that Peak 3 sites are less efficiently phosphorylated than Peak 1 and Peak 2 sites.

The Aurora B sites in MCAK conform to the consensus sequence derived from known Aurora B substrates (Figure 2E; Cheeseman et al., 2002). All three sites in MCAK are preceded by one or more K or R residues and often, but not always, are followed by a hydrophobic residue. Alignment of the N termini of MCAK and its orthologs with the closely related Kif2 kinesins reveals that the Aurora B phosphorylation sites identified here are highly conserved in all Kinl kinesins (Figure 2F). The Kif2 kinesins regulate cytoplasmic microtubules during neurite extension (Homma et al., 2003). The conservation of sites in the Kif2's with those identified in MCAK suggests a conserved mechanism of regulating the activity of these enzymes.

Aurora B Phosphorylates MCAK In Vivo

In order to test the phosphorylation of MCAK in cells, we used a synthetic phosphopeptide derived from phosphorylation Site 1 in human MCAK (Figure 2E) to generate novel anti-MCAK antibodies. We used repeated rounds of affinity purification to isolate antibodies that specifically recognized MCAK phosphorylated on Ser92 (α-P-Ser92) and antibodies that recognized both dephosphorylated and phosphorylated MCAK (α-Ser92). Figure 3A shows that α-P-Ser92 only recognizes the phosphopeptide antigen, but not the desphosphopeptide in an ELISA assay, while α-Ser92 recognizes both forms of the peptide. In addition, α-P-Ser92 only recognized MCAK on immunoblots after phosphorylation with recombinant Ipli1p/Sli15p (Figure 3B). By contrast, control antibodies recognized both nonphosphorylated and phosphorylated forms of MCAK on the same blot. Together, these results suggest that the α-P-Ser92 antibody recognizes phosphorylated MCAK.

To examine the phosphorylation state of MCAK in cells, we performed immunoblots of lysates from control and nocodozole-arrested HeLa cells with α-P-Ser92. Figure 3C shows a series of slow-migrating forms of MCAK enriched in nocodozole-arrested lysates. α-P-Ser92 only recognized the slowest migrating bands, and showed highest reactivity after nocodozole arrest, suggesting that MCAK phosphorylation is highest in mitotic cells. Localization of MCAK phosphorylation by immunofluorescence revealed that α-P-Ser92 recognized centromeric MCAK in prometaphase cells (Figure 3D). We also noted abundant α-P-Ser92 signal throughout the cell, suggesting that cytoplasmic MCAK may also be phosphorylated at Ser92. Both the centromeric and cytoplasmic signals were blocked with the P-Ser92 peptide but not the Ser92 peptide, confirming the specificity of α-P-Ser92 in cells.

While we noted an increase in mitotic MCAK phosphorylation both on immunoblots and by immunofluorescence (Figures 3C and 3D), closer examination revealed differences in MCAK phosphorylation across the centromere. In prometaphase and metaphase cells transfected with wtMCAK-GFP, we detected similar amounts of MCAK at sister centromeres and kinetochores, yet significant differences in the level of α-P-Ser92 staining (Figure 3E). These differences in antibody staining may occur due to changes in antigen accessibility or because of differences in MCAK phosphorylation. We have never observed systematic asymmetry in MCAK staining between sister centromeres or kinetochores with other MCAK antibodies (see Figure 1), suggesting that the phosphorylation state of MCAK at centromeres and kinetochores at Ser92 may be dynamic.

We next asked whether in vivo phosphorylation of MCAK at Ser92 was dependent on Aurora B. HeLa cells were treated with nocodozole and transfected with a siRNA targeted to human Aurora B (see Experimental Procedures). Aurora B depletion was assayed both biochemically (Supplemental Figure S2) and by immunofluorescence in single cells. In cells depleted of Aurora B, the phospho-specific α-P-Ser92 antibody reactivity at the centromere was largely abolished (Figure 3F). By contrast, reactivity of the α-Ser92 antibody, which recognizes both phosphorylated and nonphosphorylated MCAK (Figure 3B), remained unchanged. This suggests that phosphorylation of centromeric MCAK at Ser92, a major site of MCAK phosphorylation in vitro, also occurs in vivo and is dependent on Aurora B. In addition, after depletion of Aurora B by RNAi, the migration of MCAK on a 2D gel changes from pI $\sim$6.5 to pI $\sim$8.5, consistent with a loss of phosphorylation (Supplemental Figure S2).

Aurora B Phosphorylation Inhibits the Activity of MCAK

We next assayed whether the phosphorylation of MCAK by Aurora B affected MCAK's depolymerization activity in vitro using a microtubule sedimentation assay. In the absence of MCAK, the vast majority of tubulin from

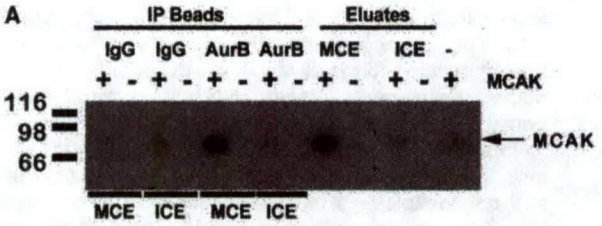

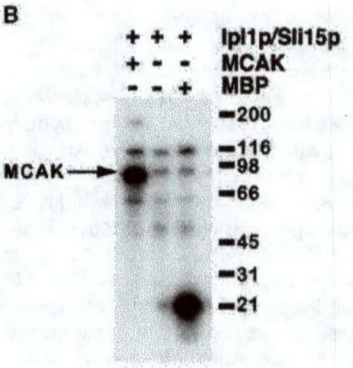

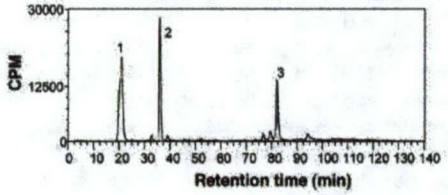

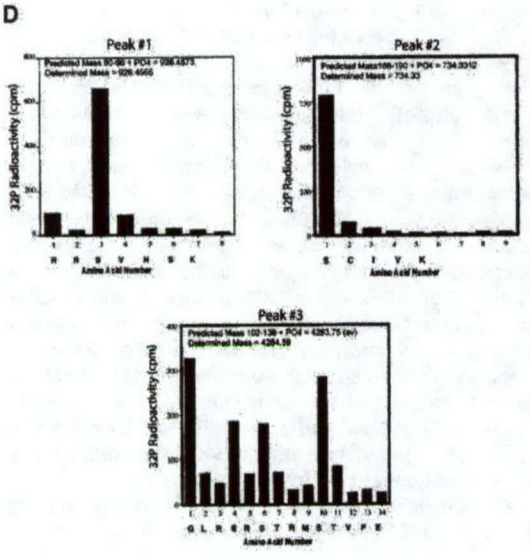

E

```
CgMCAK          87  KQKRRSVNSKI
                101 KEGLRSRSTRM
                181 PARRKSCIVKE

Histone H3       5  QTARKSTGGKA
                 23 KAARKSAPATG

HsCENP-A         2  GPRRRSRKPEA

ScDam1p         20  TEYRLSIGSAP
                257 KLRRKSILHTI
                267 HTIRNSIASGA
                292 PNNRISLGSGA

Spc34p          199 NQRRKTIFVED

Ndc80p          100 SVSRLSINQLG

Ask1p           200 RKRKISLLLQQ
```

F

```
                                  Peak 1                                - Peak3 -
CgMCAK          77 LPLQENVTVPKQKRRSVNSKIPAPKEG--------------LRSRSTRMSTVPEVRIATQENEMEVELPV..
HsMCAK          80 LPLQENVTIQKQKRRSVNSKIPAPKES--------------LRSRSTRMSTVSELRITAQENDMEVELPA..
RnKRP2          26 --TATAGERNHPKAKTQVRQLQNSRS--------------KRRPSKRSTRISTVSEVRIPAQENEMEVELPVS..
XlKCM1          79 MPPQRNVSSQNHKRKTI-SKIPAPKEVAAKNSLLSESGAQSVLRERSTRMTAIHETLPYENEMEAE-STPL..
HsKIF2          52 PASSAKVNKIVKNRRTVASIKNDPPSRDN-----------RVVGSARARPSQFPEQSSSAQQNGSVSDISPV..
MmKIF2          51 -SSSSKVNKIVKNRRTVAAVKNDPPPRDN-----------RVVGSARARPSQLPEQSSSAQQNGSVSDISPV..
MmKIF2b         51 PSSSSKVNKIVKNRRTVAARAVKNDPPPR-----------DNRVVGSARPSQLPEQSSSAQQN----------..
XKIF2           76 PAPTTKVNKIVKNRRTVAPVKNETPAKDN---------RVAAVGSARARPIQPIEQSASRQQNGSVSDISPD..

                                                                  Peak 2
CgMCAK         156 ELPLSMVSEEAEEQVHPTRSTSSAN---------PARRKSCIVKEMEKMKNKREEKRAQ
HsMCAK         159 EIPLRMVSEEMEEQVHSIRGSSSANPV------NSVRRKSCLVKEVEKMKNKREEKKAQ
RnKRP2         105 ELPLLMISEEAEEQAHSTRSTSSANPG------NSVRRKSCIVKEMEKMKNKREEKRAQ
XlKCM1         158 RSRSTKVSIAEEPRLQTRISEIVEESLPSGRNNQGRRKSNIVKEMEKMKNKREEQRAQ
HsKIF2         125 ----------------------------------PSRRKSNCVKEVEKLQEKREKRRLQ
MmKIF2         124 ----------------------------------PSRRKSNCVKEVEKLQEKREKRRLQ
MmKIF2b        106 ----------------------------------ARRKSNCVKEVEKLQEKREKRRLQ
XKIF2          151 ----------------------------------ASRRKSNCVKEVEKLQEKREKRRRLQ
DmKlp10A       180 AAASAGPAAQGVATAATTQGAGG----------ASTRRSHALKEVERLKENREKRRAR
CfDSK           24 ------------------------------MNAANRRKSTSTVGITGRKDATRMKIEQ
```

taxol-stabilized microtubules sediments in the pellet (Figure 4A, "P"; lanes 5–8). MCAK incubated with control beads retained full depolymerization activity (Figure 4A, "S"; lanes 3 and 4). In contrast, the activity of MCAK phosphorylated by the immunopurified Aurora B complex was significantly reduced (Figure 4A, lanes 1 and 2), suggesting that in vitro phosphorylation by Aurora B inhibits the microtubule depolymerizing activity of MCAK. Similarly, a mixture of recombinant Ipl1p and Sli15p (Kang et al., 2001) also reduced MCAK's in vitro microtubule depolymerizing activity (Figure 4B, lanes 1 and 2).

To assess the effect of MCAK phosphorylation in vivo, we transfected HeLa cells with GFP-MCAK constructs bearing mutations in the phosphorylation sites we identified in Figure 2 and then measured the amount of polymerized tubulin present in transfected cells by immunofluorescence (Ovechkina et al., 2002). Transfection of GFP fused to wild-type MCAK (wtMCAK) efficiently depolymerized most of the microtubules in the cell (Figures 4C and 4D). All constructs bearing single S→A or S→E mutations efficiently depolymerized microtubules in this in vivo assay (data not shown). In addition, transfection with either double S→A mutants or the quintuple S92A/S106A/S108A/S112A/S186A MCAK, "AAAAA-MCAK," caused no detectable effect on microtubule depolymerization. In contrast, cells transfected with either double S→E mutations or the quintuple S92E/S106E/S108E/S112E/S186E MCAK, "EEEEE-MCAK," contained significantly more tubulin polymer, suggesting that MCAK proteins bearing these phosphorylation-mimicking mutations are less active than wtMCAK or the various S→A mutants. Together, these in vitro and in vivo results suggest that phosphorylation inhibits MCAK catalytic activity.

Phenotypes and Localization of MCAK Phosphorylation-Site Mutants

We next assessed the effect of introducing MCAK constructs bearing mutations in the Aurora B phosphorylation sites on the mitotic spindle. In Figures 5A–5C, we show four representative examples of each construct. HeLa cells transfected with wtMCAK fused to GFP formed normal mitotic spindles, with apparently bioriented chromosomes and GFP-MCAK localization indistinguishable from the endogenous protein (Figure 5C). Transfection of cells with either AAAAA-MCAK (Figure 5A), or EEEEE-MCAK (Figure 5B), produced aberrant mitotic figures with frequent misoriented chromosomes. In cells expressing AAAAA-MCAK, we observe a significant increase in monopolar chromosomes and chromosomes with apparently syntelic (both kinetochores attached to same pole) or monotelic kinetochore-microtubule attachments (one kinetochore attached to microtubules from one pole). Expression of EEEEE-MCAK caused a high frequency of mitotic figures with poorly aligned chromosomes that were often clustered on the periphery of the mitotic spindle (Figure 5B). Cytological analysis of mitotic progression revealed that EEEEE-MCAK increased the frequency of prometaphase figures, whereas AAAAA-MCAK increased the frequency of metaphase figures (Figure 5D).

Since MCAK localization normally changes from the inner centromere to the inner kinetochore during prometaphase (Figure 1), we determined the localization of the different MCAK mutants. AAAAA-MCAK often localized away from the inner centromere, closer to ACA staining, even in prometaphase figures where MCAK is normally localized to the inner centromere (Figure 5E, see also Figure 1). In contrast, EEEEE-MCAK localized to the inner centromere even in metaphase chromosomes where MCAK normally localizes to the inner kinetochore (Figure 5E). The visual impression gained in Figure 5E is quantified in Figure 5F. We conclude that multiple MCAK binding sites may be present on chromosomes and MCAK's association with these sites depends on its phosphorylation state.

We next used fluorescence recovery after photobleaching (FRAP) of the MCAK mutants to determine if the phosphorylation state of MCAK affects its association with centromeres and kinetochores in living cells. We bleached GFP-MCAK and then examined the recovery of fluorescence, to assay the association of the different MCAK mutants with centromeres and kinetochores. wtMCAK, EEEEE-MCAK, and AAAAA-MCAK all recovered rapidly, although the recovery rate for AAAAA-MCAK was noticeably slower (Figures 6A–6C). We noted that wtMCAK recovers more slowly on aligned chromosomes (Figure 6D, blue bars) than on unaligned chromosomes (Figure 6D, red bars), suggesting a change in the affinity of MCAK for the centromere/kinetochore as chromosomes align. Although we do not have sufficient resolution or fiduciary marks in this live cell experiment to distinguish centromere- and kinetochore-associated populations of MCAK, our localization data

Figure 2. Aurora B Phosphorylation of MCAK In Vitro

(A) Autoradiograph of SDS-PAGE gel of recombinant full-length MCAK phosphorylated in the presence of ^{32}P-ATP using Aurora B immunoprecipitated from *Xenopus* mitotic chromosomal eluate (MCE), Aurora B from *Xenopus* interphase chromosomal eluate (ICE), control immunoprecipitations from MCE and ICE, or crude MCE or ICE alone. As a further control, MCAK alone was incubated in kinase buffer in the presence of ^{32}P-ATP.

(B) Autoradiograph of SDS-PAGE gel of recombinant full-length MCAK phosphorylated in the presence of ^{32}P-ATP using active recombinant Ipl1p/Sli15 complex. Myelin basic protein is included as a control (right lane). Weakly phosphorylated bands present in all lanes are derived from Sli15p.

(C) Recombinant hamster MCAK was phosphorylated with mitotic Aurora B and digested with LysC endoproteinase. Peptides were separated by RP-HPLC and the three radioactive peptides peaks isolated.

(D) Radiolabeled phosphopeptides were identified by MALDI-TOF (see Supplemental Table S1) and the position of the phosphorylated residue(s) determined by solid-phase Edman sequencing, monitoring release of radioactivity at each cycle.

(E) Comparison of MCAK phosphorylation sites with known Aurora B substrates (Cheeseman et al., 2002).

(F) Alignment of conserved Aurora B phosphorylation sites (red), and basic (green) and hydrophobic residues (blue) in Kinl kinesins. The alignment of *Xenopus* XKCM1 with its mammalian orthologs in the region of Site 2 differs from that previously published (Walczak et al., 2002).

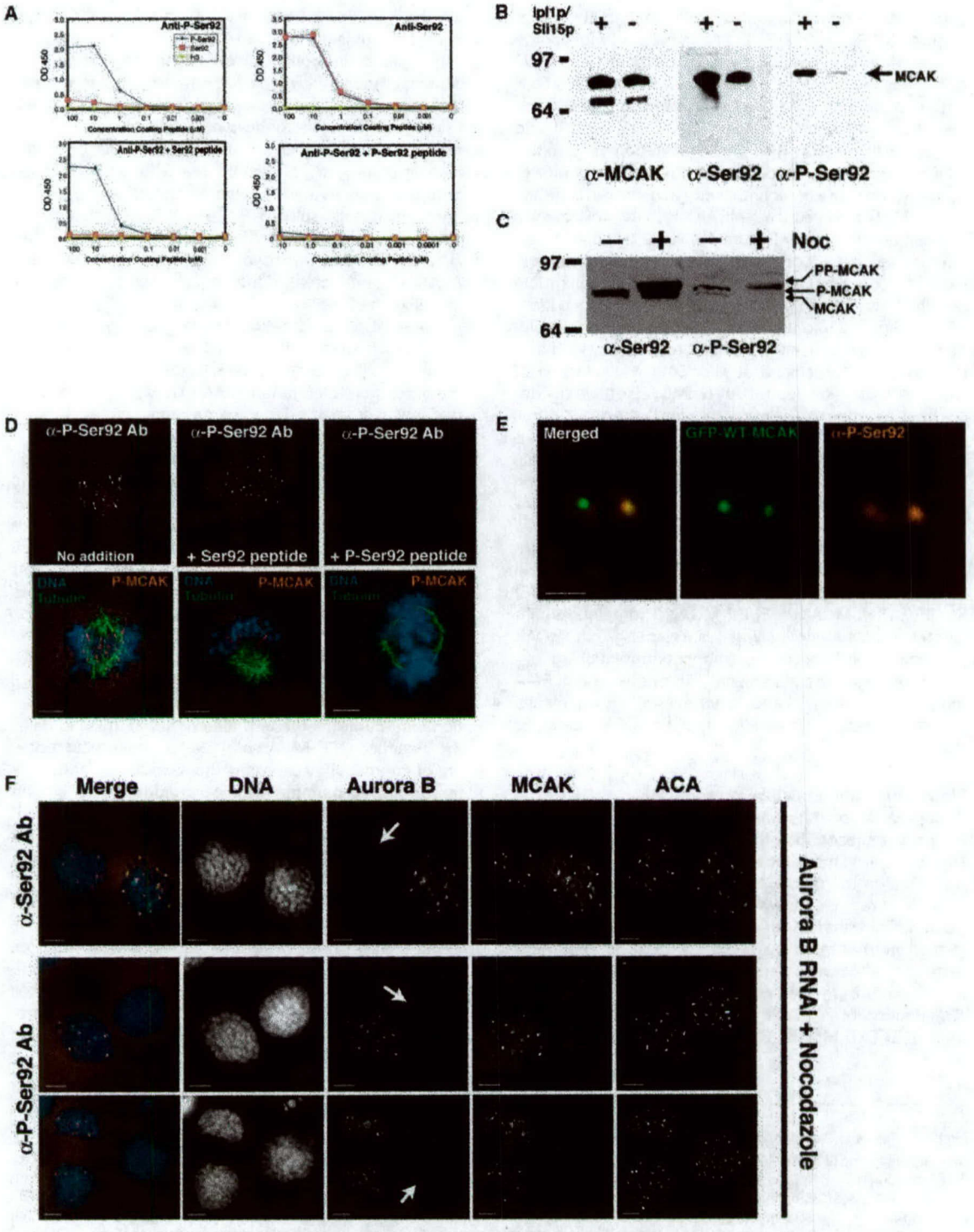

Figure 3. α-Phospho-Ser92 Antibodies Show Aurora B-Dependent MCAK Phosphorylation In Vivo

(A) Specificity tests of affinity-purified α-P-Ser92 and α-Ser92 antibodies. Upper panels, ELISAs with P-Ser92 peptide (blue), Ser92 peptide (pink), Histone H3 Ser10 peptide (yellow). Lower panels, ELISAs after preblocking antibodies.

(B) α-P-Ser92 antibody detects full-length recombinant MCAK only when MCAK has been phosphorylated in vitro with Ipl1p/Sli15p (right-hand panel). Control antibodies are polyclonal sheep α-MCAK Ab and α-Ser92.

(C) α-P-Ser92 antibody recognizes only lower mobility MCAK species in Western blots of whole-cell extracts of asynchronous HeLa cells or HeLa cells arrested with nocodazole for 16 hr. α-Ser92 antibody reacts with all MCAK species on identical blots.

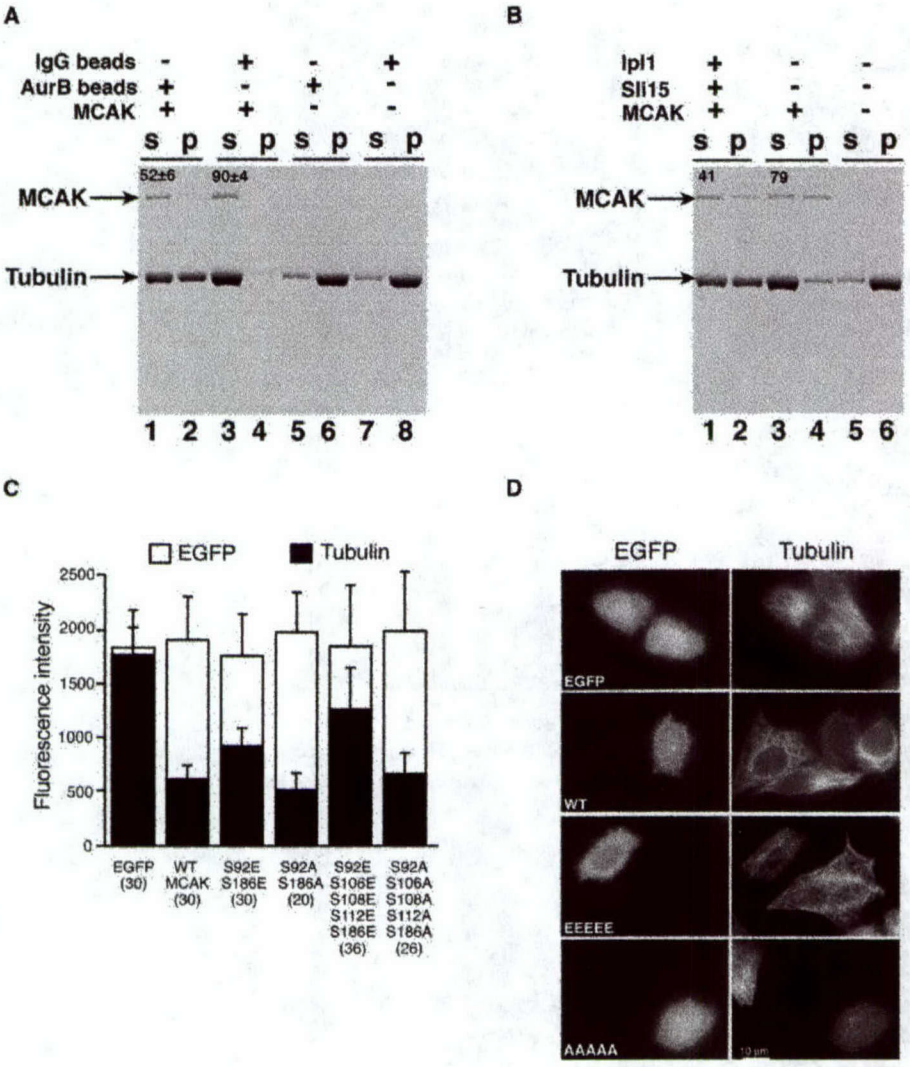

Figure 4. Aurora B-Mediated Phosphorylation Inhibits the Microtubule Depolymerization Activity of MCAK In Vitro and In Vivo

MCAK was incubated with Aurora B complex immunoprecipitated from MCE with α-Aurora B beads or with control beads (A) or with recombinant Ipl1p-Sli15p complex.

(B) Taxol-stabilized microtubules (1500 nM) were added to the phosphorylation reactions containing 24 nM MCAK dimer and 1 mM ATP and incubated for 10 min at RT and then analyzed by sedimentation assay. % tubulin released into the supernatant is shown as mean ± σ (N = 3). In each case, the upper band on the gel is MCAK and the lower band is tubulin.

(C) In vivo analysis of GFP-MCAK and phosphorylation site mutants. CHO cells were transfected with MCAK or MCAK mutants and then fixed and stained for tubulin. Cells were quantified for microtubule loss as described previously (Ovechkina et al., 2002). Total MCAK protein was measured by GFP fluorescence (white bars). Total tubulin polymer was measured by indirect immunofluorescence (black bars).

(D) Images of typical GFP-MCAK-transfected CHO cells used for measurements shown in (C).

(D) α-P-Ser92 antibody recognizes centromeric MCAK in fixed HeLa cells (left). Upper panels are grayscale images of P-Ser92 staining; lower panels are merged images showing DNA (blue), tubulin (green), and P-Ser92 (red). Preblocking with Ser92 peptide had no effect on MCAK reactivity (middle), whereas preblocking with P-Ser92 abolished MCAK reactivity (right).

(E) HeLa cells transfected with wtMCAK-GFP were fixed and stained with α-P-Ser92. P-Ser92 can be detected asymmetrically across sister centromeres/kinetochores. Scale 1 μm.

(F) Aurora B-dependent phosphorylation of MCAK at Ser92. HeLa cells were treated simultaneously with nocodazole (to prevent MCAK delocalization; see text and Figure 7) and Aurora B siRNA (see Experimental Procedures), for 16 hr. Cells were fixed and stained for DAPI (blue), Aurora B (green), MCAK (red; either α-Ser92 or α-P-Ser92), and ACA (not shown on merged image, far right-hand panel in grayscale). Arrows indicate Aurora B-depleted cells. α-P-Ser92 staining is lost in cells depleted of Aurora B while α-Ser92 is not affected. Scale, 5 μm.

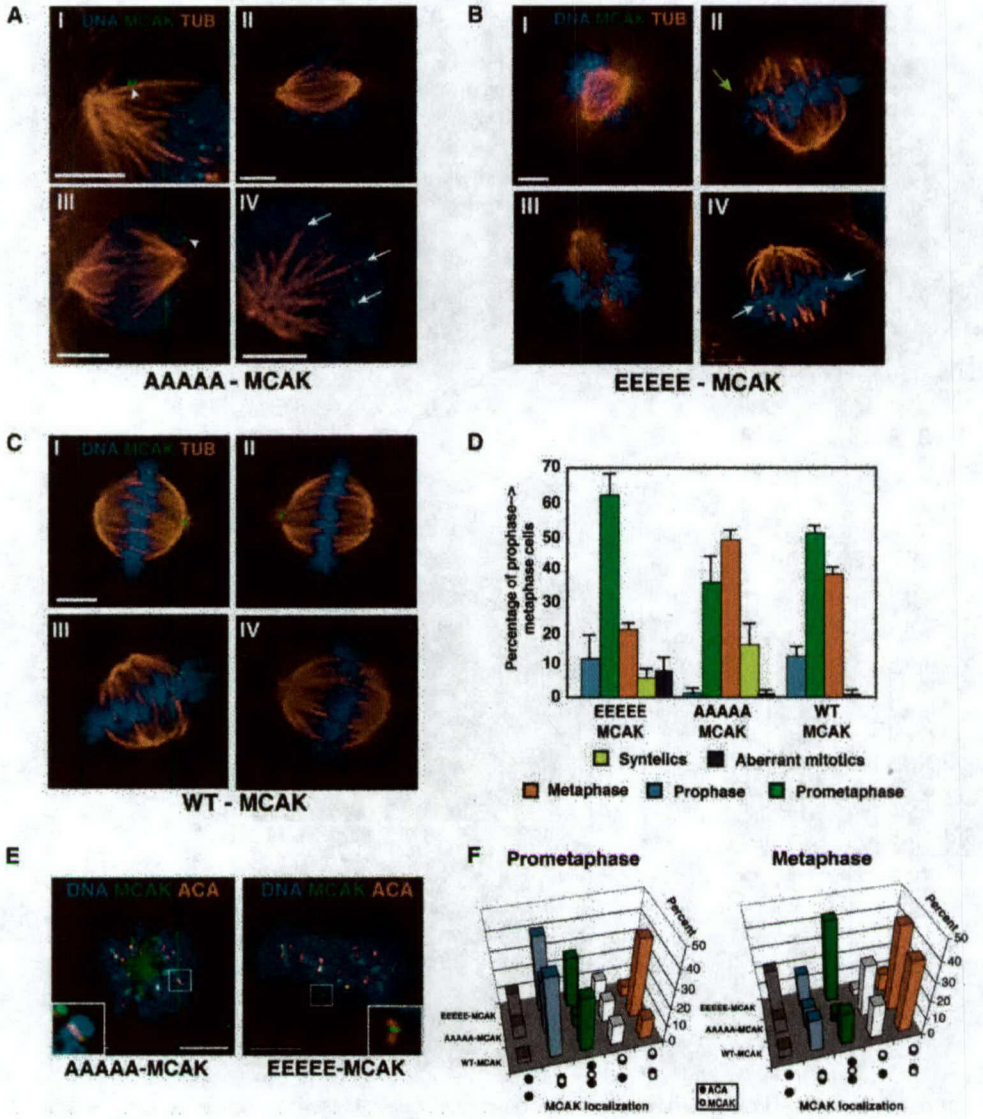

Figure 5. Expression of Phosphorylation-Site Mutants Causes Aberrant Mitotic Phenotypes

HeLa cells transfected with wtMCAK and mutant MCAK plasmids were fixed and stained for tubulin (red) and DNA (blue).

(A) AAAAA-MCAK expression causes accumulation of cells with monopolar chromosomes (arrowheads; panels I–III) and syntelic attachments (arrows; panel IV).

(B) EEEEE-MCAK expression causes aberrant metaphase figures reminiscent of Aurora B or BubR1 RNAi (this study; Ditchfield et al., 2003; Hauf et al., 2003) where chromosomes are clustered around a bipolar spindle (panels I and III) as well as irregularly formed mitotic spindles (panel II; yellow arrow) and syntelic attachments (panel IV; arrows).

(C) wtMCAK expression results in normal metaphase figures.

(D) Analysis of cell cycle position and spindle phenotypes after expression of different forms of MCAK.

(E) Localization of MCAK mutants (green) with respect to ACA staining (red) and DNA (blue). AAAAA-MCAK was found mainly to reside outside the ACA-stained region even in prometaphase (see inset). EEEEE-MCAK mainly is found between ACA-pairs even in metaphase cells (see inset).

(F) Quantitation of MCAK localization using ACA antigen staining as a fiduciary marker. The results shown are the average of two experiments (N = 60 cells). MCAK was categorized as either absent from ACA domains; overlapping with ACA where sister centromeres are not under tension; between separated ACA pairs in sisters under tension; overlapping or distal to separated ACA pairs, but asymmetrically localized; or overlapping with separated ACA pairs, but symmetrically localized. In prometaphase, AAAAA-MCAK is predominantly localized distal or overlapping with separated ACA pairs. In metaphase, EEEEE-MCAK is predominantly localized in between ACA pairs.

(Figure 1) suggest that this difference in MCAK association mirrors a difference in localization. We were unable to find a large number of EEEEE-MCAK transfected cells that successfully entered mitosis, but those we studied showed a less pronounced difference between aligned and unaligned chromosomes (Figure 6D). This result, together with EEEEE-MCAK's preferential localization to the inner centromere in fixed cells (Figure 5E) and

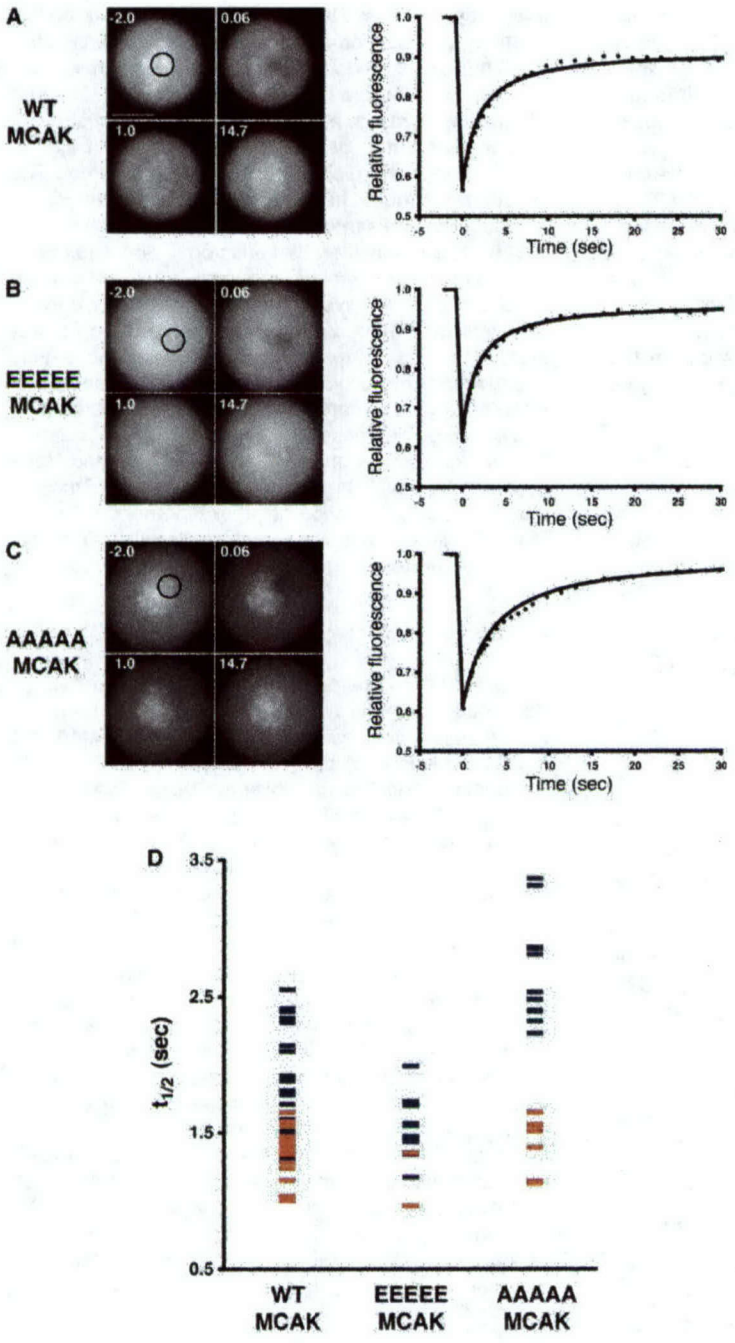

Figure 6. FRAP Analysis of Association of wtMCAK and Phosphorylation-Site Mutants

(A–C) Images before bleaching (−2.0 s), immediately after the photobleach event (0.06 s), during recovery (1.0 s), and later in the time course (14.7 s). Graphs show percent fluorescence recovery versus time for each protein. Dotted lines show the measured data; solid lines show the modeled recovery. (A) wtMCAK. (B) EEEEE-MCAK. (C) AAAAA-MCAK. AAAAA-MCAK displays a longer recovery time than for wild-type or the EEEEE mutant.

(D) Scatter plot of $t_{1/2}$ (horizontal lines) for wtMCAK and mutant MCAKs. Results from aligned centromeres are shown in blue and for unaligned centromeres in red. AAAAA-MCAK recovery $t_{1/2}$s for aligned chromosomes are significantly longer than for wtMCAK or EEEEE-MCAK.

wtMCAK's observed behavior in fixed cells, leads us to speculate that EEEEE-MCAK's faster recovery time is due to its inner-centromeric localization. By contrast, AAAAA-MCAK on aligned chromosomes clearly showed a significantly slower fluorescence recovery rate compared to wtMCAK (Figure 6D). Consistent with AAAAA-MCAK's localization distal to the inner centromere in fixed cells (Figure 5E), our FRAP data suggest the presence of a second MCAK binding site. We therefore postulate the existence of at least two different binding sites for MCAK on chromosomes, whose properties are differentially sensitive to the phosphorylation state of MCAK.

Aurora B Disruption Delocalizes MCAK from Centromeres

Aurora B is required for the localization of dynein, CENP-E, and BubR1 and therefore is a critical regulator of kinetochore function (Ditchfield et al., 2003; Hauf et al., 2003; Murata-Hori et al., 2002). To determine if Aurora

B is required for MCAK localization, we transiently expressed the "kinase-dead" KR mutant of Aurora B, which causes defects in chromosome movement, spindle structure, and dynein/CENP-E localization (Murata-Hori et al., 2002). Cells were transfected with CFP fused to either wt Aurora B or Aurora B (KR) and cotransfected with YFP-MCAK (YFP-FL MCAK) or a construct bearing a deletion of the MCAK motor domain (YFP-ML MCAK; Ovechkina et al., 2002). After transfection with CFP-Aurora B, YFP-FL MCAK localization was indistinguishable from the endogenous protein (Figure 7A). In cells transfected with CFP-Aurora B (KR), YFP-FL MCAK was not concentrated at the inner centromere in either prometaphase or metaphase cells, but was found in the cytoplasm and on the spindle and spindle poles (Figure 7A). A similar effect was observed on endogenous MCAK (data not shown). YFP-ML MCAK was also largely delocalized by CFP-Aurora B (KR) (Figure 7A), but a relatively small population did appear to remain associated with centromeres/kinetochores, the significance of which is currently unclear. These results suggest that Aurora B kinase activity is required for inner centromere targeting of MCAK and that this localization is largely independent of the MCAK motor domain and hence the microtubule depolymerization activity of MCAK.

To confirm our observations with the Aurora B (KR) mutant, we depleted Aurora B by RNAi in HeLa cells and assayed MCAK localization. Figure 7B shows representative prometaphase and metaphase cells from four independent experiments, 12–18 hr posttransfection using Aurora B siRNA or control (scrambled) siRNA duplexes. Aurora B and MCAK levels were quantified in single cells using digital fluorescence imaging (see Experimental Procedures) and in cell lysates by immunoblotting (see Supplemental Figure S2). In Aurora B-depleted cells, we detected no significant change in total cellular MCAK (Figure 7B; also see Supplemental Figure S2). However, after Aurora B depletion, MCAK was no longer concentrated at the inner centromere/kinetochore, but instead was localized throughout the cytoplasm and on the mitotic spindle.

Previous work has shown that the loss of CENP-E and dynein from kinetochores after expression of Aurora B (KR) depends on the presence of microtubules (Murata-Hori et al., 2002). To determine if MCAK's behavior is similar, we added nocodozole to cells after transfection with Aurora B siRNA or Aurora B (KR) cDNA. In cells depleted of Aurora B (Figure 3F) or expressing Aurora B (KR) (data not shown), MCAK still localized to centromeres. We conclude that MCAK's dependence on Aurora B for localization is likely to be similar to other critical kinetochore effectors.

Interfering with Aurora B function causes defects in spindle morphology and chromosome alignment on the metaphase plate (Figure 7C; Andrews et al., 2003; Carmena and Earnshaw, 2003). A chromosome alignment defect was also observed after microinjection of anti-XKCM1 antibodies into mitotic cells (Kline-Smith and Walczak, 2002). To determine if Aurora B RNAi affected microtubule stability within the mitotic spindle, we measured the amount of tubulin polymer at kinetochores by immunofluorescence. Tubulin polymer at kinetochores increased significantly after Aurora B RNAi (Figure 7D), suggesting increased microtubule stability at the kinetochore in the absence of Aurora B and MCAK. By contrast, there was no detectable difference between control RNAi and Aurora B RNAi cells in the total amount of tubulin polymer in mitotic spindles (data not shown). This suggests that delocalized MCAK did not significantly change the global level of tubulin polymer. The proportion of MCAK localized to centromeres in normal mitotic cells represented 33.5 $\pm$ 4.9% of the total cellular MCAK. It seems unlikely that this population, if released into the cytoplasm, would produce a significant change in tubulin polymer levels. Finally, Aurora B RNAi leads to a significant decrease in average centromere-centromere distances compared to control cells, most likely because loss of Aurora B delocalizes MCAK and other factors required for force generation at the kinetochore. The observed decrease in tension after Aurora B depletion is significant, but less than in taxol-treated HeLa cells (see Figure 7E, legend). This partial relief of tension may be due to presence of other kinetochore factors that engage microtubules, or alternatively that residual MCAK generates this result.

Discussion

In this study, we present evidence that the centromeric Kinl kinesin MCAK is a substrate for the Aurora B protein kinase during mitosis. Aurora B phosphorylated five conserved serines in the N terminus of MCAK in vitro. A phospho-specific antibody against one of these sites demonstrated Aurora B-dependent MCAK phosphorylation in vivo. Phosphorylation by Aurora B inhibits MCAK's microtubule depolymerizing activity in vitro, and mutagenesis of MCAK phosphorylation sites inhibits the activity of MCAK in vivo. Aurora B and MCAK colocalize on mitotic centromeres before establishment of bipolar attachment, but become spatially separated when centromeres are under tension at metaphase. The phosphorylation-site mutants concentrate at different locations, either within the inner centromere or at the inner kinetochore, and their expression in cells leads to defects in chromosome biorientation. Disruption of Aurora B function decreases MCAK phosphorylation and leads to a microtubule-dependent loss of MCAK from the inner centromere, increased kinetochore microtubule density, and decreased tension across sister centromeres. These data establish a direct link between Aurora B activity and MCAK function at the centromere and kinetochore.

MCAK Is Phosphorylated In Vitro and In Vivo by Aurora B

Our results demonstrate the phosphorylation of a Kinl kinesin and identify MCAK as a critical downstream effector of the Aurora B kinase. MCAK was phosphorylated by Aurora B at two sites in the N terminus and one in the neck region. These sites are conserved in most Kinl kinesins and represent good consensus Aurora B phosphorylation sites. Using a phospho-specific antibody, we demonstrated that Ser92 is phosphorylated in vivo, in an Aurora B-dependent manner. Interestingly, we detected asymmetry in phospho-specific antibody

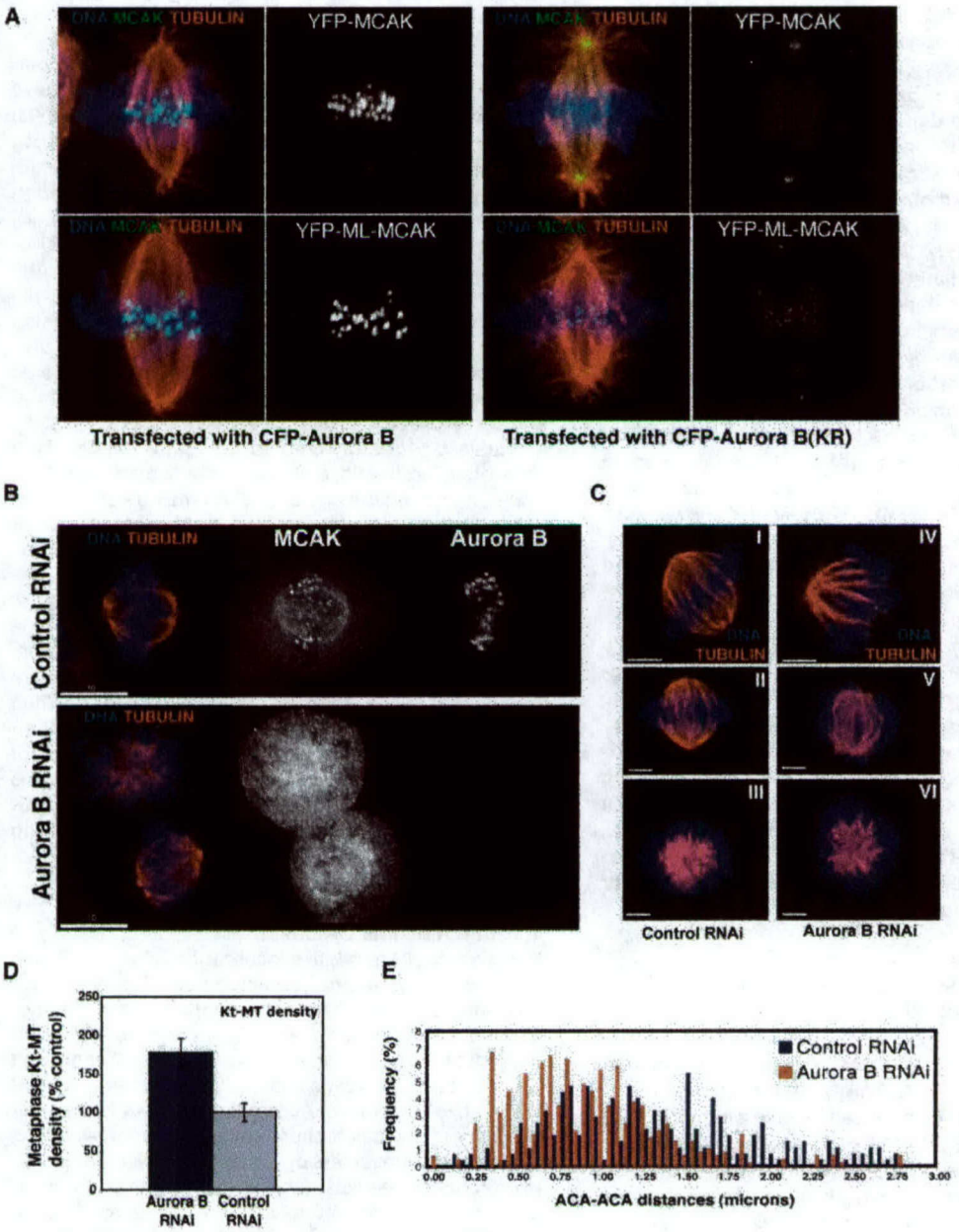

Figure 7. Disruption of Aurora B Function Delocalizes MCAK

(A) Kinase-dead Aurora B (KR) mutant expression results in loss of MCAK from centromeres. CHO cells were transfected with CFP-Aurora B (left) or CFP-Aurora B (KR) (right). Tubulin (red), YFP-MCAK or YFP-motorless (ML) MCAK (green), and DNA (blue). In all panels, CFP-Aurora B has been omitted for clarity. Images are maximum intensity projections of deconvolved 3D data sets.

(B) Aurora B RNAi causes MCAK delocalization from the inner centromere. Tubulin (red), DNA (blue). Top, control RNAi-treated mitotic cell. Bottom, Aurora B RNAi-treated cells. Images are single optical sections of 3D deconvolved data sets acquired under identical conditions and scaled identically.

(C) Spindle structure is aberrant in Aurora B RNAi cells. Aurora B-depleted cells were stained for Aurora B (not shown), tubulin (red), and DNA (blue). Maximum-intensity volume projections were generated from 3D deconvolved data sets. Images show typical spindles for control cells (left panel) or Aurora B RNAi cells (right panel) viewed from two different angles; the lower image is rotated about the x axis by 90°.

(D) Aurora B RNAi increases density of microtubules at kinetochores. Graph shows mean $\pm$ σ of total background-corrected fluorescence in a 9 $\times$ 10 pixel box located adjacent to the kinetochore (N = 30).

(E) Aurora B RNAi causes reduced sister centromere tension. Centromere-centromere distances in metaphase cells measured using ACA-ACA distance (N = 20 cells). Control RNAi, 1.34 $\pm$ 0.60 μm (N = 496); Aurora B RNAi 0.89 $\pm$ 0.45 μm (N = 270). Note that this latter value is significantly higher than that obtained in HeLa cells treated with taxol (Trinkle-Mulcahy et al., 2003), suggesting that tension is reduced, not eliminated.

reactivity across sister centromeres in mitosis, suggesting that phosphorylation of this site could be dynamic.

Phosphorylation at Ser186 occurs in the basic neck region of MCAK, a domain postulated to form a weak electrostatic interaction with the acidic C terminus of tubulin. The neck region may mediate diffusional motility of MCAK on the microtubule lattice (Hunter et al., 2003; Niederstrasser et al., 2002; Ovechkina et al., 2002). Phosphorylation of MCAK by Aurora B might therefore reduce the basic charge in this critical domain and thus disrupt key electrostatic interactions between MCAK and the carboxy-terminal tail of tubulin. Indeed, phosphorylation of MCAK by Aurora B inhibits MCAK microtubule depolymerization activity in vitro, and mimicking phosphorylation with point mutants inhibits depolymerization in vivo. Whether the four other phosphorylation sites we have identified all affect MCAK in the same way is not yet clear. In our in vivo microtubule depolymerization assay (Figure 4), EEEEE-MCAK showed less activity that any of the double or single S→E mutants. However, it seems likely that further biophysical and functional analyses will reveal separable functions of the individual sites.

The conservation of these Ser residues in other Kinl's suggests a general mechanism for regulating the function of these enzymes. Indeed, a Ser or Thr residue is often C-terminal to the K-loop in several Kif1's, so phosphorylation may be a common mechanism for modulating K-loop function. Recently, the targeting of the chromosome-associated kinesin Kid has also been found to depend on phosphorylation (Ohsugi et al., 2003), suggesting that cell cycle-dependent posttranslational modification may be a common mechanism for targeting microtubule motors.

MCAK Phosphorylation Determines Localization to Centromeres and Kinetochores

Using two different approaches, we have identified distinct binding sites for MCAK at centromeres and kinetochores. In fixed cells, AAAAA-MCAK often localizes to a domain near the ACA antigen even in prometaphase, whereas the EEEEE-MCAK often remains in the inner centromere between ACA sites, even in metaphase cells (Figure 5E), suggesting that MCAK's phosphorylation status governs its preference for centromeres or kinetochores. Consistent with this, in living cells, we find that the FRAP recovery times of wtMCAK differ on aligned and unaligned chromosomes, which may mirror the localization differences between prometaphase and metaphase observed in fixed cells (Figure 1). AAAAA-MCAK recovers much more slowly than wtMCAK, suggesting a second binding site with different binding properties. In contrast, EEEEE-MCAK always recovers quickly, possibly reflecting this mutant's preference for occupancy of an inner centromere binding site, as observed in fixed cells (Figure 5E). Thus, the association of MCAK with different binding sites may depend on MCAK phosphorylation. ICIS, a recently discovered MCAK targeting factor, is likely to be the receptor for at least one of these sites (Ohi et al., 2003).

MCAK Phosphorylation in Biorientation and Mitosis

Aurora B is required for the establishment of bipolar orientation and may be involved in resolving syntelic attachments on mitotic chromosomes (Hauf et al., 2003; Tanaka et al., 2002). As disruption of MCAK function by microinjection of anti-MCAK antibodies (Kline-Smith and Walczak, 2002) or transfection of MCAK phosphorylation site mutants into mitotic cells (Figures 5A–5D) causes similar chromosome alignment defects as interfering with Aurora B function, it seems possible that Aurora B promotes biorientation and possibly syntelic resolution through MCAK. A major unresolved question is how Aurora B, MCAK, and ICIS collaborate to promote correct chromosome biorientation. Incorrect (e.g., syntelic) attachments may be selectively destabilized through MCAK's microtubule depolymerase activity. Alternatively, oscillatory chromosome movements driven through microtubule end depolymerization may help promote correct orientation. MCAK may be only one of many Aurora B targets involved in this process. Other studies have shown that disruption of Aurora B by RNAi, or by expression of Aurora B (KR), leads to loss of kinetochore CENP-E and cytoplasmic dynein (Murata-Hori et al., 2002), and to loss of kinetochore BubR1 and Mad2 (Ditchfield et al., 2003). Delocalization of MCAK from centromeres using an N-terminal dominant-negative fragment of MCAK does not affect CENP-E localization (Walczak et al., 2002), implying Aurora B separately directs the centromere targeting, and thus the function of MCAK and CENP-E. It therefore appears that Aurora B directs two separable pathways, one involving MCAK localization and function, and a second involving CENP-E and BubR1.

Protein Phosphorylation and Chromosome Dynamics

It is clear that the relative localization of Aurora B and MCAK changes during prometaphase (Figure 1). Furthermore, once attached to the mitotic spindle, chromosomes display dynamic oscillatory movement, indicating rapid changes in microtubule dynamics (Rieder and Salmon, 1994; Skibbens et al., 1993). We speculate that the relative positions of Aurora B and MCAK in the inner centromere and kinetochore could permit the switching of directional movement by asymmetrically altering local microtubule dynamics. Indeed, we find that Aurora B phosphorylates MCAK asymmetrically across metaphase centromeres (Figure 3G). This notion is attractive when one considers the recent discovery that protein phosphatase 1 (PP1), which antagonizes Aurora B (Hsu et al., 2000; Sassoon et al., 1999) and also regulates its activity (Murnion et al., 2001), is localized to the outer kinetochore in metaphase (Trinkle-Mulcahy et al., 2003). An additional level of control of depolymerizing activity may be afforded by modulating the affinity of MCAK for the different centromere/kinetochore binding sites through phosphorylation. The dynamic balance of phosphorylation of motors such as MCAK mediated by Aurora B and PP1 might then regulate the dynamic movements of chromosomes in the mitotic spindle. Moreover, it will be important to determine whether MCAK phosphorylation affects the dynamics of mono-oriented chromosomes in living cells.

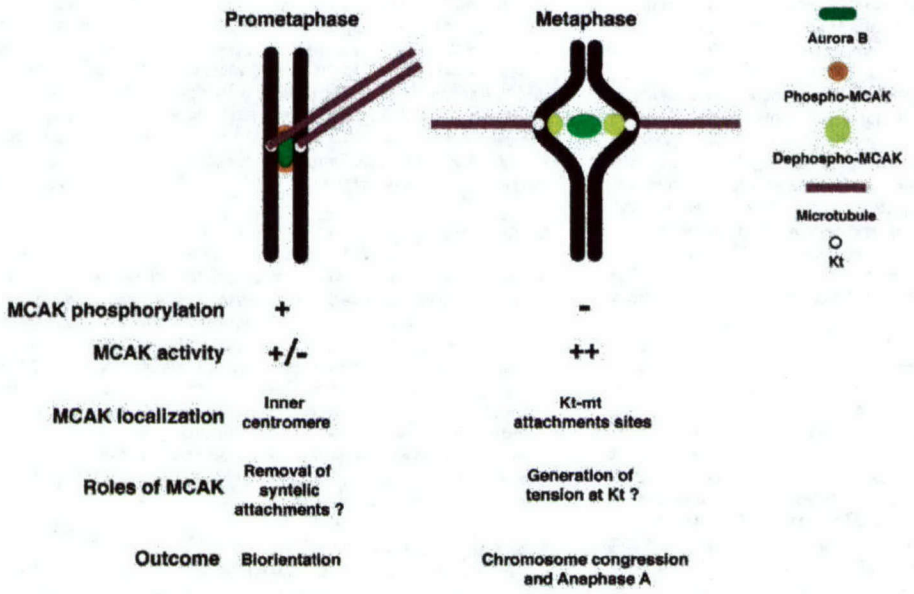

Figure 8. Model for the Regulation of MCAK by Aurora B in Mitosis

We propose a model for the role of Aurora B in regulating of MCAK activity during biorientation and throughout the process of chromosome congression, adapted from a previous suggestion (Tanaka et al., 2002). First, MCAK is targeted to the centromere by Aurora B phosphorylation. MCAK activity is inhibited by Aurora B phosphorylation, thereby increasing the probability that microtubule capture will result in stable kinetochore-microtubule interactions. MCAK activity is likely not completely inhibited, allowing it to destabilize incorrect (e.g., syntelic) attachments. After bipolar attachment initiates, the bioriented sister centromeres are under tension and the distance between them increases. MCAK separation from Aurora B favors its dephosphorylation, possibly by kinetochore-targeted PP1. Dephosphorylated MCAK would lose affinity for its inner-centromere binding site and gain affinity for its inner-kinetochore binding site concomitant with an increased catalytic activity, causing an increase in tension across the sister centromeres and full catalytic activity in anaphase.

Our finding that a phospho-mimic MCAK mutant is concentrated at the inner centromere and a nonphosphorylatable MCAK mutant is at the kinetochore, coupled with the observation that loss of Aurora B results in the appearance of MCAK on the spindle microtubules, suggests that inner-centromeric MCAK is phosphorylated and localized by its proximity to Aurora B in the absence of tension (Figure 8). At this point, MCAK activity is inhibited, possibly to prevent reversal of the initial microtubule-kinetochore attachments. Once bipolar attachment is established, MCAK and Aurora B are physically separated, MCAK phosphorylation decreases due to its proximity to PP1, and MCAK switches its affinity from centromeres to kinetochores/microtubule ends. Concomitantly, MCAK activity increases, allowing it to participate in force generation at the kinetochore. Whether this change in localization causes the MCAK microtubule depolymerase to switch from an error correction activity to a force generation machine can now be tested.

Experimental Procedures

Materials and Cell Culture

General laboratory reagents were purchased from Sigma or Merck. Microcystin-LR was the generous gift of Dr. C. MacKintosh (University of Dundee). HeLa cells were maintained in DMEM supplemented with 10% FBS (Sigma), 2 mM glutamate, and 10 U/ml Penicillin/Streptomycin at 37°C, 5% CO_2. Sheep anti-hamster MCAK polyclonal antiserum was produced via standard immunization and bleeding protocols (Pocono Rabbit Farm & Laboratory Inc., Canadensis, PA) using purified baculovirus-expressed hamster MCAK (Maney et al., 1998), affinity purified with immobilized bacterially expressed human MCAK (Ovechkina et al., 2002).

Immunofluorescence Microscopy

For immunofluorescence, cells grown on coverslips were fixed after washing once in 37°C PBS by incubation in 3.7% formaldehyde/PBS (pH 6.8) for 2 times 5 min at 37°C. Cells were permeabilized in PBS-0.1%Triton X-100 for 10 min at 37°C. Cells were blocked in AbDil (Cramer and Desai, 1995) supplemented with 0.1% normal donkey serum for 1 hr at room temperature. Anti-AIM1 (HsAurora B) monoclonal antibody (BD Biosciences) was used at 1:200 dilution. Affinity-purified sheep anti-human MCAK polyclonal antibody was diluted to 1 μg/ml. Rat anti-α-tubulin (Serotec) was used at a 1:500 dilution. Human CREST autoantisera (ACA; the generous gift of Professor Bill Earnshaw, University of Edinburgh) was diluted 1:10,000. All second antibodies (labeled with either FITC, Texas-Red, TRITC, or Cy5) were purchased from Jackson Laboratories.

3D data sets were acquired using a MicroMax cooled CCD camera (5 MHz: Roper Scientific), on a DeltaVision Restoration Microscope (Applied Precision, LLC, WA), built around a Nikon TE200 Eclipse stand with a 100 x/1.4NA PlanApo lens, or using a CoolSnap HQ cooled CCD camera on a DeltaVision Spectris Restoration Microscope built around an Olympus IX70 stand, with an a 100 x/1.4NA lens (Applied Precision, LLC, WA). Optical sections were recorded every 0.2 μm, and 3D data sets were deconvolved using the constrained iterative algorithm (Swedlow et al., 1997; Wallace et al., 2001) implemented in SoftWoRx software (Applied Precision LLC). Image data were quantified using SoftWoRx software. Kinetochore tubulin density was quantified in single optical sections using a 9 × 10 pixel box positioned at the plus end of kinetochore fibers. Integrated pixel intensities were measured for over 20 individual fibers in control and Aurora B RNAi cells. ACA-ACA distances were measured for clearly distinguishable metaphase centromere pairs lying along the pole-to-pole axis, using individual optical sections from 3D data sets from a large number of control and Aurora B RNAi cells.

Phospho-Specific Antibody Generation and Characterization

Phospho (CIQKQKRRS(Phos)VNSKIPA) and dephospho (CIQKQKR RSVNSKIPA) MCAK peptides encompassing the Ser92 phosphorylation site were synthesized and purified by Dr. G. Bloomberg (University of Bristol, UK). Phospho-Ser92 peptides were coupled to KLH (Calbiochem, UK) using standard protocols (Field et al., 1998) and used to immunize sheep (Diagnostics Scotland, UK). Phospho- and dephospho-peptides were coupled to Affigel 10 active ester agarose (BioRad) using iodoacetic acid N-Hydroxy-succinamide ester as described (Field et al., 1998). Serum was diluted 1:1 with TBS/0.1% Triton X-100, filtered, and repeatedly (5×) applied to a dephospho-peptide column. After washing with TBS and TBS/TX-100, antibodies were eluted with 0.2 M glycine (pH 2.6), and 0.1 M NaCl and immediately neutralized. Fractions containing antibody were pooled and dialyzed overnight against TBS. The flowthrough from the dephospho-peptide column was applied to the phospho-peptide column and then washed as above. Phospho-specific antibody was eluted as described above. For ELISA, serial dilutions (ranging from 100 μM to 0.001 μM; in 50 mM sodium carbonate buffer [pH 9.5]) of phospho-peptide, dephospho-peptide, or control Histone H3 serine 10 peptide were coated onto 96-well plates washed extensively (PBS, 0.05% Tween 20), blocked with 0.1% BSA/PBS, and washed (PBS, 0.05% Tween 20), and then diluted purified antiserum (1 μg/ml) was added to each well for 2 hr at room temperature. Bound antibody was detected with diluted (1:5000) anti-sheep-HRP conjugate and TMB solution (Sigma). Assay was read at 450 nm in a plate reader. To pre-block antibody with either the phospho-peptides or dephospho-peptide, 1 μg antibody was incubated with 0.5 mM peptide on ice for 1 hr prior to its addition to the ELISA. The antibodies were tested by Western blotting recombinant MCAK that had previously been either mock phosphorylated or phosphorylated by recombinant Ipl1p/Sli15p. Antibody specificity was similarly tested in fixed HeLa cells by preblocking antibody (10 μg Ab with 5 mM peptide).

Fluorescence Recovery after Photobleaching

Fluorescence recovery after photobleaching (FRAP) on wild-type and phosphorylation site mutant GFP-MCAK was performed on HeLa cells 18–24 hr after transfection with GFP-wtMCAK and GFP-AAAAA-MCAK and GFP-EEEEE-MCAK plasmids. All experiments were conducted using a FRAP-enabled DeltaVision Spectris (as above) fitted with a 10 mW 488 nm solid-state laser. The laser was focused to a diffraction-limited spot and spot bleaching performed with a single 50 ms stationary pulse at 90% laser power. The first image was acquired approximately 50 ms after the bleach event. For the first second, images were acquired every 150 ms, for the following 2 s every 300 ms, then at 800 ms intervals in the following 8 s, after which images were acquired every 1.5 s for the remainder of the experiment. Recovery models were generated and half-times calculated using the method of Axelrod (Axelrod et al., 1976) as implemented within SoftWoRx software. Centromeres were individually targeted for photobleaching and categorized as either aligned (congressed) or unaligned (noncongressed).

Aurora B Kinase Isolation, In Vitro Phosphorylation, and Phosphorylation Site Identification

Mitotic and interphase chromatin eluates (MCE and ICE, respectively) were prepared from in vitro-assembled *Xenopus* (Murnion et al., 2001; Swedlow, 1999) and used as a source of cell cycle-regulated Aurora B kinase activity. Aurora B complex was immunoprecipitated from MCE or ICE using an affinity-purified rabbit anti-Xaurora B polyclonal antibody raised against a peptide (CTTPSSATAAQRVL-RKEP) in the N terminus of *Xenopus* Aurora B conjugated to KLH (Field et al., 1998). This antibody recognizes a single band on Western blots and immunoprecipitates active Aurora B-INCENP complex from MCE and inactive Aurora B-INCENP complex from ICE (Murnion et al., 2001; data not shown). Control immunoprecipitations were performed in parallel using normal rabbit IgG bound to Affiprep Protein A beads. Bacterially expressed and purified Ipl1p-GST and Sli15p-GST were the generous gifts of N. Rachidi, University of Dundee. For in vitro phosphorylation studies, 2–4 μl Aurora B kinase beads were incubated with 0.2 μg recombinant hamster MCAK (Maney et al., 2001), in a 20 μl reaction buffer containing 2 μl [γ-^{32}P] ATP (10 mCi/ml: specific activity > 5000 Ci/mmol), 0.2 mM cold ATP, 1 x XBE2, 5 mM $MgCl_2$, and 1 μM Microcystin-LR, for 1 hr at 22°C, with shaking. Kinase reactions were terminated with Laemmli sample buffer, heated to 70°C for 5 min, and subjected to SDS-PAGE. After electrophoresis, gels were stained with Coomassie and destained and MCAK bands were excised. Phosphorylation site analysis was performed (Lizcano et al., 2002), except for the use of LysC for enzymatic digestion in order to determine MCAK phosphorylation sites more readily.

2D Gel Electrophoresis

To detect modification of human MCAK in Aurora B/control RNAi-treated HeLa cells (see below for details), whole-cell extracts (Feijoo et al., 2001) were prepared in the presence of phosphatase inhibitors, TCA precipitated, and rehydrated in sample buffer supplemented with 50 mM DTT and appropriate ampholytes. Isoelectric focusing was performed overnight using a BioRad Protean IEF Cell System, employing pH 6–11 Immobiline DryStrip isoelectric focusing strips (Amersham PLC). Proteins were separated in the second dimension on NuPAGE 4%–12% Bis-Tris IPG gels (Novex) run in MOPS buffer (Novex). 2D gels were blotted onto Protrans nitrocellulose membrane (Schleicher and Schuell). ECL was used for immunoblot detection (Amersham, PLC).

Microtubule Depolymerization Assays

Baculovirus-expressed 6His-hamster MCAK (Maney et al., 1998) was phosphorylated by incubation at 22°C for 90 min in 20 μl of 8 mM K-HEPES (pH 7.7), 65 mM KCl, 40 mM sucrose, 6 mM $MgCl_2$, 4 mM K-EGTA (pH 7.7), 60 mM Imidazole, 1 mM DTT, 0.2 mM ATP, 1 μM Microcystin-LR (Sigma), and 0.03% Triton X-100 in the presence of Aurora B complexes precipitated with rabbit α-Aurora B Ab-protein A-agarose beads (or rabbit IgG-protein A-agarose beads). Microtubule depolymerization was performed as described previously (Maney et al., 2001; Ovechkina et al., 2002). pEGFP-CgMCAK (pYOY71) was made by subcloning of BspE1-HindIII CgMCAK cDNA into pEGFP-C1 vector (Clontech). CgMCAK mutants were made by overlapping PCR mutagenesis using PfuTurbo DNA polymerase (Stratagene) and sequenced. CHO cells were cultured and transfected as described previously (Maney et al., 2001; Ovechkina et al., 2002).

Transfection and Imaging of Aurora B (KR)

Rat Aurora B and Aurora B (KR) were excised from GFP-Aurora B and GFP-Aurora B (KR) (a kind gift of Yu-Li Wang) and ligated into ECFP-N1 (Clontech). Full-length hamster MCAK was excised from pYOY71 (described above) and ligated into EYFP-C1 (Clontech). Motorless MCAK was excised from GFP-ML-MCAK (Maney et al., 1998) and ligated to EYFP-C1 (Clontech). CHO cells were cotransfected with CFP-Aurora or CFP-Aurora B (KR) in combination with either YFP-MCAK or YFP-ML MCAK. The cells were cultured for 16 hr, fixed in 1% glutaraldehyde in PBS for 20 min, and reduced in 5% $NaBH_4$/PBS for 20 min. Microtubules were labeled with DM1 (Sigma) and Texas Red-conjugated secondary antibodies.

RNAi

A 21 nt siRNA (AAGAGCCUGUCACCCCAUCUG: Dharmacon Research Inc., USA) corresponding to position +149 → +169 of the human Aurora B (STK12) coding sequence was used for Aurora B RNAi, depleting Aurora B protein levels by more than 75% in less than 24 hr. Lamin A/C siRNA and a scrambled random siRNA duplex (Dharmacon Research, Inc.) were used as controls. For RNAi, HeLa cells were seeded onto 13 mm coverslips and grown overnight in medium without antibiotics. Transfection was performed using Oligofectamine (Invitrogen, Inc.) using 60 pmol siRNA per well following manufacturer's protocols. Coverslips were fixed at intervals between 5 and 48 hr posttransfection and processed for immunofluorescence. The siRNA duplex used significantly decreases Aurora B protein levels within 10 to 24 hr in single cells (data not shown). Previously, we have characterized the dynamic range of our microscope system and shown that we can accurately measure relative intensities over ~2.5 orders of magnitude with a coefficient of variation of ~6%–9% (Swedlow et al., 2002). We have used this capability to accurately measure the depletion of Aurora B, as detected by

immunofluorescence and score phenotypes in single cells with Aurora B levels <1% of control cells. The mean depletion of Aurora B assayed by quantifying fluorescence in single cells was 76.9 ± 19.6% (N = 15; also see Supplemental Figure S2), which was similar to the value obtained from immunoblots of whole-cell lysates, suggesting that immunofluorescence, at least in this case, can be used to quantify Aurora B levels in fixed cells. Images for Aurora B RNAi and control RNAi cells were acquired and processed under identical conditions. For analysis of protein levels on 2D gels, the RNAi treatment was scaled up using 900 pmol siRNA duplexes.

Acknowledgments

We thank Bill Earnshaw for the ACA antibody, Yu-Li Wang for the kinase-dead Aurora B, Najma Rachidi for Ipl1p/Sli15p and many useful discussions, Iain Porter and Guennadi Khodouli for assistance with 2D gels, past and present members of Swedlow lab for help with *Xenopus* extracts, and Tomo Tanaka for critical reading of the manuscript and many thoughtful discussions. This work was supported by grants from the Wellcome Trust and Cancer Research UK (to J.R.S.) and from the Department of Defense (DAMD17-01-1-0450) (to L.W). J.R.S. is a Wellcome Trust Senior Research Fellow.

Received: May 23, 2003
Revised: August 22, 2003
Accepted: December 11, 2003
Published: February 9, 2004

References

Adams, R.R., Maiato, H., Earnshaw, W.C., and Carmena, M. (2001). Essential roles of *Drosophila* inner centromere protein (INCENP) and Aurora B in histone h3 phosphorylation, metaphase chromosome alignment, kinetochore disjunction, and chromosome segregation. J. Cell Biol. *153*, 865–880.

Andrews, P.D., Knatko, E., Moore, W.J., and Swedlow, J.R. (2003). Mitotic mechanics: the Auroras come into view. Curr. Opin. Cell Biol. *15*, 672–683.

Axelrod, D., Koppel, D.E., Schlessinger, J., Elson, E., and Webb, W.W. (1976). Mobility measurement by analysis of fluorescence photobleaching recovery kinetics. Biophys. J. *16*, 1055–1069.

Biggins, S., Severin, F.F., Bhalla, N., Sassoon, I., Hyman, A.A., and Murray, A.W. (1999). The conserved protein kinase Ipl1 regulates microtubule binding to kinetochores in budding yeast. Genes Dev. *13*, 532–544.

Carmena, M., and Earnshaw, W.C. (2003). The cellular geography of Aurora kinases. Nat. Rev. Mol. Cell Biol. *4*, 842–854.

Cheeseman, I.M., Anderson, S., Jwa, M., Green, E.M., Kang, J., Yates, J.R., 3rd, Chan, C.S., Drubin, D.G., and Barnes, G. (2002). Phospho-regulation of kinetochore-microtubule attachments by the Aurora kinase Ipl1p. Cell *111*, 163–172.

Cramer, L., and Desai, A. (1995). (http://mitchison.med.harvard.edu/protocols/gen1.html).

Desai, A., Verma, S., Mitchison, T.J., and Walczak, C.E. (1999). Kin I kinesins are microtubule-destabilizing enzymes. Cell *96*, 69–78.

Ditchfield, C., Johnson, V.L., Tighe, A., Ellston, R., Haworth, C., Johnson, T., Mortlock, A., Keen, N., and Taylor, S.S. (2003). Aurora B couples chromosome alignment with anaphase by targeting BubR1, Mad2, and Cenp-E to kinetochores. J. Cell Biol. *161*, 267–280.

Feijoo, C., Hall-Jackson, C., Wu, R., Jenkins, D., Leitch, J., Gilbert, D.M., and Smythe, C. (2001). Activation of mammalian Chk1 during DNA replication arrest: a role for Chk1 in the intra-S phase checkpoint monitoring replication origin firing. J. Cell Biol. *154*, 913–923.

Field, C.M., Oegema, K., Zheng, Y., Mitchison, T.J., and Walczak, C.E. (1998). Purification of cytoskeletal proteins using peptide antibodies. Methods Enzymol. *298*, 525–541.

Giet, R., and Glover, D.M. (2001). *Drosophila* Aurora B kinase is required for histone H3 phosphorylation and condensin recruitment during chromosome condensation and to organize the central spindle during cytokinesis. J. Cell Biol. *152*, 669–682.

Hauf, S., Cole, R.W., LaTerra, S., Zimmer, C., Schnapp, G., Walter, R., Heckel, A., Van Meel, J., Rieder, C.L., and Peters, J.M. (2003). The small molecule Hesperadin reveals a role for Aurora B in correcting kinetochore-microtubule attachment and in maintaining the spindle assembly checkpoint. J. Cell Biol. *161*, 281–294.

He, X., Rines, D.R., Espelin, C.W., and Sorger, P.K. (2001). Molecular analysis of kinetochore-microtubule attachment in budding yeast. Cell *106*, 195–206.

Homma, N., Takei, Y., Tanaka, Y., Nakata, T., Terada, S., Kikkawa, M., Noda, Y., and Hirokawa, N. (2003). Kinesin superfamily protein 2A (KIF2A) functions in suppression of collateral branch extension. Cell *114*, 229–239.

Hsu, J.-Y., Sun, Z.-W., Li, X., Reuben, M., Tatchell, K., Bishop, D.K., Grushcow, J.M., Brame, C.J., Caldwell, J.A., Hunt, D.F., et al. (2000). Mitotic phosphorylation of histone H3 is governed by Ipl1/aurora kinase and Glc7/PP1 phosphatase in budding yeast and nematodes. Cell *102*, 279–291.

Hunter, A.W., and Wordeman, L. (2000). How motor proteins influence microtubule polymerization dynamics. J. Cell Sci. *113*, 4379–4389.

Hunter, A.W., Caplow, M., Coy, D.L., Hancock, W.O., Diez, S., Wordeman, L., and Howard, J. (2003). The kinesin-related protein MCAK is a microtubule depolymerase that forms an ATP-hydrolyzing complex at microtubule ends. Mol. Cell *11*, 445–457.

Kaitna, S., Mendoza, M., Jantsch-Plunger, V., and Glotzer, M. (2000). Incenp and an aurora-like kinase form a complex essential for chromosome segregation and efficient completion of cytokinesis. Curr. Biol. *10*, 1172–1181.

Kang, J.S., Cheeseman, I.M., Kallstrom, G., Velmurugan, S., Barnes, G., and Chan, C.S. (2001). Functional cooperation of Dam1, Ipl1, and the inner centromere protein (INCENP)-related protein Sli15 during chromosome segregation. J. Cell Biol. *155*, 763–774.

Kline-Smith, S.L., and Walczak, C.E. (2002). The microtubule-destabilizing kinesin XKCM1 regulates microtubule dynamic instability in cells. Mol. Biol. Cell *13*, 2718–2731.

Lizcano, J.M., Deak, M., Morrice, N., Kieloch, A., Hastie, C.J., Dong, L., Schutkowski, M., Reimer, U., and Alessi, D.R. (2002). Molecular basis for the substrate specificity of NIMA-related kinase-6 (NEK6). Evidence that NEK6 does not phosphorylate the hydrophobic motif of ribosomal S6 protein kinase and serum- and glucocorticoid-induced protein kinase in vivo. J. Biol. Chem. *277*, 27839–27849.

Maney, T., Hunter, A.W., Wagenbach, M., and Wordeman, L. (1998). Mitotic centromere-associated kinesin is important for anaphase chromosome segregation. J. Cell Biol. *142*, 787–801.

Maney, T., Wagenbach, M., and Wordeman, L. (2001). Molecular dissection of the microtubule depolymerizing activity of mitotic centromere-associated kinesin. J. Biol. Chem. *276*, 34753–34758.

Murata-Hori, M., and Wang, Y.L. (2002). The kinase activity of Aurora B is required for kinetochore-microtubule interactions during mitosis. Curr. Biol. *12*, 894–899.

Murata-Hori, M., Tatsuka, M., and Wang, Y.L. (2002). Probing the dynamics and functions of aurora B kinase in living cells during mitosis and cytokinesis. Mol. Biol. Cell *13*, 1099–1108.

Mumion, M.E., Adams, R.A., Callister, D.M., Allis, C.D., Earnshaw, W.C., and Swedlow, J.R. (2001). Chromatin-associated protein phosphatase 1 regulates aurora-B and histone H3 phosphorylation. J. Biol. Chem. *276*, 26656–26665.

Niederstrasser, H., Salehi-Had, H., Gan, E.C., Walczak, C., and Nogales, E. (2002). XKCM1 acts on a single protofilament and requires the C terminus of tubulin. J. Mol. Biol. *316*, 817–828.

Ohi, R., Coughlin, M.L., Lane, W.S., and Mitchison, T.J. (2003). An inner centromere protein that stimulates the microtubule depolymerizing activity of a Kinl kinesin. Dev. Cell *5*, 309–321.

Ohsugi, M., Tokai-Nishizumi, N., Shiroguchi, K., Toyoshima, Y.Y., Inoue, J., and Yamamoto, T. (2003). Cdc2-mediated phosphorylation of Kid controls its distribution to spindle and chromosomes. EMBO J. *22*, 2091–2103.

Ovechkina, Y., Wagenbach, M., and Wordeman, L. (2002). K-loop insertion restores microtubule depolymerizing activity of a "neckless" MCAK mutant. J. Cell Biol. *159*, 557–562.

Rieder, C.L., and Salmon, E.D. (1994). Motile kinetochores and polar ejection forces dictate chromosome position on the vertebrate mitotic spindle. J. Cell Biol. *124*, 223–233.

Sassoon, I., Severin, F.F., Andrews, P.D., Taba, M.R., Kaplan, K.B., Ashford, A.J., Stark, M.J., Sorger, P.K., and Hyman, A.A. (1999). Regulation of *Saccharomyces cerevisiae* kinetochores by the type 1 phosphatase Glc7p. Genes Dev. *13*, 545–555.

Skibbens, R.V., Skeen, V.P., and Salmon, E.D. (1993). Directional instability of kinetochore motility during chromosome congression and segregation in mitotic newt lung cells: a push-pull mechanism. J. Cell Biol. *122*, 859–875.

Swedlow, J.R. (1999). Chromosome assembly in vitro using Xenopus egg extracts. In Chromosome Structural Analysis, W.A. Bickmore, ed. (Oxford: Oxford), pp. 167–182.

Swedlow, J.R., Sedat, J.W., and Agard, D.A. (1997). Deconvolution in optical microscopy. In Deconvolution of Images and Spectra, P.A. Jansson, ed. (New York: Academic Press), pp. 284–309.

Swedlow, J.R., Hu, K., Andrews, P.D., Roos, D.S., and Murray, J.M. (2002). Measuring tubulin content in *Toxoplasma gondii*: a comparison of laser-scanning confocal and wide-field fluorescence microscopy. Proc. Natl. Acad. Sci. USA *99*, 2014–2019.

Tanaka, T.U., Rachidi, N., Janke, C., Pereira, G., Galova, M., Schiebel, E., Stark, M.J.R., and Nasmyth, K. (2002). Evidence that the Ipl1-Sli15 (Aurora kinase-INCENP) complex promotes chromosome bi-orientation during mitosis by altering kinetochore-spindle pole connections. Cell *108*, 317–329.

Trinkle-Mulcahy, L., Andrews, P.D., Wickramasinghe, S., Sleeman, J., Prescott, A., Lam, Y.W., Lyon, C., Swedlow, J.R., and Lamond, A.I. (2003). Time-lapse imaging reveals dynamic relocalization of PP1gamma throughout the mammalian cell cycle. Mol. Biol. Cell *14*, 107–117.

Walczak, C.E., Mitchison, T.J., and Desai, A. (1996). XKCM1—a Xenopus kinesin-related protein that regulates microtubule dynamics during mitotic spindle assembly. Cell *84*, 37–47.

Walczak, C.E., Gan, E.C., Desai, A., Mitchison, T.J., and Kline-Smith, S.L. (2002). The microtubule-destabilizing kinesin XKCM1 is required for chromosome positioning during spindle assembly. Curr. Biol. *12*, 1885–1889.

Wallace, W., Schaefer, L.H., and Swedlow, J.R. (2001). A workingperson's guide to deconvolution in light microscopy. Biotechniques *31*, 1076–1097.

Waters, J.C., Skibbens, R.V., and Salmon, E.D. (1996). Oscillating mitotic newt lung cell kinetochores are, on average, under tension and rarely push. J. Cell Sci. *109*, 2823–2831.

Westermann, S., Cheeseman, I.M., Anderson, S., Yates, J.R., 3rd, Drubin, D.G., and Barnes, G. (2003). Architecture of the budding yeast kinetochore reveals a conserved molecular core. J. Cell Biol. *163*, 215–222.

Wordeman, L., Wagenbach, M., and Maney, T. (1999). Mutations in the ATP-binding domain affect the subcellular distribution of mitotic centromere-associated kinesin (MCAK). Cell Biol. Int. *23*, 275–286.

Zeitlin, S.G., Shelby, R.D., and Sullivan, K.F. (2001). CENP-A is phosphorylated by Aurora B kinase and plays an unexpected role in completion of cytokinesis. J. Cell Biol. *155*, 1147–1157.

Appendix 4

FEBS Letters 572 (2004) 80–84 FEBS 28658

MCAK, a Kin I kinesin, increases the catastrophe frequency of steady-state HeLa cell microtubules in an ATP-dependent manner in vitro

Cori N. Newton[a,1], Michael Wagenbach[b,2], Yulia Ovechkina[b,2], Linda Wordeman[b,2], Leslie Wilson[a,*]

[a] *Department of Molecular, Cellular, and Developmental Biology, and The Neuroscience Research Institute, University of California, Santa Barbara, CA 93106, USA*

[b] *Department of Physiology and Biophysics, University of Washington School of Medicine, Seattle, WA USA*

Received 23 June 2004; accepted 30 June 2004

Available online 23 July 2004

Edited by Jesus Avila

Abstract Mitotic-centromere-associated kinesin (MCAK) is a member of the KIN I (internal motor domain) subfamily of kinesin related proteins. MCAK and its homologues destabilize microtubules both in cells and in vitro. Here, we analyzed the effects of MCAK in the presence and absence of ATP on the dynamic instability behavior of steady state microtubules assembled from purified HeLa cell tubulin. In the presence of ATP, substoichiometric levels of full length MCAK and a segment (A182) consisting of the motor and neck domains strongly increased the catastrophe frequency of the microtubules. These data demonstrate that MCAK is a microtubule-catastrophe promoting factor in vitro, and support the hypothesis that MCAK may serve as a catastrophe-promoting factor in cells.
© 2004 Published by Elsevier B.V. on behalf of the Federation of European Biochemical Societies.

Keywords: Microtubule dynamic instability; Regulation of microtubule dynamics; Catastrophe promoting factor

1. Introduction

Dynamic instability, the switching at microtubule ends between growth and shortening [1–3], is critical for many microtubule-mediated cellular processes including chromosome movements during mitosis and the development of cell polarity [4,5]. Although dynamic instability is an intrinsic property of microtubules composed solely of tubulin, the dynamic instability behavior of microtubules in cells is considerably greater than that of microtubules composed of pure tubulin in vitro [6–10]. Specifically, microtubules assembled from purified HeLa cell tubulin in vitro display highly attenuated dynamic instability behavior, indicating that the robust dynamic instability behavior displayed by microtubules in dividing cells is created by regulatory proteins [10].

A protein that appears to destabilize microtubules and increase microtubule dynamic instability in cells is mitotic-centromere-associated kinesin (MCAK) a member of the KIN I (internal motor domain) subfamily of kinesin-related proteins [11,12]. Unlike most other kinesins that utilize ATP hydrolysis to move along microtubules, MCAK and its KIN I family members exhibit no motile activity [12–16]. Instead, they induce microtubule depolymerization in vitro in an ATP dependent manner [14,17] and in cells [16,18–20]. Specifically, incubation of MCAK with taxol- or GMPPNP stabilized microtubules in vitro induces depolymerization [16,17,19], as does the overexpression of MCAK in CHO cells [16,18]. Furthermore, immunodepletion or inactivation of XKCM1 (the Xenopus homologue of MCAK) by antibody addition in frog extracts induces the formation of abnormally long non-dynamic microtubules, supporting the idea that one of XKCM1's functions is to increase the dynamic instability of microtubules [13]. Direct analysis of the changes in the dynamics of axoneme-seeded microtubules incubated in the immunodepleted frog extracts revealed a 4-fold decrease in the catastrophe frequency (switching from growth to shortening), supporting the idea that XKCM1 might have catastrophe-promoting activity in cells [13]. In further support of this idea, overexpression of XKCM1 in PtK2 interphase cells enhanced the catastrophe frequency by 4.5-fold [20].

The effects of MCAK and its homologues on the dynamic instability of non-stabilized microtubules in vitro in the absence of other regulatory proteins at steady state have not been described. Thus, we determined the effects of MCAK on the individual dynamic parameters at plus ends of purified steady state microtubules in vitro, using highly purified HeLa cell microtubules, which exhibit intrinsically tempered dynamics. We found that substoichiometric quantities of full length MCAK potently and selectively increased the plus-end catastrophe frequency in an ATP-dependent manner, supporting the hypothesis that MCAK binds to the plus ends to convert the microtubule from a growing or attenuated (paused) state to a shortening state. In contrast to the ATP-dependent effects of MCAK on the catastrophe frequency, MCAK reduced the microtubule polymer mass in the absence of ATP. Thus, the ability of MCAK to destabilize microtubules (decrease polymer mass) and act as a catastrophe-promoting factor may be brought about by more than a single mechanism.

* Corresponding author. Fax: +805-893-8094.
E-mail address: wilson@lifesci.ucsb.edu (L. Wilson).

[1] Fax: +805-893-8094.
[2] Fax: +206-685-0619.

0014-5793/$22.00 © 2004 Published by Elsevier B.V. on behalf of the Federation of European Biochemical Societies.
doi:10.1016/j.febslet.2004.06.093

2. Materials and methods

2.1. MCAK expression, HeLa cell tubulin purification, determination of MCAK concentrations

Full-length hamster MCAK (FL-MCAK) was expressed in baculovirus and purified as previously described [18]. The hamster MCAK motor domain and the A182 fragment were bacterially expressed and purified as described in [19]. Purified HeLa cell tubulin was isolated as described by Newton et al. [10]. HeLa cell tubulin and the MCAK proteins were exchanged into 80 mM Pipes, 1 mM $MgCl_2$, 1 mM EGTA, 0.5% NP-40, and 60 mM KCl, pH 6.8 [BRB80], by concentrating the solutions in a Biomax-30 centrifugal filter (Millipore) and by centrifugation in a Sorvall centrifuge (SS34 rotor, 10 000 rpm, 4 °C). Aliquots of the protein solutions were frozen in liquid nitrogen and stored at −70 °C until use. The concentrations of active FL-MCAK dimer, A182, and the motor domain negative control were determined by measuring their ATP binding activities [21]. The ratios of active (able to bind ATP) to inactive (unable to bind ATP) for FL-MCAK, A182, and the motor domain were 1:5. FL-MCAK activity is reported as a dimer (two ATP binding sites per dimer), while the protein concentrations of A182 and the core motor domain proteins are reported as the monomers [21]. MCAK inhibits microtubule polymerization and thus two criteria were used to determine the concentrations of the MCAK proteins used for the dynamics experiments; the highest concentration at which we obtained adequate numbers and lengths of assembled microtubules, and the concentration at which we could detect a change in dynamic instability behavior as compared with the inactive motor domain control. Tubulin concentration was determined by the Bradford method using bovine serum albumin as the standard [22].

2.2. Determination of HeLa cell microtubule dynamic instability in the presence of full-length MCAK, A182, and the MCAK Motor Domain

Samples containing 15.5 μM tubulin and 58.9 nM FL-MCAK, 3.5 nM A182 or 30 nM core MCAK motor domain (see Fig. 1) were mixed with 0.5 mg/ml casein in BRB80 buffer containing 1 mM GTP and 1 mM DTT and incubated on ice for no more than 15 min. ATP, when used, was added at a final concentration of 2 mM. Flow-through chambers were assembled with double-stick tape and pre-cleaned glass coverslips and slides. Diluted *Strongylocentrotus purpuratus* axonemes were flowed through the chambers and after incubation on ice for 5 min, unattached axonemes were washed out by addition of 5 mg/ml casein in BRB80 buffer and slides were further incubated to allow binding of casein to the chamber surfaces. The chambers were then washed with BRB80 buffer. The pre-mixed sample containing HeLa cell tubulin and MCAK was then flowed through the chamber and sealed with 1:1:1 vasoline, lanolin, and paraffin. The slide was placed on a pre-warmed (35 °C) differential interference contrast (DIC) microscope stage and incubated for 30 min to reach steady-state. Individual microtubules were then imaged and analyzed at 35 °C as previously described [10].

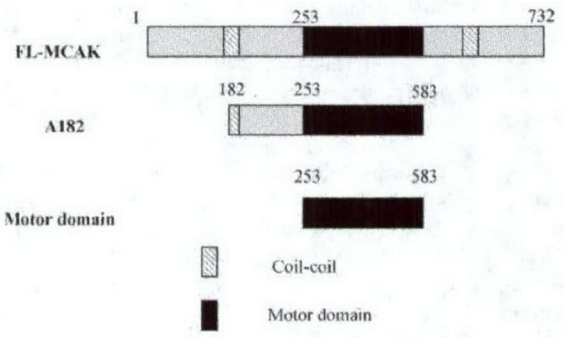

Fig. 1. Schematic showing the different MCAK constructs used. FL is full-length Hamster MCAK (732 amino acids). A182 is a truncated form of MCAK which contains the motor domain and the region amino-terminal to the motor domain (amino acids 182–583). The motor domain is the core motor domain of MCAK only (amino acids 253–583).

3. Results

3.1. Effects of MCAK on the Dynamic instability of HeLa cell microtubules

In an effort to understand MCAK's role as a regulator of microtubule dynamics, we analyzed the effects of three MCAK constructs in the presence and absence of 2 mM ATP on the dynamic instability behavior of steady state microtubules composed of HeLa cell tubulin (15.5 μM). These microtubules display intrinsically tempered dynamic instability behavior [10], making them very useful for analysis of regulators that increase dynamics. The concentration of active FL MCAK dimer (Fig. 1) chosen for use in this study was 59 nM. This concentration was the highest concentration that yielded sufficient polymer mass and microtubule lengths for analysis. We also analyzed the effects of a fragment called A182 at 3.5 nM using the same criteria for choice of concentration (containing the core motor domain between residues 253 and 583 and a region near the amino-terminus from residue 182 to 253 called the "neck domain") and, as a negative control, a fragment consisting only of the core motor domain (30 nM) which is devoid of microtubule depolymerizing activity [16,19] (Fig. 1).

Life-history traces showing length changes with time of microtubules assembled in the presence of 2 mM ATP with the inactive core motor domain, FL-MCAK, and A182, are shown in Fig. 2. The traces demonstrate that microtubules assembled with the inactive core motor domain (Fig. 2A) display minimal dynamic instability behavior, as do control HeLa cell microtubules composed solely of tubulin (data not shown) [10]. In contrast with microtubules assembled from brain tubulin, microtubules assembled from highly purified HeLa cell tubulin rarely display growth or shortening or transitions to shortening (catastrophes) [10]. By comparison, both FL-MCAK (Fig. 2B) and the active A182 fragment (Fig. 2C) significantly increased the catastrophe frequency.

The effects of the three MCAK constructs on the individual steady state dynamic instability parameters in the presence and absence of 2 mM ATP are shown quantitatively in Table 1. Neither FL-MCAK nor A182 significantly changed the growth or shortening rates as compared with the inactive motor domain, nor did they induce significant differences in the mean length grown per growth event or the mean length shortened per shortening event (99% confidence level, Student's t test). However, both FL-MCAK and the active A182 fragment significantly increased the catastrophe frequency. Specifically, low ratios both of dimeric FL-MCAK and monomeric A182 (1/263 moles of active FL-MCAK/mole of tubulin and 1:4428 moles of A182/mole of tubulin) increased the catastrophe frequency by ~7-fold (from 0.03 min^{-1} with the inactive motor domain to 0.2 min^{-1}, both with FL-MCAK and A182, Table 1). Interestingly, the monomeric A182 exerted much more potent catastrophe promoting activity than the dimeric FL-MCAK, as 16.8-fold more FL-MCAK exerted the same catastrophe-promoting activity as A182. In addition, it appears that both FL-MCAK and A182 decreased the rescue frequency (frequency of transitions from shortening to either growth or an attenuated state) by 61% and 46%, respectively (Table 1). As a result of the increased catastrophe frequency, microtubules in the presence of FL-MCAK and A182 spent ~88% more time shortening than in the presence of the motor domain control (Table 1). In addition, as would be expected with a factor that increases the catastrophe frequency thereby

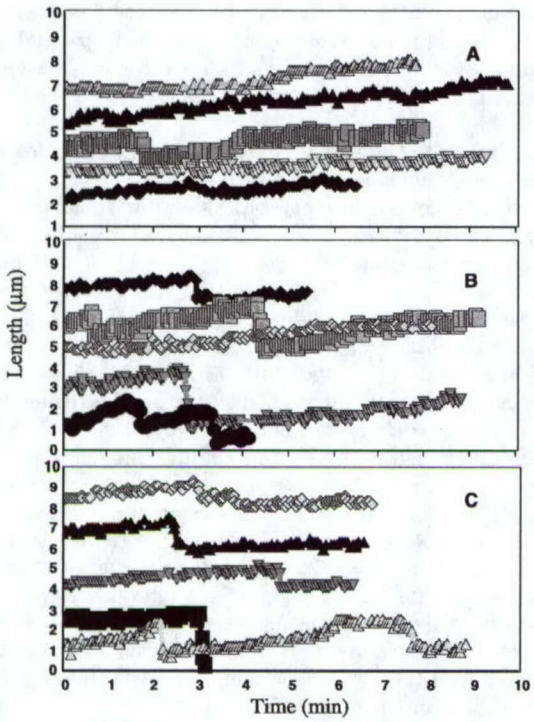

Fig. 2. Life-history traces of individual axoneme-seeded HeLa cell microtubules. Panel A, microtubules incubated with the core motor domain (30 nM). Panel B, microtubules incubated with FL-MCAK (58.9 nM). Panel C, microtubules in the presence of A182 (3.5 nM). The tubulin concentration was 15.5 μM.

increasing the rate tubulin would appear in the soluble pool, MCAK and A182 increased the percentage of time the microtubules grew (by 33% and 21%, respectively) (Table 1). Finally, FL-MCAK and A182 increased the dynamicity (overall detectable growth and shortening per unit time) by ~2.5-fold as compared to the motor domain control (Table 1).

3.2. The catastrophe promoting activity of MCAK and A182 requires ATP

The catastrophe-promoting activity of FL-MCAK and A182 MCAK requires ATP (Table 1), confirming suggestions of previous studies [14,17,23]. In the absence of any added ATP, the catastrophe frequency with FL- MCAK or A182 was no different than the catastrophe frequency with the core motor domain (Table 1). These experiments also show that GTP, which was present at a concentration of 1 mM, could not substitute for ATP.

3.3. Microtubule length changes in the presence of MCAK

In preliminary experiments we found that MCAK and A182, but not the motor domain which had similar lengths and numbers of microtubules as buffer alone (unpublished data),

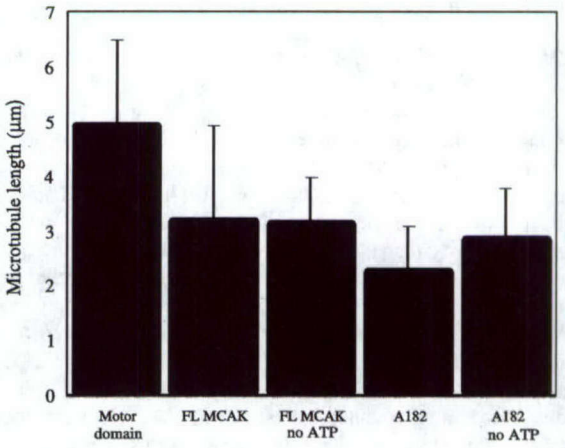

Fig. 3. Average microtubule length for axoneme-seeded HeLa cell microtubules. The microtubules were measured in the following conditions (shown left to right), in the presence of the core motor domain (1:520 mole of motor domain: mole of tubulin), in the presence of FL-MCAK (1:260 mole of FL-MCAK: mole of tubulin) ± ATP, and in the presence of A182 (1:4400 mole of A182: mole of tubulin) ± ATP.

Table 1
Dynamic instability parameters of HeLa cell microtubules in the presence of MCAK's core motor domain, A182 and FL-MCAK

Parameter	Motor domain (plus ATP)	FL (plus ATP)	FL (no ATP)	A182 (plus ATP)	A182 (no ATP)
Rate (μm/min)					
Growing	0.39 ± 0.4	0.38 ± 0.2	0.36 ± 0.3	0.42 ± 0.3	0.32 ± 0.2
Shortening	23.4 ± 9.8	16.5 ± 9.4	18.3 ± 6.3	13.4 ± 7.8	13.9 ± 11.6
Mean length (μm/event)					
Growing	0.6 ± 0.4	0.7 ± 0.4	0.6 ± 0.5	0.5 ± 0.3	0.5 ± 0.3
Shortening	1.1 ± 0.9	1.5 ± 1.3	1.1 ± 0.4	0.9 ± 0.6	0.9 ± 0.4
Transition frequencies (min^{-1})					
Catastrophe	0.03	0.2	0.04	0.2	0.03
Rescue	20.0	7.8	15.4	10.7	11.1
Percentage of time					
Growing	33.0	49.1	26.2	41.3	30.7
Shortening	0.2	1.6	0.2	1.8	0.3
Attenuated	66.8	49.3	73.6	56.9	69.0
Dynamicity (μm/min)	0.17	0.45	0.14	0.41	0.14

Changes in length at plus ends of microtubules assembled with 15.5 μM HeLa cell tubulin in the presence of 30 nM MCAK core motor domain, 58.9 nM FL-MCAK and 3.5 nM A182 were measured for a total of 205, 160 and 153 min, respectively. Values are shown as means ± S.D. The rates and mean lengths were not significantly different (99% confidence level, Student's t test).

reduced the lengths and numbers of microtubules assembled at the ends of axonemal seeds. Thus, to measure the effects of MCAK and A182 on the dynamic instability of microtubules, we chose to use the highest concentration of FL-MCAK and A182 that still yielded adequate numbers and lengths of microtubules at the ends of the seeds (59 nM FL-MCAK and 3.5 nM A182). At the concentrations used, MCAK and A182 reduced the lengths of the microtubules in the presence of ATP. Surprisingly, the microtubule lengths were also reduced in the absence of ATP (Fig. 3). For example, MCAK reduced the mean length to a similar extent, by 37%, either in the presence or absence of ATP. MCAK and A182 also reduced the number of microtubules polymerized at the ends of the axoneme-seeds either in the presence or absence of ATP as compared with the number of microtubules assembled in the presence of the motor domain control (data not shown).

4. Discussion

Previous work from a number of laboratories has shown that MCAK and other members of the Kin I family of internal motor domain kinesins, including XKCM1 and the neuronal family member XKIF2, do not "walk" along microtubules as do most other kinesins, but rather, destabilize microtubules apparently by acting at the microtubule ends [14,16–20]. MCAK and its homologues bind to microtubules preferentially at their ends [14,17,23] and their localization at the kinetochores of mitotic chromosomes and at spindle poles during mitosis places them near the ends [11,18,20]. Considerable evidence indicates that MCAK induces microtubule depolymerization both in cells [16,18] and in vitro [16,17,19]. In addition, evidence both in cells and with microtubules reconstituted in vitro has suggested that MCAK homologues can act as catastrophe-promoting factors [15,20]. For example, overexpression of XKCM1 in PtK2 cells increases the catastrophe frequency of microtubules [20] and depletion or inhibition of XKCM1 in *Xenopus* egg extracts induces formation of large asters with abnormally long, non-dynamic microtubules [13]. The strongest direct evidence indicating that an MCAK homologue is a bona fide catastrophe factor was obtained under non-steady state conditions [15]. However, in order to demonstrate unambiguously that MCAK is a bone fide catastrophe factor, it is necessary to measure the catastrophe promoting activity under conditions in which the microtubules are at or near steady state, with the soluble tubulin concentration constant. For example, under non-steady state conditions, a tubulin-sequestering factor would decrease the soluble tubulin concentration, which would result in net microtubule disassembly and induce a transient increase in the catastrophe frequency.

In the present study, we analyzed the effects of MCAK and A182, consisting of the motor and neck domains, on the individual dynamic instability parameters of microtubules assembled to steady state in the presence of the Kin I proteins. We used microtubules that were assembled from highly purified tubulin, from dividing cells, and thus a normal substrate for MCAK. Finally, the microtubules were analyzed in the absence of any other regulatory proteins, so the effects of MCAK alone could be determined with microtubules that in the absence of MCAK display highly tempered dynamic instability behavior. We find that MCAK acts as a potent microtubule catastrophe-factor in vitro, increasing the switching frequency from the growing or attenuated (paused) state without exerting significant effects on the rate or extent of steady state growth or shortening.

4.1. *Catastrophe promoting activity of MCAK and A182 at steady state in vitro*

In the presence of inactive MCAK motor domain, the purified HeLa cell microtubules rarely switched from the growing or an attenuated state to shortening (Table 1, 0.03 per min, or only once every 33 min). Essentially, the same catastrophe frequency was obtained with steady state HeLa cell microtubules in the absence of any regulatory proteins (1 every 50 min) [10]. In contrast, only 1 molecule of FL-MCAK dimer per 263 molecules of tubulin increased the catastrophe frequency by ~6.7-fold to ~ once every 5 min. The MCAK-induced increase in the catastrophe frequency was not high enough to cause an increase in the soluble tubulin level and thus increase the growth rate. These results further support the conclusion that the microtubules were at a true steady state. The observed reduction in the rescue frequency in the presence of MCAK is probably not meaningful because the time the microtubules spent shortening was exceedingly small and the lengths of the microtubules were short, making it difficult to accurately measure transitions from shortening to growth. In accord with the observation that FL-MCAK increased the catastrophe frequency, it also increased total visibly detectable tubulin subunit exchange (dynamicity), which resulted from an increase in the percentage of time the microtubules spent shortening and growing (Table 1). Thus, it is clear that MCAK potently increases the catastrophe frequency of HeLa cell microtubules in vitro.

It is interesting to note that the catastrophe frequency of HeLa cell microtubules in the presence of MCAK is still quite low compared to the catastrophe frequency of microtubules in living cells [5,9]. While we do not know the concentration of active MCAK at microtubule ends in cells, the data support the idea that multiple regulatory factors must be necessary to achieve not only the high catastrophe frequency of cellular microtubules but also the fast rates of growth [5–10]. Additional studies involving the combination of multiple microtubule regulatory factors and purified HeLa cell microtubules would help provide further insight into the regulation of microtubule dynamics in cells.

4.2. *A182 is a more potent catastrophe-promoting factor than FL-MCAK*

Like full-length dimeric MCAK, the monomeric A182 increased the catastrophe frequency of the microtubules without significantly affecting the growth or shortening rates (Table 1). Surprisingly, A182 was much more potent than full-length MCAK (Table 1). Specifically, more than 16 times the amount of full-length MCAK than A182 was needed to elicit a similar increase in the catastrophe frequency. One possible explanation for the increased potency of A182 is that it is a monomer rather than a dimer, and that the monomer is more potent than the dimer. Another possibility is that the missing regions of A182 play a regulatory role in MCAK's catastrophe-promoting activity. A recent study by the Wordeman lab has shown that the C-terminal end of FL-MCAK inhibits lattice-stimulated ATPase activity of the motor supporting the idea that protein regions outside the truncated MCAK (A182) play a

regulatory role (unpublished data, Ayana Moore and Linda Wordeman). Future studies involving a detailed analysis of the relationship between MCAK structure and its catastrophe-promoting activity should help resolve this issue.

4.3. Reduction in the microtubule polymer mass by MCAK

Consistent with previous studies [14,20], MCAK reduced the length of the axoneme-seeded steady state microtubules by 36% and A182 reduced the length by 64% (Fig. 3). In addition to the reduction in the length of the microtubules, there was also a reduction in the number of microtubules assembled from the seeds. Surprisingly, the reduction in the mean lengths and microtubule number occurred both in the presence and absence of ATP, while the catastrophe-promoting activity only occurred in the presence of ATP. One possible reason for the reduction in microtubule mass could be that MCAK was binding to soluble tubulin inactivating or sequestering it. In support of this idea, several studies have shown that MCAK is capable of binding to tubulin dimers. For example, Desai et al. [14] showed that MCAK homologues could bind tubulin dimers in the presence of AMPPNP. In addition, soluble tubulin is capable of stimulating the ATPase activity of MCAK [17,23] further supporting the idea that MCAK is capable of binding to tubulin dimers. There are several plausible reasons for why MCAK might bind to soluble tubulin in our dynamics assays. One reason is that the binding of MCAK to tubulin dimer in the absence of nucleotide is a step in MCAK's enzymatic pathway. Moores et al. [23] proposed that MCAK homologues in a nucleotide free (inactive) state allow MCAK to search for a "productive binding site" such as the terminal tubulin dimers of capped microtubules. It is thought based on this model that soluble GTP-tubulin would have similar structural attributes to terminal tubulin dimers at the microtubule ends. Finally, we cannot rule out the possibility that the enzymatically inactive fraction of the MCAK in this work (unable to bind ATP) sequesters tubulin in a non-physiological manner.

4.4. How might MCAK increase the catastrophe frequency?

We found that the catastrophe-promoting activity of FL-MCAK and A182 was dependent on the presence of ATP (Table 1). To test whether ATP hydrolysis was necessary for MCAK's catastrophe promoting activity, we also analyzed the effects of MCAK on the catastrophe promoting activity in the presence of the non-hydrolyzable ATP analogue, AMPPNP (2 mM). The catastrophe-promoting activity of MCAK in the presence of AMPPNP was the same as in the absence of ATP, suggesting that ATP hydrolysis is necessary for MCAK's microtubule catastrophe-promoting activity (data not shown). These results are consistent with those of Hunter et al. [17] who found that ATP hydrolysis is necessary for MCAK's depolymerizing activity, and are consistent with the hypothesis of Moores et al. [23] that the hydrolysis of ATP is required for converting a growing microtubule end to a shortening end.

Several studies have led to the idea that MCAK and its homologues destabilize microtubules by inducing a conformational change at the end of a microtubule, which promotes microtubule shortening [14,23]. Our results also support the idea that MCAK destabilizes microtubules by acting at microtubule ends. Perhaps, MCAK specifically binds to the stabilizing tubulin-GDP-Pi or GTP cap, converting it to the strained rapidly disassembling tubulin-GDP form [24]. The observed increase in the catastrophe frequency of HeLa cell microtubules in the presence of MCAK must be due to the binding of MCAK to the microtubules. Furthermore, extremely small quantities of MCAK were capable of increasing the catastrophe frequency, suggesting that MCAK's destabilizing activity is the result of MCAK binding at microtubule ends. Quantitatively, based on our data and experimental conditions, only 1 molecule of FL-MCAK was present for every 263 tubulin dimers (both soluble tubulin and in microtubules), suggesting that for a microtubule that is 3 μm in length (1690 dimers/μm) there would be ~9 molecules available per microtubule end, indicating that only a few molecules of MCAK are needed to elicit catastrophes at the ends of microtubules. In summary, the data indicate that MCAK is a potent ATP-dependent catastrophe factor, which mechanistically binds to and destabilizes microtubule ends in vitro, supporting the idea that MCAK is a catastrophe-promoting factor in cells.

Acknowledgements: This work was supported by USPHS Grant NS13560, the Materials Research Program of the National Science Foundation under award NSF DMR 0080034, and by the Department of Defense DAMD17-01-1-0450. We thank Drs. Kathy Kamath Mitchelson and Doug Thrower for critically reading the manuscript.

References

[1] Mitchison, T.J. and Kirschner, M. (1984) Nature 312, 237–242.
[2] Horio, T. and Hotani, H. (1986) Nature 321, 605–607.
[3] Walker, R.A., O'Brien, T.O., Pryer, N.R., Soboeiro, M.F., Voter, W.A., Erickson, H.P. and Salmon, E.D. (1988) J. Biol. Chem. 107, 1437–1448.
[4] Hyams, J.S. and Lloyd, C.W. (1994) Microtubules. In: Mod. Cell Biol., 13, pp. 1–439, Wiley-Liss, New York.
[5] Desai, A. and Mitchison, T.J. (1997) Annu. Rev. Cell Dev. Biol. 13, 83–117.
[6] McNally, F.J. (1996) Mol. Cell. Biol. 8, 23–29.
[7] Anderson, S.S.L. (1999) BioEssays 21, 53–60.
[8] Cassimeris, L. (1999) Curr. Opin. Cell Biol. 11, 134–141.
[9] Kinoshita, K., Arnal, I., Desai, A., Drechsel, D.N. and Hyman, A.A. (2001) Science 294, 1340–1343.
[10] Newton, C.N., DeLuca, J.G., Himes, R.H., Miller, H.P., Jordan, M.A. and Wilson, L. (2002) J. Biol. Chem. 277, 42456–42462.
[11] Wordeman, L. and Mitchison, T.J. (1995) J. Cell Biol. 128, 95–104.
[12] Vale, R.D. and Fletterick, R.J. (1997) Annu. Rev. Cell Dev. Biol. 13, 745–777.
[13] Walczak, C.E., Mitchison, T.J. and Desai, A. (1996) Cell 84, 37–47.
[14] Desai, A., Verma, S., Mitchison, T.J. and Walczak, C.E. (1999) Cell 96, 69–78.
[15] Kinoshita, K., Arnal, I., Desai, A., Drechsel, D.N. and Hyman, A.A. (2001) Science 294, 1340–1343.
[16] Maney, T., Wagenbach, M. and Wordeman, L. (2001) J. Biol. Chem. 276, 34753–34758.
[17] Hunter, A.W., Caplow, M., Coy, D.L., Hancock, W.O., Diez, S., Wordeman, L. and Howard, J. (2002) Mol. Cell 11, 445–457.
[18] Maney, T., Hunter, A.W., Wagenbach, M. and Wordeman, L. (1998) J. Cell Biol. 142, 787–801.
[19] Ovechkina, Y., Wagenbach, M. and Wordeman, L. (2002) J. Cell Biol. 159, 557–562.
[20] Kline-Smith, S.L. and Walczak, C.E. (2002) Mol. Biol. Cell 13, 2718–2731.
[21] Coy, D.L., Wagenbach, M. and Howard, J. (1999) J. Biol. Chem. 274, 3667–3671.
[22] Bradford, M.M. (1976) Anal. Biochem. 72, 248–254.
[23] Moores, C.A., Hekmat-Nejad, M., Sakowicz, R. and Milligan, R.A. (2003) J. Cell Biol. 163, 963–971.
[24] Panda, D., Miller, H.P. and Wilson, L. (2002) Biochemistry 41, 1609–1617.

Biochemical Journal Immediate Publication. Published on 13 Jul 2004 as manuscript BJ2004

The Carboxyl-Terminus of Mitotic Centromere-Associated Kinesin (MCAK) Inhibits Its Lattice Stimulated ATPase Activity

Ayana Moore* and Linda Wordeman
University of Washington School of Medicine, Department of Physiology and Biophysics, Seattle, WA

*Corresponding author:
Ayana Moore
Department of Physiology and Biophysics
1959 NE Pacific St.
Box 357290
Seattle WA 98195
(206) 543-9184 (lab)
(206) 685-0619 (fax)
atmoore@u.washington.edu

Dr. Linda Wordeman
Department of Physiology and Biophysics
1959 NE Pacific St.
Box 357290
Seattle WA 98195
(206) 543-4135 (office)
(206) 685-0619 (fax)
worde@u.washington.edu

Condensed title: C-terminus Inhibits Lattice ATPase

Character count: 35,503

Key words: XKCM1, Kin I, kinesin, mitosis, microtubule, depolymerization

Copyright 2004 Biochemical Society

Biochemical Journal Immediate Publication. Published on 13 Jul 2004 as manuscript BJ20040736

Abstract:

Mitotic Centromere-Associated Kinesin (MCAK) is a microtubule (MT) destabilizing molecular motor. Here we show that the final eight amino acids of MCAK's carboxy-terminus (C-terminus) inhibit lattice-stimulated ATPase activity of the motor. Surprisingly, loss of this C-terminal "tail" (MCAK-Q710) leads to more rapid depolymerization of MTs relative to full length MCAK (wt-MCAK). Biochemical and microscopic assays revealed that MCAK-Q710 bound to the MT lattice with higher apparent affinity as compared to wt-MCAK. End-stimulated depolymerization was similar for both enzymes. These data suggest that lattice-bound MCAK can increase the rate of MT depolymerization but at an energy cost. The function of MCAK's C-terminus may be to selectively inhibit lattice-stimulated ATPase activity resulting in limited interactions of the motor with the MT lattice. This increases the coupling between ATP hydrolysis and tubulin dimer release, but it also limits MT depolymerization.

Copyright 2004 Biochemical Society

Biochemical Journal Immediate Publication. Published on 13 Jul 2004 as manuscript BJ20040736

Introduction:

The kinesin superfamily consists of motor proteins that convert chemical energy, through ATP hydrolysis, into physical work [1-4]. These motors are involved in a wide range of cellular functions such as vesicle transport along MT tracks, signal transduction, and MT polymer dynamics [1, 2, 5]. Mitotic Centromere Associated Kinesin (MCAK, the hamster orthologue of mouse Kif2C [6, 7]) belongs to the Kin I (Internal motor domain) or M-type [6] subfamily of kinesin-related proteins and shares a highly conserved ATP-hydrolyzing motor (head) domain with other members of this subfamily [2, 8]. Unlike many other kinesins, which transport cargo along the surface of MTs, MCAK and its homologues depolymerize them [9-12]. This activity is critical for proper cell division [10, 13-15] and in modulating interphase MT dynamics [10, 11].

In the presence of ATP, purified MCAK and its homologues are very efficient microtubule (MT) depolymerizers. However, where on the MT and when, exactly, MCAK hydrolyzes ATP is still a matter of debate. Because MCAK localizes preferentially to the ends of stabilized MTs in the presence of a non-hydrolysable form of ATP (AMP-PNP) [9], one current model suggests that MCAK associates loosely with the lattice of MTs, perhaps through electrostatic interactions, and then translocates via one-dimensional diffusion to the MT ends where depolymerization takes place [9, 16, 17]. MT destabilization (in the form of protofilament peels) occurs even in the presence of AMP-PNP when the stoichiometry of Kin I motor to tubulin in polymer is high [18]. These data led researchers to propose that the sole purpose of ATP hydrolysis is to trigger the dissociation of the terminal tubulin dimer [9, 17].

In contrast to MCAK, conventional kinesin translocates along the MT lattice using a mechanism that is tightly coupled to ATP hydrolysis [19, 20]. Conventional kinesin exists in two different conformations, compact/folded and unfolded [21]. Folding is promoted by an interaction between the C-terminus and the head/neck region. In the folded state, ATP hydrolysis is inhibited [22, 23]. Irrespective of the striking functional differences, we show here that when the C-terminus of MCAK is truncated, MT-

Copyright 2004 Biochemical Society

Biochemical Journal Immediate Publication. Published on 13 Jul 2004 as manuscript BJ20040736

stimulated ATPase activity is increased. Interestingly, the MT depolymerization rate is increased both *in vivo* and *in vitro* in the absence of the C-terminus. Truncated MCAK (MCAK-Q710) binds with higher apparent affinity to the MT lattice as compared to the full-length protein (wt-MCAK). These results suggest that inhibition of lattice ATPase by the C-terminus may be a fundamental property of N-type and M-type kinesins.

We propose that the C-terminus of wt-MCAK, analogous to conventional kinesin, acts as a selective inhibitor of ATP hydrolysis that negatively influences the protein's interaction with the MT lattice. For MCAK, the tail may inhibit a process we call "lattice priming," in which the motor becomes tightly coupled to the MT lattice during specific stages of the ATP hydrolysis cycle. As the MT ends approach, active motors present along the lattice can participate in depolymerization thus affording the system more effective depolymerization as it mitigates the limitations of the simple diffusive end targeting of the wild type motor.

Copyright 2004 Biochemical Society

Biochemical Journal Immediate Publication. Published on 13 Jul 2004 as manuscript BJ20040736

Materials and Methods

Constructs

MCAK constructs were made by ligating MCAK PCR products (from pOPRSVICAT-GFP-MCAK [15]) with TOPO NT-GFP fragments (Invitrogen Corp., Carlsbad, CA). Deletions were confirmed by DNA sequencing.

Cell culture, transfection and immunofluorescence

Cells were cultured, fixed and immunofluorescently labeled as described [11]. For cells cultured in the presence of paclitaxel, 15μM paclitaxel was added 2 hours into the transfection (using Lipofectamine, Carlsbad, CA) and maintained 20 hours until fixation. Tubulin was labeled with mouse anti-tubulin DM1α (Sigma ImmunoChemicals, St. Louis, MO) and Texas Red anti-mouse (Jackson ImmunoResearch, Inc., West Grove, PA). Analysis was done with a Nikon FX-A microscope equipped with a 60X/1.4 NA Plan Apo oil objective. Digital images were acquired with a Sensys cooled CCD camera (Photometrics, Tucson, AZ) controlled by QED camera software (QED Imaging, Inc., Tucson, AZ).

Quantitation of MT depolymerization *in vivo*

GFP:MCAK fusion constructs were transfected into CHO cells and cultured in the presence of 15μM paclitaxel for 20 hours. Cells were then fixed and labeled with DM1α. Digital images were acquired using a cooled CCD camera. Images of transfected cells were collected for GFP and MT fluorescence using the same exposure times, respectively. Images were saved as 8-bit TIFF files with a 256 gray scale range. Quantification was performed using NIH Image 1.62 and Microsoft Excel. Interphase cells chosen for quantitation displayed similar levels of cytoplasmic GFP expression. The average pixel intensity (mean gray value) of GFP in the cytoplasm was measured for both constructs to control for variations in the extent of nuclear sequestration. Using a gray scale image of MTs, where MTs appear in intensity between white and light gray (grayscale value between 0 and 120) on a nearly black (grayscale value near 256) background, we recorded the pixels present within the grayscale range of 0 and 120. This

Copyright 2004 Biochemical Society

number was divided by the total pixels in the cell. The resulting number gave us a normalized value representing the amount of tubulin polymer per cell.

Expression and purification of recombinant MCAK

MCAK-Q710 was constructed by ligating a PCR fragment containing the truncated C-terminus into pVL1393-MCAK digested with NotI and NcoI. EGFP labeled MCAK constructs were made by digesting EGFP-MCAK from pYOY152 (from Y. Ovechkina) and ligating it into the Baculovirus expression vector, pVL1393 (Pharmingen, San Diego CA). Baculovirus expression of recombinant 6x-histidine tagged MCAK in Sf9 cells (Pharmingen, San Diego, CA) and its purification on a nickel-nitrilotriacetic (Ni-NTA) agarose columns (Qiagen Inc., Chatsworth, CA) were performed as previously described [15]. Peak fractions in elution buffer [15] were stored at -70° C. The number of active nucleotide binding sites was measured radiometrically as previously described [23]. Because MCAK is a dimer [15], the concentrations are always expressed as the number of active heads.

***In vitro* MT assembly**

Bovine brain tubulin was acquired from Cytoskeleton (Denver, CO). For *in vitro* pelleting assays, 2.2μM of tubulin was added to BRB80 (80mM Pipes, pH 6.8, 1mM EGTA, 1mM $MgCl_2$) with 6mM $MgCl_2$, 1.5mM GTP, and 1.4M DMSO and incubated for 30 minutes at 37° C. Following the incubation, MTs were diluted 1:20 in 37° C BRB80 plus 10μM paclitaxel. Variable MT lengths were achieved by passing MTs through a 30-gauge syringe of either 0.5 inches in length (Becton Dickinson, Franklin Lakes, NJ) or 2.0 inches in length (Hamilton Co., Reno NV). Resulting lengths (5μm and 15μm, respectively) were determined via immunofluorescent microscopy. Unsheared MTs can extend to ~40μm in length but may retain bundled MT polymer and have a less consistent length distribution as compared to the sheared polymer. For ATPase assays, 11μM of tubulin was added to BRB80 with 8mM $MgCl_2$, 2mM GTP and 1.9M DMSO, and grown at 37° C as before. MTs were then diluted 1:2 with BRB80 plus paclitaxel for a final paclitaxel concentration of 7.5μM.

Copyright 2004 Biochemical Society

Biochemical Journal Immediate Publication. Published on 13 Jul 2004 as manuscript BJ20040736

GMP-CPP rhodamine labeled MTs were grown by combining 4 μg unlabeled bovine brain tubulin and 1 μg rhodamine-labeled bovine brain tubulin, 6mM $MgCl_2$, 1.5mM GMP-CPP, and 1.4M DMSO and incubated for 30 minutes at 37° C. Following the incubation, MTs were diluted 1:12.5 in 37° C BRB80. MTs were then spun in an airfuge at 149,000 x g for 10 minutes in order to separate out any unincorporated tubulin. All MTs were used within 24 hours of being polymerized.

***In vitro* MT depolymerization assays**

Elution buffer containing 50nM of active motor protein was mixed with 0.8mM DTT, 1.2mM MgATP, 75mM KCl and 2.2μM paclitaxel stabilized MT polymer. Reactions were incubated at room temperature for 16 minutes and centrifuged in an airfuge at 149,000 x g for 10 minutes. (50μM MgATP and a three-minute incubation were used to generate the binding curve for the motor.) Supernatants and pellets were assayed for the presence of tubulin and motor on Coomassie stained SDS-polyacrylamide gels (Invitrogen, Carlsbad, CA). Bands were quantified using NIH Image 1.62. The extent of depolymerization with the 2 constructs was assayed by comparing the total amount of tubulin in the supernatant minus the supernatant of a no-motor control. Motor affinity was assayed by comparing the percentage of motor in the pellet over a range of motor to tubulin stoichiometries. Asymptotic values were obtained using an exponential association curve (see **ATPase assays** below)

***In vitro* motor/rhodamine-MT squashes**

1.8 mM of rhodamine-labeled MTs was combined with 30nm of active EGFP labeled motor. MT/motor mixture was incubated in BRB80 containing 3mM AMP-PNP or ADP (or no nucleotide), 75 mM KCl, 1mg/ml BSA, and an anti-fade solution consisting of 40mM D-glucose, 200 μg/ml glucose oxidase, 35 μg/ml catalase, 1mM DTT, and 0.5% BME. After 5 minutes, 2 μl of this solution was squashed onto a microscope slide under a glass coverslip. ADP.Pi mimicked experiments (ADP.AlFx) were performed as previously described [24] with the minor substitution of using NaF as opposed to KF.

Copyright 2004 Biochemical Society

Biochemical Journal Immediate Publication. Published on 13 Jul 2004 as manuscript BJ20040736

ATPase assays

Assays were performed as previously described [17].

'On' and 'off' rates for ATPase experiments were evaluated with an exponential association curve fit over a 60-minute time interval: $F(t) = A(1 - e^{-k_{OB}t})$

A: asymptotic value; t: time; k_{OB}: observed association rate expressed in inverse time; k_{OB}: k_{ON}[MCAK] + k_{OFF}

Constants were determined with a non-linear least squares fit. Regression analysis and curves were generated using MATLAB (The MathWorks Inc.) and Microsoft Excel.

Copyright 2004 Biochemical Society

Biochemical Journal Immediate Publication. Published on 13 Jul 2004 as manuscript BJ20040736

Results

C-terminal truncations of MCAK exhibit increased MT depolymerization *in vivo*

Chinese Hamster Ovary (CHO) cells transfected with full-length MCAK (wt-MCAK) display a complete loss of MT polymer by 20 hours post-transfection (figs. 1a, 1b). However, when wt-MCAK transfected cells are cultured for the same time duration in the presence of 15μM paclitaxel, they exhibit only a partial loss of MT polymer (figs. 1c, 1d). Partial abrogation of MCAK activity with paclitaxel allowed us to differentiate between MCAK constructs with slightly dissimilar rates of MT depolymerization.

Maney et al. [11] observed that wt-MCAK exhibited slightly lower MT depolymerization activity than a construct of MCAK missing the entire C-terminus (the region immediately following the motor domain). In order to precisely map this inhibitory domain, we prepared successively smaller C-terminus deletions of MCAK and transfected these constructs into CHO cells cultured in the presence of 15μM paclitaxel. By inspection, cells transfected with C-terminus deletions between S583 and Q710 exhibited equally enhanced MT depolymerization when compared to wt-MCAK (fig. 1g). We determined that it is the terminal eight amino acids that are responsible for the partial auto-inhibition of MT depolymerization activity of full length MCAK.

Quantitation of the C-terminal inhibition of MT depolymerization *in vivo*

MCAK-Q710 was chosen for quantitative comparison with wt-MCAK as it was the most intact truncation construct with maximally enhanced MT depolymerization. Figs. 1e and 1f show a cell transfected with MCAK-Q710, cultured in the presence of paclitaxel. MCAK-Q710 is able to depolymerize bundled MTs to a significantly greater extent than wt-MCAK.

In order to quantitate the extent of depolymerization for both MCAK constructs, we devised a method using digital images of transfected cells (described in the Methods).

Copyright 2004 Biochemical Society

Biochemical Journal Immediate Publication. Published on 13 Jul 2004 as manuscript BJ20040736

The relative amount of tubulin polymer remaining in a population of transfected cells is shown in fig. 2a. Wt-MCAK and MCAK-Q710 transfected cells exhibited a significant difference in the extent of polymer loss according to a paired t-Test with 95% confidence. In addition, we measured the relative levels of cytoplasmic MCAK expression and found that these two populations of cells exhibited statistically indistinguishable levels of cytoplasmic protein expression (fig. 2b). This suggests that the difference in depolymerization is not due to sequestration of MCAK-Q710 away from cytoplasmic MTs.

In vitro MT depolymerization is enhanced by the loss of MCAK's C-terminus

To confirm that the difference in MT depolymerization seen *in vivo* was intrinsic to the motor and not the result of interactions with other cellular proteins, we performed a series of *in vitro* depolymerization assays. Wt-MCAK and MCAK-Q710 purified from SF9 cells (see Methods) were incubated with paclitaxel-stabilized MTs (about 15μm in length, on average), and MgATP and then pelleted. The amount of tubulin released into the supernatant was quantified on an SDS-gel as an indication of the extent of MT depolymerization. Any motor found in the supernatant is either unbound or associated with free tubulin. Motor seen with the pellet is presumably bound to the MT polymer. Quantitation of these gels revealed that MCAK-Q710 was approximately 25% more potent as a MT depolymerizer than wt-MCAK *in vitro* (fig. 3a). In addition, more MCAK-Q710 was found in the MT pellet as compared to wt-MCAK suggesting that the deletion construct may have a higher apparent-affinity for the MT polymer. Pelleting assays performed over a range of motor to tubulin stoichiometries confirmed that MCAK-Q710 does in fact have a higher affinity for the MT (fig 3b). Saturating experiments revealed that in the presence of 25μM MgATP and 44μM MT polymer, MCAK-Q710 saturates the MT polymer at 527μM whereas wt-MCAK saturates at 453μM, a 16% increase. (Saturating equation described in Methods.)

C-terminal truncation of MCAK increases MT lattice-stimulated ATPase activity.

Copyright 2004 Biochemical Society

Biochemical Journal Immediate Publication. Published on 13 Jul 2004 as manuscript BJ20040736

MCAK exhibits both free tubulin-stimulated and MT-stimulated ATP hydrolysis [17]. One possible model suggests that ATP hydrolysis or inorganic phosphate release may serve to dissociate MCAK from the removed terminal tubulin dimer [6, 9, 17, 18]. Some researchers believe that this happens before the tubulin/MCAK complex dissociates from the MT protofilament, resulting in processive depolymerization [17]. Others believe that it occurs afterwards [6, 18]. In either case, we wanted to determine if MCAK-Q710 had a higher depolymerization rate because it was able to more quickly promote the dissociation of the motor from the terminal tubulin dimer. To test this, we measured the tubulin-stimulated ATPase activity for both wt-MCAK and MCAK-Q710 (figs. 4a, 4b). MCAK-Q710 and wt-MCAK had nearly identical tubulin-stimulated phosphate release rates, suggesting that the enhanced MT depolymerization of MCAK-Q710 is not due to an enhanced rate of tubulin dissociation from the motor.

We measured the MT-stimulated ATPase activity using paclitaxel-stabilized MTs. MCAK-Q710 exhibited a higher rate of ATPase activity in the presence of MTs as compared to wt-MCAK (figs. 4c, 4d, 4e). This was most significantly pronounced with longer MTs, which have a higher ratio of lattice to ends.

We fit our ATPase data (the phosphate released in the experiments) to an exponential association curve (described in Methods). We interpreted the ATPase activity in these experiments as an indicator of an ATP stimulating, tight coupling reaction between MCAK and the MT. This particular measurement does not discriminate between end and lattice binding. 'On' and 'off' rates were determined by varying MCAK concentrations (data not shown).

We chose 15μm MTs because their length is more consistent with those found in cells. 'On' and 'off' rates are listed in Table 1a. The MT on-rate for wt-MCAK, as indicated by the hydrolysis of ATP, is approximately 2.3-fold less than that of MCAK-Q710 suggesting that MCAK-Q710 finds high affinity, ATPase stimulating, binding sites more quickly than wt-MCAK. In contrast, the off-rates for both were comparable for the two proteins (Table 1a).

Copyright 2004 Biochemical Society

We evaluated the initial velocities of ATPase activities for both wt-MCAK and MCAK-Q710 in order to compare the initial motor/MT interactions (Table 1b). It can be seen for each MT length that MCAK-Q710 has an approximate 3-fold increase in ATPase activity at the initial rates.

To compare ATPase activity to MT depolymerization, we plotted the tubulin released from comparable pelleting assays at a number of time points, along side the ATPase curve (fig. 5). It can be seen that wt-MCAK displays an ATPase activity that more closely tends toward a 1:1 stoichiometry with tubulin dimer release in comparison to MCAK-Q710. The ATPase activity of MCAK-Q710 quickly diverges from the rate of tubulin release.

MCAK-Q710 binds lattice more readily in the zero ATP state.

In order to determine microscopically where MCAK was interacting with the MT during ATP hydrolysis, we constructed and purified EGFP fusion constructs of both motors. We incubated EGFP fusion motors with MTs in the presence of AMP-PNP (to mimic the ATP-bound state), ADP.AlFx (which mimics the ADP.Pi state), ADP, and no nucleotide. The results are shown in figs. 6a and 6b (ADP.AlFx data not shown). Both EGFP:wt-MCAK and EGFP:MCAK-710 accumulate at MT ends in AMP-PNP. In the ADP.Pi state, there was very little detectable binding of wt-MCAK to the MT within the first 15 minutes of the incubation (data not shown). After a 45-minute incubation, there was a slight increase in binding (from approximately 1%-10%) solely at the microtubule ends. We were unable to detect any association of MCAK-Q710 in this ADP.PI mimicked state with MTs within 45 minutes. This is likely to reflect a difference in the limits of detection of MCAK-Q710 (due to its tendency to aggregate less as seen in figs. 6a and 6b, motor only) rather than a difference in end binding between the two proteins. In the presence of ADP, there is no detectable binding of either motor to the MT on the lattice or the MT end.

Copyright 2004 Biochemical Society

In the absence of nucleotide, both MCAK constructs significantly bundle MTs. However, there is a distinct difference in the lattice decoration of EGFP:wt-MCAK in comparison to EGFP:MCAK-Q710. Wt-MCAK appears to sparsely decorate the lattice in a punctate fashion whereas MCAK-Q710 appears to bind more uniformly throughout the lattice.

We tested the hypothesis that ATP is required to free MCAK from free tubulin dimers by determining whether incubation with free tubulin could inhibit the MT bundling observed in the nucleotide free state. At a 1:1 stoichiometry of free to polymerized tubulin, MT bundling was reduced ~20%. At an 8:1 stoichimoetry, bundling was reduced ~90%. Results were similar for both motors. These data suggest that tubulin can sequester MCAK away from the MT lattice in the absence of nucleotide.

Copyright 2004 Biochemical Society

Biochemical Journal Immediate Publication. Published on 13 Jul 2004 as manuscript BJ20040736

Discussion

MCAK has a high affinity for MT ends which is the substrate for its depolymerizing activity [17]. Here we show that lattice-bound MCAK can also significantly increase the efficacy of MT depolymerization although at an energy cost (uncoupling). The interaction of MCAK with the lattice is inhibited by eight amino acids at the C-terminus of the protein. Therefore, MCAK has a mechanism to suppress lattice interactions in preference for end-binding which is the productive substrate for MT depolymerization [17]. What is surprising however is that lattice-bound MCAK increases the velocity with which MTs are depolymerized rather than serving as a sink for unproductive interactions.

The extreme C-terminus of MCAK is an auto-inhibitor of ATPase activity along the MT lattice

Wt-MCAK and MCAK-Q710 exhibit a significant difference in MT-stimulated ATPase activity. This disparity increased with the length of the MTs (and by extension, with longer exposure to the MT lattice), presumably because MCAK-Q710 can interact productively (in a manner that stimulates ATP hydrolysis) with more sites along the MT lattice in comparison to wt-MCAK.

A comparison of the on-rates revealed that MCAK-Q710 finds an ATPase stimulating binding site along the MT at a rate 2.3 times faster than wt-MCAK. Furthermore, by comparing ATPase activity to MT depolymerization, we saw that wt-MCAK tends toward a 1:1 stoichiometry where as MCAK-Q710 quickly diverges from this trend. This suggests that with paclitaxel stabilized MTs, ATP hydrolysis is more strongly coupled to MT depolymerization for wt-MCAK. Our data suggests that when the ratio of lattice to ends increases, both motors tend to exhibit non-end stimulated ATP-hydrolysis. Hunter et al. also observed that wt-MCAK exhibited low lattice stimulated ATPase activity in particular, when the concentration of motor exceeded the concentration of exposed MT ends [17]. However, wt-MCAK significantly suppresses this activity in comparison to MCAK-Q710. Again, this suggests that the role of the C-terminus may be to suppress

Copyright 2004 Biochemical Society

lattice stimulated ATPase activity. Relief of inhibition by the C-terminus (via protein interactions or clipping) might be one method that organisms could employ to rapidly disassemble long cellular MTs.

Our experiments indicate an on-rate for wt-MCAK that is approximately 8-fold less than that found by Hunter et al. [17] However, two important differences in experimental design should be noted. The first is that different MT stabilizing mechanisms were used – paclitaxel verses GMP-CPP. It has not yet been determined if the differences in these stabilizations affects the method or efficiency in which MCAK depolymerizes MTs. It can however be noted that the extreme disparity that Hunter et al. observed between the tubulin-stimulated ATPase activity and that stimulated by MTs is not present in our experiments. Our measurements are more consistent with Moores et al. [25] in which they saw comparable maximum ATPase activity with free tubulin and paclitaxel stabilized polymer. The second difference is that there is a considerable difference in our MT lengths. MTs from Hunter et al. were on the order of 2.2μm whereas ours are approximately 15μm. If we consider the notion that wt-MCAK primarily employs Brownian motion to diffuse to MT ends, and MT ends are the primary site of ATP hydrolysis for wt-MCAK, then the difference in diffusion times may account for the difference in the on-rates.

A model: enhanced depolymerization of MCAK-Q710 may result from additional motors being distributed along the MT lattice

We propose that MCAK, analogous to kinesin and myosin II [22, 26], may exist in 2 conformations: folded (inactive, limited ATPase activity) and unfolded (active ATPase activity). The C-terminus of MCAK may contribute to keeping the motor in the folded conformation when not at the highest affinity binding site (MT ends) to inhibit excess ATP hydrolysis along the lattice (fig. 7). This may serve as an important regulatory mechanism particularly when the cell is not actively remodeling its MT array. Once MCAK encounter a protofilament end, high-affinity binding to the conformationally distinct terminal tubulin [27, 28] may out compete the C-terminus for the binding of the

Copyright 2004 Biochemical Society

motor and releases the ATPase inhibition. Alternatively, the MCAK C-terminus may possess a binding domain for the end of the terminal tubulin dimer, comparable to that of ncd [29] (fig. 7a). Selective binding to the terminal tubulin dimer may also provide some insight as to why MCAK, unlike most other kinesins, has free tubulin stimulated ATPase activity.

Fig. 7a illustrates our proposed ATP hydrolysis cycle of wt-MCAK. The model is similar to others that have been put forth [6, 17] in that it suggests that MCAK's binding to the MT lattice promotes the release of ADP which results in the binding of ATP. We suggest that the motor oscillates in the ATP-bound state until it finds a MT end. This is supported by our observation that MCAK binds with significantly lower affinity to MT ends in the ADP.Pi state in comparison to the ATP bound state. ATP hydrolysis may promote the active release of the terminal tubulin dimer from the MT ends. Subsequent release of inorganic phosphate might then trigger the dissociation of the released dimer from the MCAK motor leaving the motor in the ADP state and ready for another cycle. Our assays do not resolve whether or not MCAK functions as a processive motor (both cases are illustrated in fig. 7a). Our model for the activity of MCAK-Q710 accommodates either case.

We have identified the C-terminus as an inhibitor of high affinity, ATPase stimulating, lattice interactions. We have also demonstrated that MCAK-Q710 exhibits increased depolymerization activity relative to wt-MCAK. Lattice binding is presumed to be a sink for end-stimulated depolymerization. How do we reconcile these observations? We put forth two plausible explanations.

The first possibility is compatible with the observation that MCAK may be processive [17]. Biased diffusional motility of MCAK, which involves intermittent ATP hydrolysis can potentially explain the enhanced activity of MCAK-Q710. If the C-terminus tail inhibits lattice interactions that would lead to ATP hydrolysis, then the absence of the tail (MCAK-Q710) may result in ATP dependent biased diffusion of the motor along the lattice as is seen for Kif1A monomers [30]. Considering the time it would take for a

Copyright 2004 Biochemical Society

Biochemical Journal Immediate Publication. Published on 13 Jul 2004 as manuscript BJ20040736

motor to reach a MT ends via simple Brownian motion along the lattice, it stands to reason that directed movement via a processive mechanism, may result in faster end targeting. This precise mechanism has been elegantly established for Kif1A [30].

Because we have never observed such ATP-dependent lattice motility and because the processivity measured for MCAK is relatively weak [17], we also considered the formal possibility that MCAK is not processive. Our biochemical and microscopic assays confirm that the higher apparent-affinity of MCAK-Q710 is not due to enhanced accumulation of motor at the MT end but rather on the lattice. Therefore, we suggest a model in which MCAK's mechanism of MT depolymerization includes a feature that we call "lattice priming". While directed movement along the lattice and lattice priming are not mutually exclusive mechanisms it is important to note that lattice priming has the potential to mimic processivity, possibly resulting from the tendency of wt-MCAK to aggregate.

The lattice-priming model accommodates the situation in which a slightly higher apparent-affinity of the motor for the MT lattice promotes a slightly enhanced level of depolymerization. The active conformation of MCAK-Q710 may allow it to exist sparsely along the MT lattice, at a higher apparent-affinity at specific times during the ATP hydrolysis cycle. This activity will not directly translate to depolymerization because the tubulin dimers are locked within the lattice. However, as the MT ends approach, active motors tightly bound along the lattice will participate in depolymerization thus affording the system more efficient depolymerization as it will be less limited by the simple diffusive property of the full-length motor. These models are illustrated in figs. 7b and 7c.

Although we propose that MCAK-Q710 may bind with higher affinity along the MT lattice during certain stages of the ATP hydrolysis cycle, it is important to remember that this mutant, analogous to wt-MCAK, depends on loose tethering to the MT lattice through much of the cross-bridge cycle in order to maintain un-interrupted contact with the MT lattice. This is consistent with the results of our pelleting assays where salt

Copyright 2004 Biochemical Society

Biochemical Journal Immediate Publication. Published on 13 Jul 2004 as manuscript BJ20040736

concentrations were markedly increased. In these instances, both wt-MCAK and MCAK-Q710 were diminished in their ability to depolymerize MTs (data not shown).

Increasing the apparent-affinity of MCAK for MTs can enhance its MT depolymerizing activity by promoting lattice priming. In the cell, simple diffusion along long cellular MTs may not be an efficient method for targeting MT ends, particularly when rapid re-ordering of the MT array is required. This represents an excellent mechanism of priming for MCAK-dependent depolymerization activity in situations in which MT ends are blocked by assembly promoting factors (such as CLIP-170 and Eb1 [31, 32]). It is worth noting that GFP-MCAK is often seen transiently associated with the MT lattice *in vivo* (data not shown). It stands to reason that the C-terminus of MCAK serves as an inhibitor of fruitless ATP hydrolysis along the MT lattice for MCAK that is free in solution or when active MT depolymerization is not occurring. Priming of MCAK could then be promoted by any factors that interact with the C-terminus of MCAK thus relieving lattice inhibition. Furthermore, these data suggest that any factor (such as the Kin I activator ICIS [33]), that potentially increases the apparent affinity of MCAK for the MT lattice has the potential to stimulate or enhance MCAK's MT depolymerizing activity in a regulated fashion in response to the need for rapid MT remodeling.

Acknowledgements

We thank Michael Wagenbach for the unlabeled wt-MCAK protein and for the rhodamine labeled tubulin. We thank Jeremy Cooper, Will Hancock (Department of Bioengineering, Pennsylvania State University, University Park, PA), Marla Feinstein, Yulia Ovechkina, and Kathleen Rankin for many discussions and comments on the manuscript. We also thank Steve Carlson and Mark Bothwell for many useful discussions on experimental techniques. This study was supported by National Institute of Health Grant GM53654A and Department of Defense Grant DAMD 17-01-1-0450 (to L. Wordeman) and National Institute of Health Predoctoral Fellowship 1 F31 GM65061 (to A.T. Moore).

Copyright 2004 Biochemical Society

Biochemical Journal Immediate Publication. Published on 13 Jul 2004 as manuscript BJ20040736

Abbreviation list

ADP.AlFx: ADP + aluminum + sodium fluoride

AMP-PNP: adenylyl-imidodiphosphate

CHO: chinese hamster ovary

C-terminus: carboxyl terminus

EGFP: enhanced green fluorescent protein

GFP: green fluorescent protein

GMP-CPP: guanylyl-(alpha,beta)-methylene-diphosphonate

MCAK: mitotic centromere-associated kinesin

MT: microtubule

Pi: inorganic phosphate

wt: wild type

Copyright 2004 Biochemical Society

References:

1 Goldstein, L. S. and Philp, A. V. (1999) Annu Rev Cell Dev Biol **15**, 141-183
2 Vale, R. D. and Fletterick, R. J. (1997) Annu Rev Cell Dev Biol **13**, 745-777
3 Vale, R. D., Reese, T. S. and Sheetz, M. P. (1985) Cell **42**, 39-50
4 Brady, S. T. (1985) Nature **317**, 73-75
5 Vale, R. D. and Milligan, R. A. (2000) Science **288**, 88-95
6 Ogawa, T., Nitta, R., Okada, Y. and Hirokawa, N. (2004) Cell **116**, 591-602
7 Miki, H., Setou, M., Kaneshiro, K. and Hirokawa, N. (2001) Proc Natl Acad Sci U S A **98**, 7004-7011
8 Wordeman, L. and Mitchison, T. J. (1995) J Cell Biol **128**, 95-104
9 Desai, A., Verma, S., Mitchison, T. J. and Walczak, C. E. (1999) Cell **96**, 69-78
10 Walczak, C. E., Mitchison, T. J. and Desai, A. (1996) Cell **84**, 37-47
11 Maney, T., Wagenbach, M. and Wordeman, L. (2001) J Biol Chem **276**, 34753-34758
12 Homma, N., Takei, Y., Tanaka, Y., Nakata, T., Terada, S., Kikkawa, M., Noda, Y. and Hirokawa, N. (2003) Cell **114**, 229-239
13 Tournebize, R., Popov, A., Kinoshita, K., Ashford, A. J., Rybina, S., Pozniakovsky, A., Mayer, T. U., Walczak, C. E., Karsenti, E. and Hyman, A. A. (2000) Nat Cell Biol **2**, 13-19
14 Rogers, G. C., Rogers, S. L., Schwimmer, T. A., Ems-McClung, S. C., Walczak, C. E., Vale, R. D., Scholey, J. M. and Sharp, D. J. (2004) Nature **427**, 364-370
15 Maney, T., Hunter, A. W., Wagenbach, M. and Wordeman, L. (1998) J Cell Biol **142**, 787-801
16 Ovechkina, Y., Wagenbach, M. and Wordeman, L. (2002) J Cell Biol **159**, 557-62
17 Hunter, A. W., Caplow, M., Coy, D. L., Hancock, W. O., Diez, S., Wordeman, L. and Howard, J. (2003) Mol Cell **11**, 445-457
18 Moores, C. A., Yu, M., Guo, J., Beraud, C., Sakowicz, R. and Milligan, R. A. (2002) Mol Cell **9**, 903-909
19 Hua, W., Young, E. C., Fleming, M. L. and Gelles, J. (1997) Nature **388**, 390-393
20 Coy, D. L., Wagenbach, M. and Howard, J. (1999) J Biol Chem **274**, 3667-3671
21 Hackney, D. D., Levitt, J. D. and Suhan, J. (1992) J Biol Chem **267**, 8696-8701
22 Hackney, D. D. and Stock, M. F. (2000) Nat Cell Biol **2**, 257-260
23 Coy, D. L., Hancock, W. O., Wagenbach, M. and Howard, J. (1999) Nat Cell Biol **1**, 288-292
24 Rice, S., Lin, A. W., Safer, D., Hart, C. L., Naber, N., Carragher, B. O., Cain, S. M., Pechatnikova, E., Wilson-Kubalek, E. M., Whittaker, M., Pate, E., Cooke, R., Taylor, E. W., Milligan, R. A. and Vale, R. D. (1999) Nature **402**, 778-784
25 Moores, C. A., Hekmat-Nejad, M., Sakowicz, R. and Milligan, R. A. (2003) J Cell Biol **163**, 963-971
26 Alberts, B., Johnson, A., Lewis, J., Raff, M., Roberts, K. and Walter, P. (2002) Molecular Biology Of The Cell, Garland Science, New York
27 Hyman, A. A., Chretien, D., Arnal, I. and Wade, R. H. (1995) J Cell Biol **128**, 117-125
28 Severin, F. F., Sorger, P. K. and Hyman, A. A. (1997) Nature **388**, 888-891

Copyright 2004 Biochemical Society

Biochemical Journal Immediate Publication. Published on 13 Jul 2004 as manuscript BJ20040736

29 Wendt, T., Karabay, A., Krebs, A., Gross, H., Walker, R. and Hoenger, A. (2003) J Mol Biol **333**, 541-552
30 Okada, Y., Higuchi, H. and Hirokawa, N. (2003) Nature **424**, 574-577
31 Ligon, L. A., Shelly, S. S., Tokito, M. and Holzbaur, E. L. (2003) Mol Biol Cell **14**, 1405-1417
32 Perez, F., Diamantopoulos, G. S., Stalder, R. and Kreis, T. E. (1999) Cell **96**, 517-527
33 Ohi, R., Coughlin, M. L., Lane, W. S. and Mitchison, T. J. (2003) Dev Cell **5**, 309-321

Copyright 2004 Biochemical Society

Biochemical Journal Immediate Publication. Published on 13 Jul 2004 as manuscript BJ20040736

Figure Legends

Figure 1:

C-terminal truncations increase MCAK's depolymerization activity. Illustration of MT depolymerization in CHO cells transfected with wt-MCAK and MCAK-Q710. The first column (A, C, D) shows MTs, antibody labeled against α-tubulin. The second column (B, D, F) shows fluorescent expression of GFP-tagged motor protein. (A) and (B) show a cell transfected with GFP-tagged wt-MCAK. (C) and (D) show a cell transfected with GFP-tagged wt-MCAK, cultured in the presence of 15μM paclitaxel. (E) and (F) show a cell transfected with GFP-tagged MCAK-Q710 in the presence of 15μM paclitaxel. (G) illustrates C-terminal truncations of GFP-tagged MCAK in conjunction with their amino acid truncation sites. Each construct was transiently transfected into CHO cells cultured in the presence of 15μM paclitaxel. Cells were fixed 16 hours post transfection and antibody labeled against α-tubulin. The extent of MT depolymerization was scored for each of the constructs. + was the maximum observed depolymerization represented by the shortest bundles. ++++ was the minimum, represented by longer MT bundles.

Figure 2:

MCAK-Q710 shows enhanced MT depolymerization *in vivo*. (A) shows the difference in tubulin polymer levels for the same populations of cells. (B) is a comparison of the cytoplasmic MCAK expression levels between wt-MCAK and MCAK-Q710. Fluorescent intensity levels are measured over 256 gray scale values. Error bars are shown for each.

Figure 3:

MCAK-Q710 depolymerizes paclitaxel-stabilized MTs faster than wt-MCAK *in vitro* and exhibits increased apparent affinity for the MT. SDS-PAGE illustrates the

Copyright 2004 Biochemical Society

difference in localization and depolymerization activity between wt-MCAK and MCAK-Q710. (**S**)upernatant lanes show the amount of free tubulin dimer and unbound protein left in solution after the reaction was centrifuged. (**P**)ellet lanes illustrate the amount of larger polymer and any bound motor protein after centrifugation. The upper bands in the gel are MCAK motor and the lower bands are tubulin. (A) In each experiment, 50nM of active motor was added to 2200nM paclitaxel stabilized MTs and 1mM MgATP. MTs were sheared to a length of 15μm on average. The depolymerization reactions went for 16 minutes at room temperature. (B) illustrates the binding of motor to the MT over a range of motor concentrations. Saturating experiments demonstrate that in the presence of 25μM MgATP and 8.8μM MT polymer, MCAK-Q710 saturates the MT polymer at 527μM whereas wt-MCAK saturates at 453μM, a 16% increase. Curves were fit over data points from 3 independent experiments.

Figure 4:

Longer MTs increase MCAK's MT stimulated ATPase activity. 50 nM active motor was incubated in the presence of 11μM tubulin, 250μM [γ-^{32}P]-ATP (6000 Ci/mmol) and 250μM cold MgATP. All figures display inorganic phosphate release (μM) over time (seconds). Linear curve fits (A, B) were generated by Microsoft Excel. All others (C-E) were generated with MATLAB (The Mathworks Inc.) The curves fit to the data in (C-E) are exponential association curves, fit via non-linear least square regression. (A) shows free tubulin-stimulated ATPase with wt-MCAK and (B) is with MCAK-Q710. (C) shows ATPase stimulation in the presence of unsheared MTs. (D) shows ATPase stimulation in the presence of paclitaxel-stabilized MTs, 5μm in length. (E) shows ATPase stimulation in the presence of MTs, 15μm in length. Curves were fit over data points from 4 independent experiments.

Figure 5:

Copyright 2004 Biochemical Society

wt-MCAK exhibits tighter 1:1 coupling between MT depolymerization and ATP hydrolysis in comparison to MCAK-Q710. Depolymerization and ATP hydrolysis were compared for MTs 15μm in length. (A) is wt-MCAK and (B) is MCAK-Q710. The stoichiometry of ATP hydrolysis and MT depolymerization quickly diverges with MCAK-710. However, this activity is suppressed with wt-MCAK.

Figure 6:

wt-MCAK shows more significant aggregation than MCAK-Q710 and differential MT binding in the absence of nucleotide. Images of EGFP:wt-MCAK and EGFP:MCAK-Q710 bound to GMP-CPP stabilized MTs with varying nucleotide conditions are presented. 'Motor only' images illustrate the interactions of the motor alone in the absence of MTs. wt-MCAK displays more significant aggregation than MCAK-Q710. 'AMP-PNP' labeled rows illustrate the motor in the presence of MTs and AMP-PNP. Both motors bind the ends of MTs in the presence of AMP-PNP. Again, wt-MCAK displays larger aggregate on the MT ends in comparison to MCAK-Q710. 'ADP' labeled rows show the motor with MTs in the presence of ADP. Neither motor appears to bind the MT in the presence of ADP. 'No nucleotide' labeled rows show the motors with MTs but in the absence of nucleotide. Both motors bundle MTs and decorate the MT lattice. However, wt-MCAK decorates the lattice in a more punctate fashion whereas MCAK-Q710 appears to more uniformly decorate the MT lattice with increased apparent-affinity. All binding experiments were done in 75mM KCl. Incubations were for 5 minutes at room temperature.

Figure 7:

Proposed model of the difference between wt-MCAK and MCAK-Q710. (A) is a detailed illustration of the proposed ATP hydrolysis cycle of wt-MCAK based on the EGFP-wt-MCAK binding assays. The model proposes that the binding of MCAK to the MT lattice promotes the dissociation of ADP from the motor and the subsequent binding of ATP. MCAK oscillates along the lattice in the ATP bound state until it finds a MT

Copyright 2004 Biochemical Society

Biochemical Journal Immediate Publication. Published on 13 Jul 2004 as manuscript BJ20040736

end. Association with the high affinity end binding sites triggers ATP hydrolysis and terminal tubulin dimer dissociation. Phosphate release then liberates the motor from the cleaved tubulin dimer. This model does not differentiate between processivity and non-processivity. Thus, both scenarios are illustrated. (B) illustrates how wt-MCAK oscillates back and forth along the MT in a weak binding state until it finds an end, at which time the C-terminal inhibition is relieved. ATPase activity is uninhibited by this interaction and the ATP binding state then allows the motor to bind tightly to the high affinity binding site on the terminal tubulin dimer. (C) illustrates how MCAK-Q710 may interact with the MT. While it may primarily oscillate in the loose binding state, similar to wt-MCAK, it may also be able to hydrolyze ATP sporadically along the MT lattice. This ATP hydrolysis along the MT may allow the motor to bind tightly to the lattice. As the MT end approaches these tightly bound motors, may be able to facilitate more efficient MT depolymerization. This may happen as a result of more efficient end targeting via a power stroke (in comparison to the diffusion based targeting of wt-MCAK) or it may result from a cooperative interaction between the lattice bound motors and those bound to the MT end.

Copyright 2004 Biochemical Society

Biochemical Journal Immediate Publication. Published on 13 Jul 2004 as manuscript BJ20040736

Table 1:

A

	wt-MCAK	MCAK-Q710
k_{on}	$7.5 \pm 1.76\ \mu M^{-1}s^{-1}$	$16.4 \pm 1.51\ \mu M^{-1}s^{-1}$
k_{off}	$0.123 \pm 0.084\ s^{-1}$	$0.183 \pm 0.037\ s^{-1}$

11μM tubulin, 15μm MTs, 12.5nM-50nM active MCAK heads

B

	5μm MTs	15μm MTs	unsheared MTs	
initial ATPase activity	$0.102\ s^{-1}$	$0.106\ s^{-1}$	$0.26\ s^{-1}$	**wt-MCAK**
initial ATPase activity	$0.302\ s^{-1}$	$0.318\ s^{-1}$	$0.676\ s^{-1}$	**MCAK-Q710**

11μM tubulin, 50nM active MCAK heads

Copyright 2004 Biochemical Society

Biochemical Journal Immediate Publication. Published on 13 Jul 2004 as manuscript BJ20040736

Figure 1

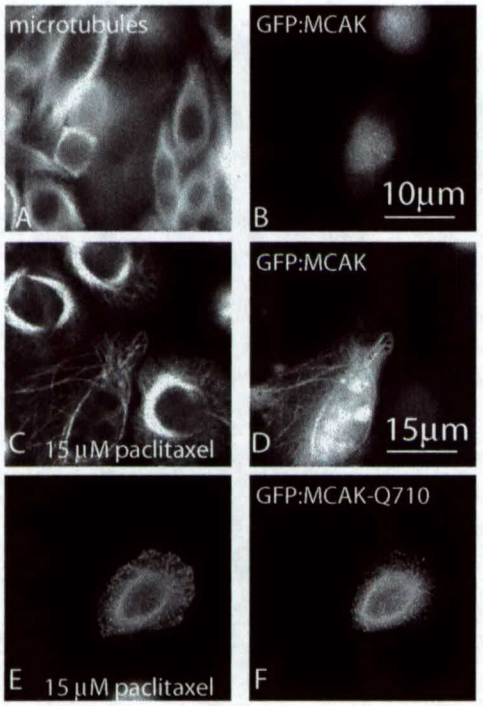

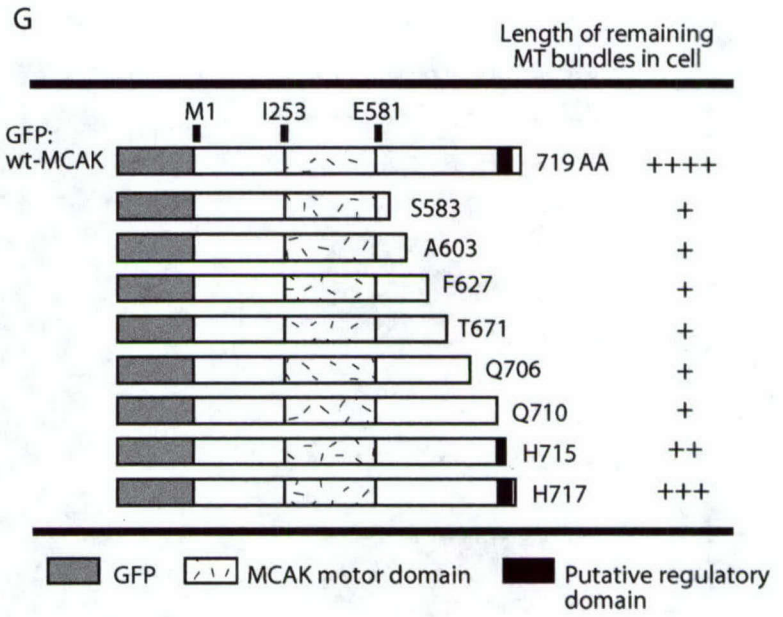

Copyright 2004 Biochemical Society

Biochemical Journal Immediate Publication. Published on 13 Jul 2004 as manuscript BJ20040736

Figure 2

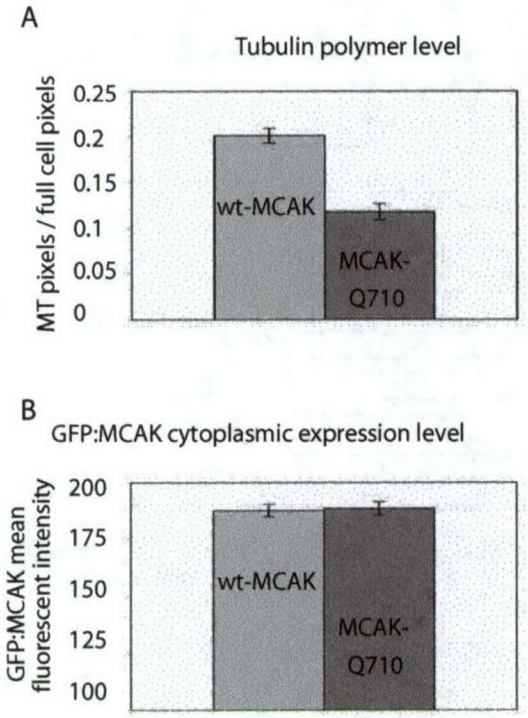

Copyright 2004 Biochemical Society

Biochemical Journal Immediate Publication. Published on 13 Jul 2004 as manuscript BJ20040736

Figure 3

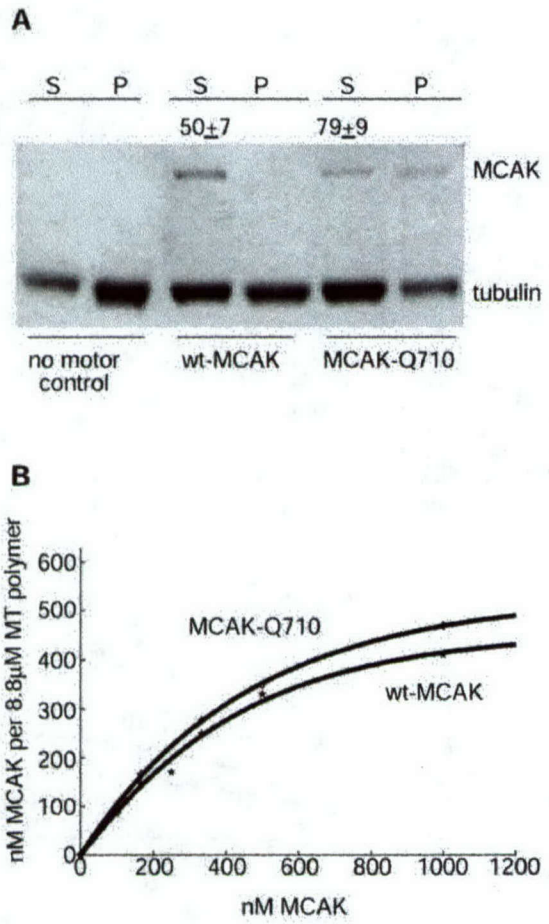

Copyright 2004 Biochemical Society

Biochemical Journal Immediate Publication. Published on 13 Jul 2004 as manuscript BJ20040736

Figure 4

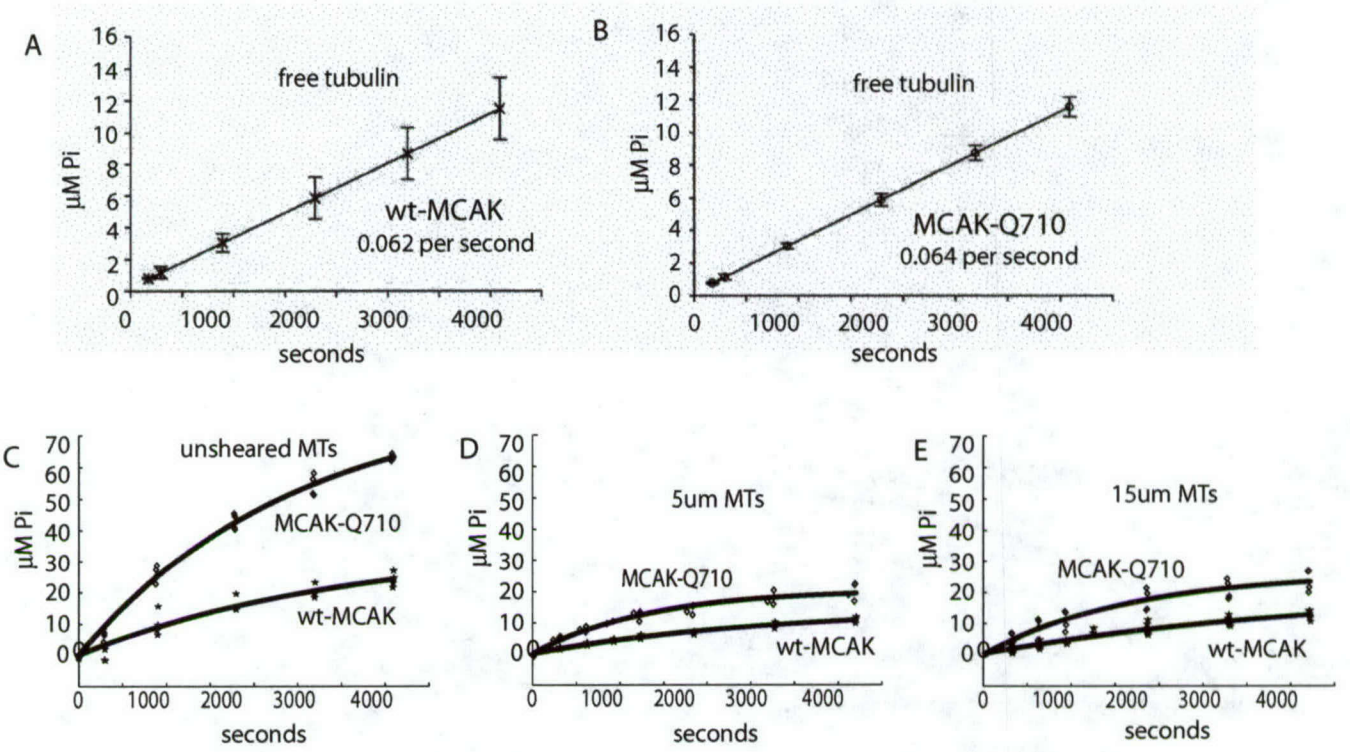

Copyright 2004 Biochemical Society

Biochemical Journal Immediate Publication. Published on 13 Jul 2004 as manuscript BJ20040736

Figure 5

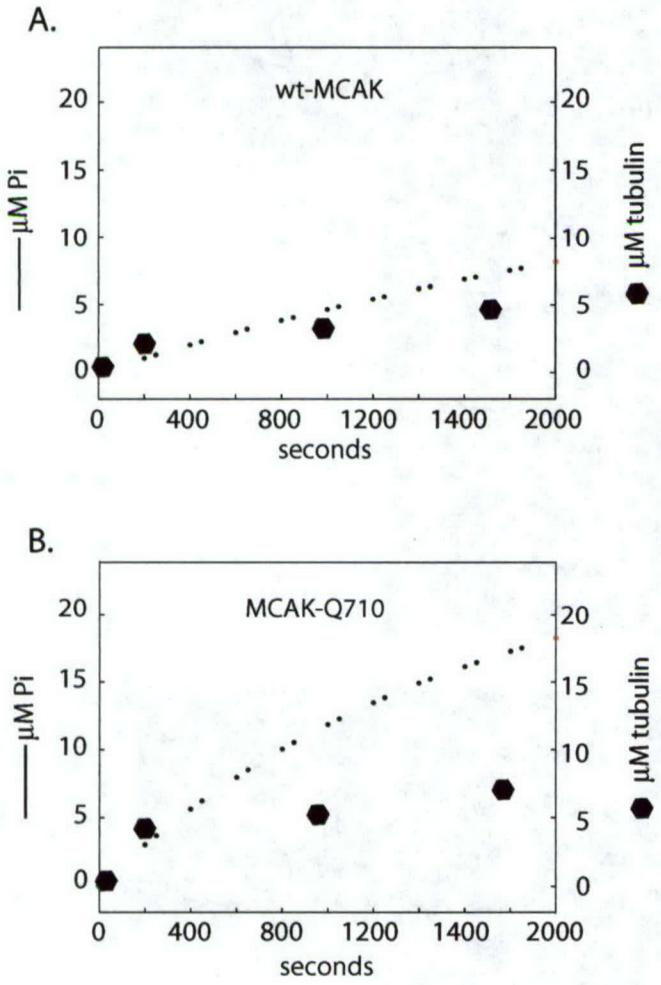

Copyright 2004 Biochemical Society

Biochemical Journal Immediate Publication. Published on 13 Jul 2004 as manuscript BJ20040736

Figure 6

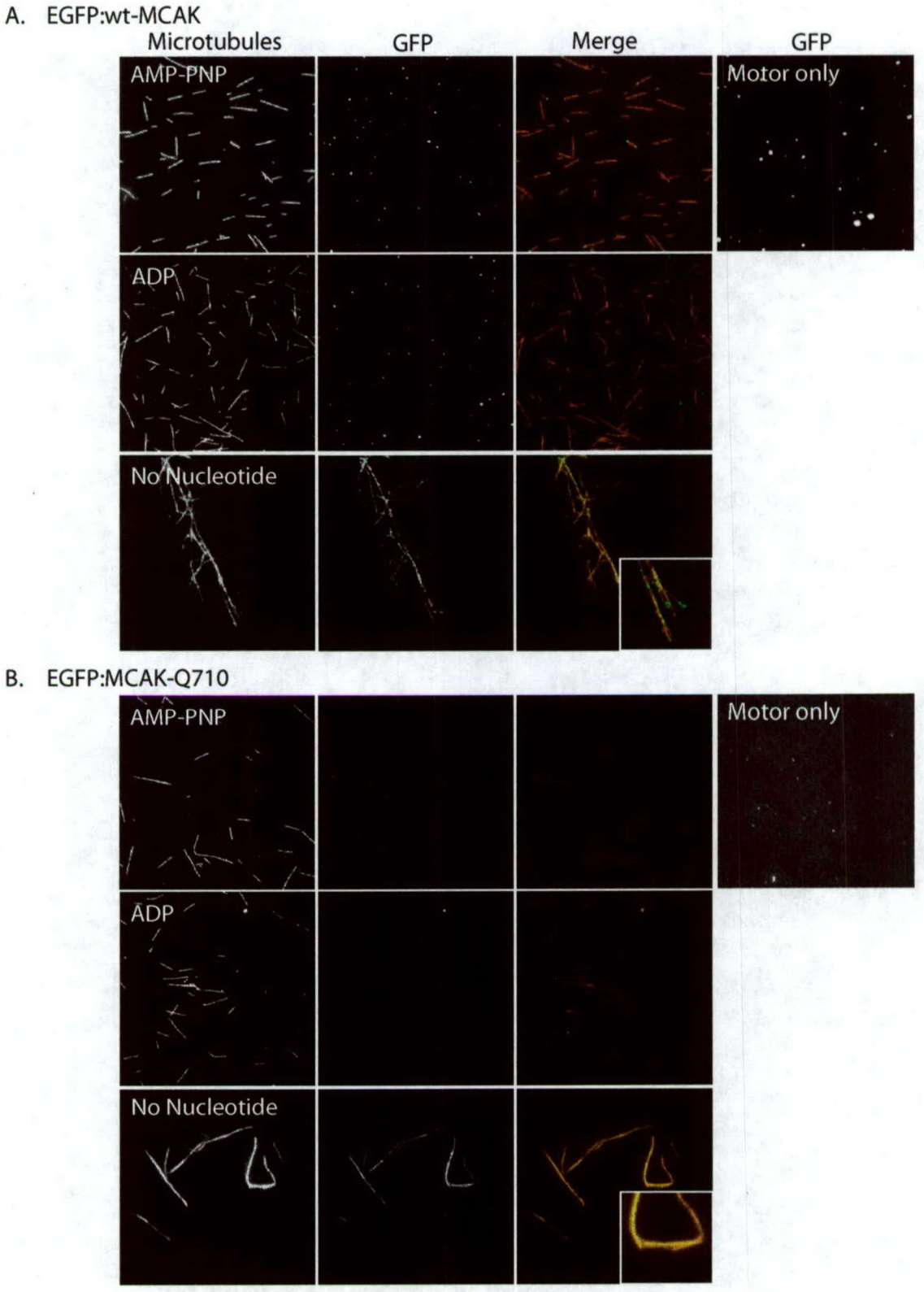

Copyright 2004 Biochemical Society

Biochemical Journal Immediate Publication. Published on 13 Jul 2004 as manuscript BJ20040736

Figure 7

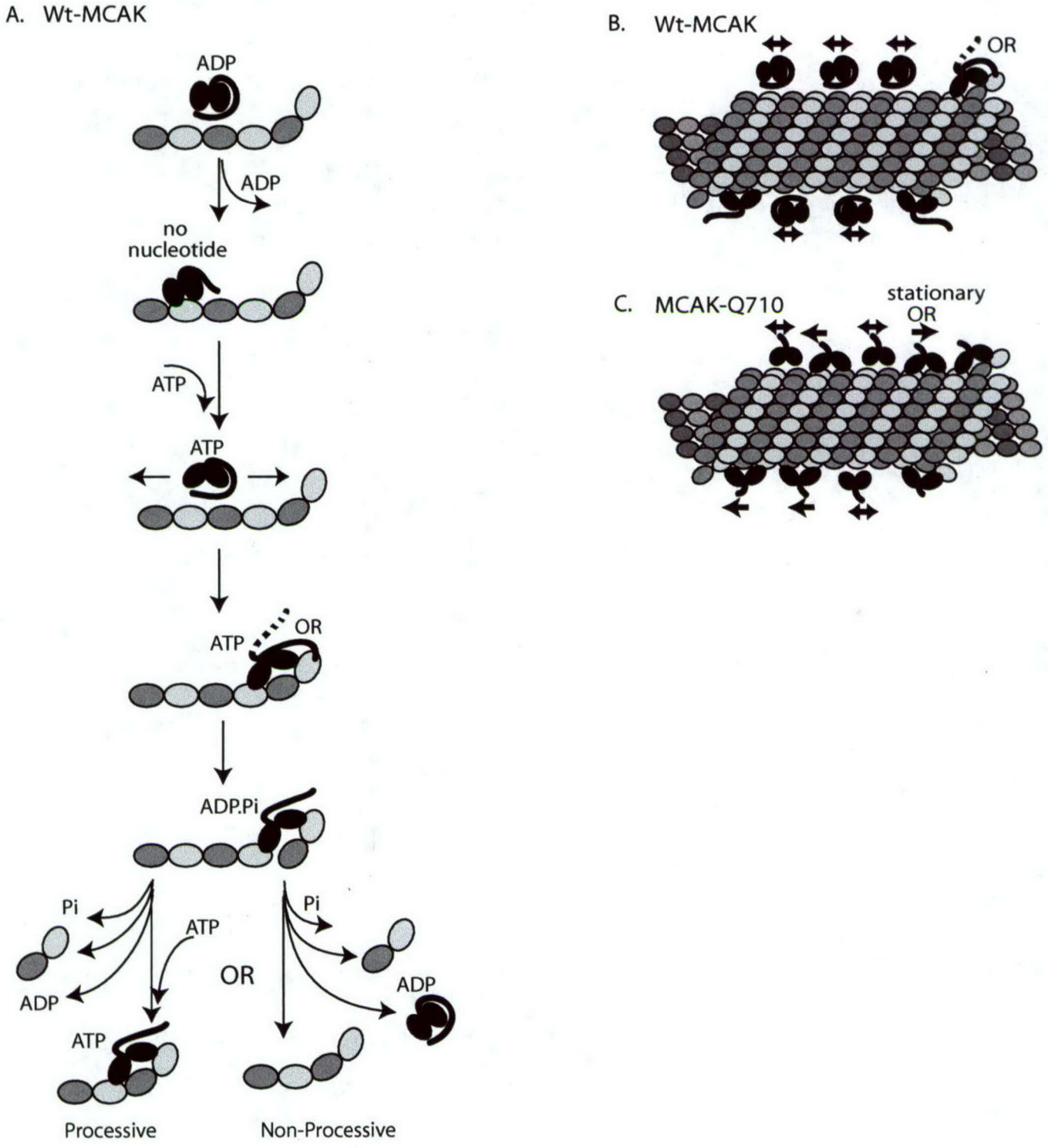

Copyright 2004 Biochemical Society

The mechanism, function and regulation of depolymerizing kinesins during mitosis

Ayana Moore and Linda Wordeman

University of Washington School of Medicine, Department of Physiology and Biophysics, Seattle, WA 98195, USA
Corresponding author: Ayana Moore (atmoore@u.washington.edu).

Kinesins are motor proteins that use the hydrolysis of ATP to do mechanical work. Most of these motors translocate cargo along the surface of the microtubule (MT). However, a subfamily of these motors (Kin-I kinesins) can destabilize MTs directly from their ends. This distinct ability makes their activity crucial during mitosis, when reordering of the MT cytoskeleton is most evident. Recently, much work has been done to elucidate the structure and mechanism of depolymerizing kinesins, particularly those of the mammalian kinesin mitotic centromere-associated kinesin (MCAK). In addition, new regulatory factors have been discovered that shed light on the regulation and precise role of Kin-I kinesins during mitosis.

Kinesins are enzymes that translocate along the surface or 'lattice' of MTs – long polymers that comprise part of the cytoskeleton (Box 1) – by coupling mechanical work to ATP hydrolysis. Because the ATP-hydrolyzing motor domain of kinesin proteins is highly conserved, it was surprising when a class of kinesins was identified that directly depolymerize MTs from either end [1,2]. This subfamily of depolymerizing kinesins also shows a structural oddity: the motor domain is generally located in the middle of the peptide sequence rather than at one end, as it is in other kinesins. For this reason, these proteins are often called 'middle' kinesins (Kin-M) or 'internal' (Kin-I) motor kinesins.

The subfamily of Kin-I kinesins is encoded by (so far) three unique genes in mammals: Kif2A [3], Kif2B [4] and MCAK (also known as Kif2C) [5]. Related kinesins with depolymerizing activity and/or sequence homology have been described in invertebrates, including *Saccharomyces cerevisiae* Kip3 [6], *Plasmodium falciparum* pKin-I [7] and *Drosophila melanogaster* Klp10A, Klp59C, Klp59D [8] and Klp67A [9]. The extent to which these genes are orthologous to their mammalian counterparts is not unequivocal. Table 1 summarizes the nomenclature and mitotic function of these kinesins in mammals and invertebrates on the basis of existing studies.

How do Kin-I kinesins affect the cell? Cooperation among many motors located at the kinetochore, centromere and centrosomes and along MTs is required to accomplish chromosome segregation during mitosis [10]. During distinct stages of this dynamic process, these motors promote tension and the movement of chromosomes and MTs [11]. MCAK and its relatives play a key role in this process by actively participating in the reordering of the MT cytoskeleton (Box 1). This crucial process is vital for ensuring high-fidelity chromosome segregation during cell division. The bulk of the existent data on these kinesins has been obtained from work on MCAK in mammalian and *Xenopus* cells with key input from other systems.

In this review, we focus on data from metazoans and discuss advances in our understanding of this important and unusual class of kinesins, including their mechanism of MT depolymerization, their role during mitosis, and regulation of their activity.

Mechanism of MT depolymerization by Kin-I kinesins

An elaborate interplay of motors facilitates the separation of genetic material during cell division. The Kin-I subfamily of kinesins participates in this process by depolymerizing MTs, thereby permitting the reordering of the MT cytoskeleton. In recent years, several investigators have provided much evidence towards elucidating the mechanism of Kin-I-mediated MT depolymerization.

MT end targeting

MCAK, a kinesin-related MT depolymerizer, exists as a homodimer in its native state, although the monomer has been shown to possess comparable, and sometimes greater, depolymerization capability [12]. Kinetic assays of the activity of MCAK have yielded surprising results for a kinesin-related protein. First, MCAK has an extraordinarily high affinity for MT ends, which are also the substrate of depolymerization [1,2]. Second, MCAK catalytically destabilizes MTs from either end with relatively little difference in the rates of disassembly [1,2].

Notably, MCAK can target MT ends in the absence of any hydrolysable ATP [1] and more rapidly than can be accounted for by three-dimensional diffusion [2]. This has fueled the hypothesis that MCAK might rapidly target MT ends in a non-motile fashion; in other words, unlike conventional kinesins, which translocate along the surface of the MT in an ATP-dependent, step-by-step fashion, MCAK might diffuse to MT ends by gliding along the surface of the MT. This diffusive activity might result from Brownian motion because MCAK targets either MT end almost indiscriminately [1].

The monomeric catalytic core of MCAK is necessary but not sufficient for depolymerization in cells and *in vitro* under physiological conditions. Inclusion of the 'neck' domain, about 50 amino acids located at the amino (N) terminus of the motor, restores full MT depolymerization activity to the MCAK core motor [12]. Neutralization of the positively charged neck by site-directed mutagenesis

markedly reduces depolymerization activity both *in vivo* and *in vitro*, suggesting that the neck might flexibly tether the motor to the negatively charged MT surface via electrostatic interactions [13].

The core motor of both pKinI (*P. falciparum* Kin-I) and MCAK can depolymerize MTs, but only in conditions of low salt [7,13]. Furthermore, the negatively charged carboxy (C)-terminal region of tubulin, or the 'hook' as it is called, is required for depolymerization to occur [7,14]. These findings suggest that balanced electrostatic interactions between Kin-I kinesins and MTs are needed for Kin-I-dependent depolymerization to proceed under physiological conditions.

Electrostatic tethering might also be involved in rapid targeting of MCAK to the MT end. Hunter *et al.* [2] combined experimental data and mathematical analysis to show that targeting of MCAK to the MT end is more rapid than can be explained by three-dimensional diffusion of the motor through solution; by contrast, one-dimensional diffusion of the motor along the lattice would be consistent with the observed rate of end targeting. Thus, MCAK might diffuse through solution, encounter the MT lattice, and then rapidly diffuse to the high-affinity end-binding site at either end of the MT. Electrostatic tethering is likely to have a role in one-dimensional diffusion along the lattice. In support of this idea, Hunter *et al.* [2] found that MTs bound to an MCAK-coated surface undergo small back-and-forth oscillations, consistent with the randomly directed processes of motors such as flagellar dynein [15], ncd [16] and Kif1A [2,17–19].

Destabilization of the MT ends

How exactly does MCAK destabilize terminal tubulin dimers? Insight into this question has been provided by electron microscopic images of depolymerization complexes formed in the presence of AMP-PNP, a non-hydrolyzable ATP analog. AMP-PNP irreversibly locks MCAK into the high-affinity binding state at the end of the MT. This irreversible binding results in the unraveling of protofilaments and the formation of curved protofilament curls or peels [1] (Box 1).

The monomeric Kin-I core motor domain has one binding site on each tubulin heterodimer [20]. The highest-affinity binding site on the longitudinal protofilament is at either end, whereas lower affinity sites are present on the lattice in between [2]. It is likely that the high-affinity end binding depends, in part, on the ability of the terminal tubulin dimer to assume a curved conformation, which favors Kin-I motor binding (Figure 1). The consistent presence of 13-fold symmetric rings comprising pKinI, AMPPNP and tubulin suggests that depolymerization might occur by bending a single protofilament longitudinally [7]. The stereotyped curvature of the ring suggests that the core motor domain of MCAK can precisely stabilize the curved GDP-bound conformation of tubulin, thereby promoting its disassembly from the MT.

A lock-and-key fit between Kin-I kinesins and the curved terminal tubulin dimer

Crystal structures of the catalytic core and neck domain of murine MCAK (known as Kif2C) have identified regions that are highly conserved among Kin-I kinesins. Seven regions in the minimal functional domain have been shown to differ significantly from other kinesin family members [21]. These regions reveal a 'lock-and-key' fit between the Kin-I motor domain and the conformationally distinct, terminal tubulin dimer.

The surface of the catalytic core of MCAK is convex in both the ATP- and ADP-bound states, preventing it from lying flat on the surface of the MT lattice. This conformation could lead to weak or unstable binding along the MT lattice (Figure 1). Indeed, microscopic images of fluorescently labeled MCAK show that it does not bind the lattice under physiological conditions in its ADP- or AMP-PNP-bound state [22]. In this conformation, the nucleotide-binding pocket seems to be in the open state, thereby preventing the hydrolysis of ATP. Once the motor makes contact with the curved terminal tubulin dimer, contact between the motor and the tubulin dimer is maximized (Figure 1c), which could then promote ATP hydrolysis [21,23]. The observation that both the ATP- and ADP-bound states have a similar convex surface has prompted Ogawa *et al.* [21] to suggest that stabilization of the curved conformation of the protofilament at the MT end might be enough to cause depolymerization in the absence of ATP hydrolysis.

The role of ATP hydrolysis in MT depolymerization

Why, then, does MCAK need to be an ATPase to trigger MT disassembly? MCAK can depolymerize MTs in the absence of ATPase activity [1,7]; however, depolymerization can occur to completion only when there is a 1:1 stoichiometry of motor to polymerized tubulin. In substoichiometric conditions, rapid and complete depolymerization occurs only in the presence of ATP [2,14].

The crystallography studies described above were done with motors lacking the N- and C-terminal arms. ATPase experiments done with the full-length motor and a hyperactive mutant lacking the final eight amino acids show that these variants have considerable differences in ATPase activity. The hyperactive mutant shows significantly enhanced ATPase activity, suggesting that ATP hydrolysis is, in fact, coupled to depolymerization [22]. At present, the best hypothesis is that ATPase activity is necessary for decoupling the dissociated terminal tubulin dimer from the motor so that the motor can be recycled for several rounds of depolymerization (Figure 1e). Whether this happens when MCAK is bound to the penultimate dimer (as suggested by the processive model of Hunter *et al.* [2]) or when it is in solution remains a subject of investigation.

Nevertheless, the interaction of MCAK with free tubulin is likely to be of key importance in cells where tubulin polymers coexist with free dimers. In the absence of ATP, free tubulin can sequester MCAK away from the MT lattice [22]. In addition, substoichiometric levels of MCAK are capable of decreasing the MT polymer mass of 'live' (non-stabilized) axoneme-seeded MTs in the absence of ATP, a result that is highly suggestive of tubulin

sequestration [24]. These data support the hypothesis that ATP hydrolysis is needed to liberate the motor from the dissociated terminal tubulin dimers.

Much work has been done *in vitro* to elucidate the mechanism by which MCAK and other members of the Kin-I family disassemble MTs; however, it should be noted that many of these studies have been done with MTs that are artificially stabilized by either the drug paclitaxel (which stabilizes lateral MT connections [25,26]) or GMP-CPP, a non-hydrolyzable form of GTP (which stabilizes longitudinal connections [27]). Notably, some data collected with paclitaxel-stabilized MTs differ significantly from data collected with GMP-CPP-stabilized MTs: namely, ATPase activity is roughly fivefold greater for GMP-CPP-stabilized MTs than for paclitaxel-stabilized MTs [2,22]. In addition, ATPase activity stimulated by free tubulin and ATPase activity stimulated by MTs are more equivalent for paclitaxel-stabilized MTs [20,22] than for GMP-CPP-stabilized MTs [2].

In GMP-CPP-stabilized MTs, the contribution of free tubulin to the kinetics of depolymerization might be suppressed because the free tubulin is complexed with GMP-CPP, which presumably makes the dimer straight in contrast to the curved conformation of the GDP-bound tubulin dimer [28] that MCAK seems to favor. Overall, this suggests that we must use caution when interpreting data derived from non-physiological systems and should work toward developing systems that more closely mimic the environment of the cell. Initial advances in this direction have come from Newton *et al.* [24], who have shown that MCAK increases the catastrophe frequency of steady-state, non-stabilized MTs purified from human HeLa cells and seeded from axonemes.

MT-depolymerizing kinesins and cell division

The MT cytoskeleton is highly reorganized during cell division. For this reorganization to occur, the MTs must be disassembled to enable formation of the mitotic spindle – the cytoskeletal structure that supports the division of duplicated genetic material (Box 1). Potent MT depolymerizers such as MCAK, which was first identified during a search for novel centromere-associated kinesins [5], are essential for this activity.

MCAK is found both on centromeres and in the cytoplasm throughout the cell cycle and is highly enriched on centromeres, centrosomes and the spindle midzone during mitosis [5,29,30] (Figure 2a). Depletion or disruption of MCAK activity leads to improper spindle maintenance and to misaligned and lagging chromosomes during metaphase and anaphase [29–31]. These data suggest that proper regulation of the activity of MCAK is necessary to maintain genetic integrity during mitosis.

Depletion and mutational analysis of several Kin-I kinesins has offered some insight into the role of MT depolymerizers and has prompted several investigators to propose some insightful and intriguing models. Notably, recent studies suggest that there might be a division of labor between centromeric (MCAK, Klp59C) and centrosomal (Kif2A, Klp10A) depolymerizers in chromosome segregation and spindle assembly [8,32].

Kinetochore and centromeric functions

Oscillation modulator

In a normal cell, paired chromosomes oscillate until they are bi-oriented (attached to both spindle poles; Box 2) and aligned at the metaphase plate [33]. Antisense and dominant-negative experiments with a motorless mutation of MCAK resulted in lagging chromosomes in mammalian cells during anaphase. Live imaging suggests that these lagging chromosomes might be caused by continued oscillations of separated chromatids during anaphase [30]. Increases in chromosome oscillations have been also observed in other systems with disruptions in Kin-I activity [31,34]. Taken together, these observations suggest that MCAK suppresses the oscillations of chromatids once they have aligned at the metaphase plate, enabling them to congress unidirectionally toward their respective poles.

Anaphase depolymerase

Analogous to MCAK, Klp59C, a *Drosophila* Kin-I kinesin that depolarizes MTs, localizes to mitotic centromeres. Downregulation of this protein results in chromosome mispositioning and also segregation defects during anaphase. Time-lapse microscopy has shown that the poleward movement (Figure 2b) of chromatids during anaphase is significantly slowed when Klp59C is inhibited, which suggests that Klp59C might contribute to chromosome-to-pole motility by 'chewing up' MT plus ends via a 'Pac-Man™-based' mechanism [8].

Corrector of MT mis-attachments

Analysis of lagging chromatids in mammalian Ptk2 cells depleted of centromeric MCAK has been used to detect morphological differences in the centromeric region. Lagging chromatids show stretched staining of CREST (an autoimmune antibody used to mark kinetochores; Figure 3a), which is indicative of a merotelic kinetochore attachment – that is, a single chromatid connected to both poles – and this finding has been confirmed by electron microscopy. These data suggest that MCAK might be involved in correcting improper kinetochore–MT attachments before anaphase [35] (Box 2).

Centrosomal functions and spindle assembly

Mitotic spindle assembly and maintenance

Functional disruptions of Kin-I kinesins in several systems have implicated a role for these kinesins in mitotic spindle assembly and maintenance. Downregulation of Klp10A [8] and Kif2A [32], which both localize primarily to spindle poles, consistently results in the formation of monopolar (only one foci) mitotic spindles. Disruptions of MCAK show minimal defects in bipolar spindle assembly and predominantly result in the formation of abnormally long spindle MTs [29,32,36,37]. These data indicate that a subset of depolymerizing kinesins has a significant role in bipolar spindle formation during mitosis.

Flux motor

Downregulation of Klp10A, the *Drosophila* Kin-I, results in an increase in MTs at the centrosomes and in

significantly inhibited translocation of chromatids towards the spindle poles [8]. These data, coupled with time-lapse microscopy, suggest that Klp10A has a role in depolymerizing MTs at their pole-associated minus ends, resulting in the movement of chromatids via 'poleward MT flux' (Figure 2b).

Compensatory and cooperative mechanisms of MT depolymerization

Although closely related structurally, the three mammalian Kin-I kinesins – Kif2A, Kif2B and Kif2C (MCAK) – have distinct functions. Originally, Kif2A was thought to have primarily a neuronal role [38]; however, Santama *et al.* [39] have demonstrated that a splice variant of Kif2A (now called Kif2Aβ) is present in dividing mouse cells (early developing hippocampus cells and fibroblasts). (Notably, a testis-specific splice variant of human MCAK has been also identified [40].) Kif2Aβ has a key role in bipolar spindle assembly in cultured mitotic human cells [32]. At present, the role of Kif2B is unknown, but Kif2Aβ and MCAK work in concert to support cell division with reliable integrity [32]. Additional cooperative mechanisms have been observed in syncytial blastoderm stage *Drosophila* embryos, in which two of the three Kin-I MT depolymerizers show a cooperative relationship during mitosis [8].

Klp10A, the probable *Drosophila* homologue of Kif2Aβ (on the basis of localization, activity and sequence homology), is implicated in poleward MT flux (Figure 2b), a process that was originally described by Mitchison [41]. Conversely, the activity of Klp59Cs is implicated in chromosome-to-pole movement (Figure 2b). Klp10A depolymerizes MTs at their pole-associated minus ends, whereas Klp59C is primarily active at kinetochore MT plus ends [8]. Thus, the localization of Kin-I kinesins to specific regions in the mitotic spindle can dictate their function (Figure 2 and Table 1).

An analogous situation might occur in the yeast *S. cerevisiae*, in which the kinesin motors Kip3p and Kar3p have both been shown to contribute to positioning of the mitotic spindle, assembly of the bipolar spindle and structural integrity of the spindle. Kar3p shows genetic and some biochemical evidence for depolymerizing activity [6,42,43]. Deletions of Kip3p, the protein found to be most similar to the vertebrate Kin-I proteins, results in extra long pre- and post-anaphase spindles. In addition, the Kip3p Kar3p double knockout is lethal [6].

The distribution of Kin-I kinesins in the cell indicates specific roles for their depolymerizing activity. So far this activity has been noted mostly on centromeres and centrosomes of mitotic cells. In *Drosophila*, Klp10A and Klp59C might partially share the role of mammalian and *Xenopus* MCAK in that their combined subcellular distribution mimics that of MCAK. Alternatively, a third as yet uncharacterized *Drosophila* Kin-I kinesin, Klp59D, seems to have arisen from a duplication of the Klp59C gene and could be a candidate for sharing a role with Klp59C. At present, no functional information is available on this kinesin. The activity of MCAK seems to extend beyond that of Klp59C. Its disruption also results in long spindle MTs [29,32,36,37] and it localizes to spindle poles [5,29], whereas Klp59C localizes only to centromeres [8]. In general, Kif2Aβ and Klp10A seem to operate more centrosomally, whereas MCAK and Klp59C seem to function more centromerically. In this way, their subcellular distribution contributes to the control of Kin-I activity. To achieve the intricate interplay of motors to support cell division, however, additional regulatory factors are warranted.

Regulation of Kin-I kinesins

The studies described above illustrate how the spatial distribution of Kin-I kinesins might control MT-depolymerizing activity by localizing it to specific subcellular regions. However, the intrinsic MT-depolymerizing activity of MCAK can be also post-translationally regulated.

Phosphorylation of MCAK

Phosphorylation of MCAK by Aurora B kinase (which is highest during mitosis) inhibits the depolymerizing activity of MCAK in both cultured cells and *Xenopus* egg extracts [44–46]. The phosphorylation sites that have been identified are highly conserved between human and *Xenopus* MCAK. Some of these sites are on the conserved neck domain, suggesting that the disruption of electrostatic interactions between the positively charged neck and the negatively charged surface of the MT is likely to be the mechanism of inhibition. This activity seems not only to affect the depolymerizing activity of MCAK, but also to reflect its sequestration to different parts of the mitotic centromere [44]. In turn, this sequestration might reflect an enhancement or antagonism of its activity because it causes the motor to be placed closer to or further away from the site of MT attachment.

Aurora B colocalizes with MCAK in chromosomes that are unattached or 'mono-oriented' (attached to only one spindle pole; Box 2) during prometaphase in mammalian cells [44]. In *Xenopus* egg extracts, colocalization is seen at mitotic centromeres, spindle midzones and midbodies [45]. Throughout mitosis, the extent of colocalization seems to decrease as a result of MT attachment and tension on the chromosomes. Both phosphorylation-specific (phosphospecific) and non-phosphospecific antibodies label centromeres, suggesting the presence of centromeric binding sites for both forms of MCAK. In addition, the intensity of the phosphospecific staining is consistently asymmetric [44,45]. These data suggest that phosphorylation has a role in regulating MCAK activity during the capture and bi-orientation of kinetochores.

Distribution of MCAK in the centromere and kinetochore

In addition, the location of MCAK on the mitotic centromere might be involved in regulating its activity. Placement of the motor in varying proximities from the point of MT attachment can alter its effects on the MT [5,30]. It has been reported that the localization of MCAK is flexible and that MCAK can appear in various places on the centromere and kinetochore (Figure 3b and Box 2), depending on tension and chromosome movement [30,35].

Further evidence suggests that MCAK might possess distinct centromeric binding sites and its localization

might depend on phosphorylation. Overexpression of a mutant mimicking phosphorylated MCAK results in consistent localization of MCAK to the inner centromere. By contrast, a non-phosphorylatable mutant is targeted to the outer face of the kinetochore, closer to the site of MT attachment, suggesting that phosphorylation has a role in targeting MCAK to the inner centromere. An interesting hypothesis is that dephosphorylation, perhaps mediated by protein phosphatase 1γ [47] enriches the outer face of the kinetochore with activated MCAK; this subset of 'outer face' MCAK is required during all stages of mitosis [44]. All centromere-associated MCAK would then be fully activated (dephosphorylated) at anaphase when Aurora B relocates from the centromere to the spindle midzone [48,49].

Another attractive hypothesis that follows from this is that localization of MCAK to the inner centromere, coupled with the reduction of its activity, promotes MT attachment while allowing MCAK to function moderately as a corrector of attachment errors. Localization on the outer kinetochore region might restore its full activity and enable it to take on another role as an anaphase depolymerase or an oscillation suppressor. Thus, the change in phosphorylation might contribute to the ability of MCAK to support many different roles during mitosis: spindle maintenance, correct attachment of MTs to the kinetochore, bi-orientation of kinetochores, alignment at the metaphase plate, and subsequent separation of sister chromatids. Defects in all of these processes have been reported in studies of the disruption of MCAK activity [30–32,35]. It is likely that the predominantly centrosomal Klp10A and Kif2Aβ also encounter regulation by phosphorylation, perhaps dependent on centrosomal Aurora A, which is localized primarily on centrosomes during mitosis [50].

Evidence that regulatory binding occurs on different sites of the centromere and kinetochore provides potential explanations for the varying degrees of phenotypes resulting from dominant-negative experiments. Disruption of endogenous MCAK by expressing exogenous motorless constructs of MCAK causes lagging chromosomes but no prometaphase defects [30,51], whereas disruption by expressing exogenous N-terminal domains of MCAK results in prometaphase and congression defects [31,35]. These disruptive constructs localize to distinctly different areas: the motorless variant to the inner centromere, the N-terminal domain to the kinetochore. As Andrews *et al.* [44] have demonstrated, disruption of activity on different parts of the centromere or kinetochore might result in different phenotypes because the position of MCAK in this region seems to regulate its activity.

Enhanced activity mediated by cofactors

Recently, an important new cofactor for Kin-I function has been identified: inner centromere Kin-I stimulator (ICIS). During prometaphase and metaphase, ICIS is seen on inner centromeres, coincident with MCAK and Aurora B. Inhibiting ICIS activity in *Xenopus* extracts results in enhanced MT growth and inhibits spindle formation [52]. Biochemical assays suggest that ICIS binds MTs directly and stimulates the MT depolymerase activity of MCAK *in vitro*. Furthermore, ICIS associates with MCAK in immunoprecipitations and its localization to the centromere is dependent on MCAK. It has been suggested that the MCAK–ICIS complex at the centromere might function, in concert with Aurora B, to prevent attachment errors between kinetochores and MTs during prometaphase and metaphase [52].

MCAK: the multitasking mitotic kinesin

MCAK seems to possess global activity throughout mitosis from spindle assembly and maintenance [29,36,37] to chromosome positioning and segregation [30,31,35]. Recent studies are just beginning to dissect how each of these tasks is controlled, in particular, at the centromere and kinetochore. Localization of the motor to specific regions of the centromere and kinetochore might be a method by which MCAK activity is regulated or a reflection of its activation.

Elucidating how centromeric MCAK is localized to different domains in the centromere will be essential to our understanding of its function during mitosis. Presumably, tension and stretch on the kinetochore, as well as MT attachment, contribute to this subcentromeric localization, because MCAK shows an asymmetric distribution across the centromere during prometaphase (a dynamic time during mitosis) [30,35]. Mechanical strain, phosphorylation and interacting proteins are all likely to be principal regulators of the localization and activation of MCAK. These layers of complexity could confer broad functional diversity on Kin-I kinesins.

MCAK and cancer

Determining how the cellular activity of MCAK is regulated is proving to be complex. Overall expression levels of the protein have been observed to increase as cells progress toward mitosis [51,53]. This observation is consistent with the fact that MCAK activity is required during the division phase of the cell cycle, when reordering of the MT cytoskeleton is most marked.

Increased levels of both MCAK and Aurora kinases have been correlated with tumorigenesis [54]. Because these proteins are normally upregulated [51,53] and highly active [50,55] as cells progress toward mitosis, an increase in their levels in tumor cells might reflect or promote the readiness of these cells to bypass checkpoints and enter cell division. Also notable is that overexpression of Aurora kinases can transform cells in culture [50]. In addition, overexpression of MCAK causes a moderate increase in the frequency of multipolar spindles [37] and monopolar spindles [56], which could contribute to the gain or loss of chromosomes in daughter cells.

Disturbances in the levels and deregulation of Kin-I kinesins could have profound effects on chromosome segregation, tumor progression and resistance to chemotherapeutic reagents. Traditionally, some of the most efficacious cancer drugs (such as Taxol™, Taxotere™, eleutherobins, epothilanes, laulimalide, sarcodictyins and discodermoide, which promote MT stability; and Vinca alkaloids, cryptophycis, halichondrins, estramustine and colchicines, which inhibit tubulin polymerization) target, in part, dynamic MTs [26,57,58]. Thus, the Kin-I kinesins

represent an important future target for anticancer therapies.

Concluding remarks

Biochemical, microscopic and crystallographic data have identified fascinating mechanisms that enable depolymerizing motors to target their high-affinity binding sites on the MT end. Moreover, they have provided the initial indications of how these motors destabilize terminal tubulin dimers. Depolymerizing kinesins are crucial to the cell because they support the reorganization of the MT cytoskeleton – an essential component of mitosis. Although much remains to be discovered, the role of MCAK and other Kin-I kinesins during mitosis is becoming clearer, and potential compensatory and cooperative mechanisms are being identified.

The regulation of MT dynamics is essential for maintaining genomic integrity, and several factors have been recently identified that support the regulation of MCAK, including phosphorylation, intracellular positioning and cofactors. Phylogenetically, it seems that the relatively small class of depolymerizing kinesins [4] might have evolved from a progenitor kinesin with motility directed towards the plus end [59,60]. Specializations that permit kinesins to regulate MT dynamics spatially confer on them an essential role in modulating cell shape, cell motility and cell division.

MCAK, one of the founding members of the Kin-I family of kinesins, has been studied from the cellular to the structural level and has been shown to be a potent MT depolymerase and a crucial participant in chromosome segregation during mitosis. Although much has been gained from these studies, many questions still remain. Does MCAK show any motility along the MT lattice? What is it about the motor and neck of MCAK that make this protein uniquely a depolymerizer? What are the structure and function of the N- and C-terminal domains of MCAK? What is MCAK doing at the centrosomes? What are the main consequences for the cell when MCAK levels are misregulated in primary cells? Does the upregulation of MCAK in tumor cells support the resistance of some tumors to Taxol™ treatment? Further investigations into depolymerizing motors are warranted at all levels: from structural to cellular to clinical.

Acknowledgements

We are indebted to Paul Andrews and Sharyn Endow for sharing ideas and for comments about the manuscript. We thank Yulia Ovechkina and Kathleen Rankin for many useful comments and for critiques of the manuscript. Because of space limitations, we limited the focus of this review primarily to metazoan depolymerizing kinesins and omitted some important studies in other systems. We apologize to those authors whose work we were unable to cite because of these constraints. L.W. is supported by a grant from the Department of Defense (DAMD 17-01-1-0450). A.T.M. is supported by a Predoctoral Fellowship from the National Institutes of Health (1 F31 GM65061).

References

1 Desai, A. *et al.* (1999) Kin I kinesins are microtubule-destabilizing enzymes. *Cell* 96, 69–78

2 Hunter, A.W. *et al.* (2003) The kinesin-related protein MCAK is a microtubule depolymerase that forms an ATP-hydrolyzing complex at microtubule ends. *Mol. Cell* 11, 445–457

3 Noda, Y. *et al.* (1995) KIF2 is a new microtubule-based anterograde motor that transports membranous organelles distinct from those carried by kinesin heavy chain or KIF3A/B. *J. Cell Biol.* 129, 157–167

4 Miki, H. *et al.* (2001) All kinesin superfamily protein, KIF, genes in mouse and human. *Proc. Natl. Acad. Sci. U. S. A.* 98, 7004–7011

5 Wordeman, L. and Mitchison, T.J. (1995) Identification and partial characterization of mitotic centromere-associated kinesin, a kinesin-related protein that associates with centromeres during mitosis. *J. Cell Biol.* 128, 95–104

6 Cottingham, F.R. *et al.* (1999) Novel roles for *Saccharomyces cerevisiae* mitotic spindle motors. *J. Cell Biol.* 147, 335–350

7 Moores, C.A. *et al.* (2002) A mechanism for microtubule depolymerization by KinI kinesins. *Mol. Cell* 9, 903–909

8 Rogers, G.C. *et al.* (2004) Two mitotic kinesins cooperate to drive sister chromatid separation during anaphase. *Nature* 427, 364–370

9 Gandhi, R. *et al.* (2004) The Drosophila kinesin-like protein KLP67A is essential for mitotic and male meiotic spindle assembly. *Mol. Biol. Cell* 15, 121–131

10 Scholey, J.M. *et al.* (2003) Cell division. *Nature* 422, 746–752

11 McIntosh, J.R. *et al.* (2002) Chromosome–microtubule interactions during mitosis. *Annu. Rev. Cell Dev. Biol.* 18, 193–219

12 Maney, T. *et al.* (2001) Molecular dissection of the microtubule depolymerizing activity of mitotic centromere-associated kinesin. *J. Biol. Chem.* 276, 34753–34758

13 Ovechkina, Y. *et al.* (2002) K-loop insertion restores microtubule depolymerizing activity of a 'neckless' MCAK mutant. *J. Cell Biol.* 159, 557–562

14 Niederstrasser, H. *et al.* (2002) XKCM1 acts on a single protofilament and requires the C terminus of tubulin. *J. Mol. Biol.* 316, 817–828

15 Vale, R.D. *et al.* (1989) One-dimensional diffusion of microtubules bound to flagellar dynein. *Cell* 59, 915–925

16 Chandra, R. *et al.* (1993) An N-terminal truncation of the ncd motor protein supports diffusional movement of microtubules in motility assays. *J. Cell Sci.* 104, 899–906

17 Okada, Y. and Hirokawa, N. (1999) A processive single-headed motor: kinesin superfamily protein KIF1A. *Science* 283, 1152–1157

18 Okada, Y. *et al.* (2003) Processivity of the single-headed kinesin KIF1A through biased binding to tubulin. *Nature* 424, 574–577

19 Okada, Y. and Hirokawa, N. (2000) Mechanism of the single-headed processivity: diffusional anchoring between the K-loop of kinesin and the C terminus of tubulin. *Proc. Natl. Acad. Sci. U. S. A.* 97, 640–645

20 Moores, C.A. *et al.* (2003) Regulation of KinI kinesin ATPase activity by binding to the microtubule lattice. *J. Cell Biol.* 163, 963–971

21 Ogawa, T. *et al.* (2004) A common mechanism for microtubule destabilizers-m type kinesins stabilize curling of the protofilament using the class-specific neck and loops. *Cell* 116, 591–602

22 Moore, A.T. and Wordeman, L. (2004) The carboxyl-terminus of mitotic centromere-associated kinesin (MCAK) inhibits its lattice stimulated ATPase activity. *Biochem. J.* 10.1042/BJ20040736 (www.biochemj.org)

23 Shipley, K. *et al.* (2004) Structure of a kinesin microtubule depolymerization machine. *EMBO J.* 23, 1422–1432

24 Newton, C.N. *et al.* (2004) MCAK, a KinI kinesin, increases the catastrophe frequency of steady-state HeLa cell microtubules in an ATP-dependent manner *in vitro*. *FEBS Lett.* 572, 80–84

25 Nogales, E. (2000) Structural insights into microtubule function. *Annu. Rev. Biochem.* 69, 277–302

26 Orr, G.A. *et al.* (2003) Mechanisms of Taxol resistance related to microtubules. *Oncogene* 22, 7280–7295

27 Hyman, A.A. *et al.* (1992) Role of GTP hydrolysis in microtubule dynamics: information from a slowly hydrolyzable analogue, GMPCPP. *Mol. Biol. Cell* 3, 1155–1167

28 Hyman, A.A. *et al.* (1995) Structural changes accompanying GTP hydrolysis in microtubules: information from a slowly hydrolyzable analogue guanylyl-(α,β)-methylene-diphosphonate. *J. Cell Biol.* 128, 117–125

29 Walczak, C.E. *et al.* (1996) XKCM1: a *Xenopus* kinesin-related protein that regulates microtubule dynamics during mitotic spindle assembly. *Cell* 84, 37–47

30 Maney, T. *et al.* (1998) Mitotic centromere-associated kinesin is important for anaphase chromosome segregation. *J. Cell Biol.* 142, 787–801

31 Walczak, C.E. *et al.* (2002) The microtubule-destabilizing kinesin XKCM1 is required for chromosome positioning during spindle assembly. *Curr. Biol.* 12, 1885–1889

32 Ganem, N.J. and Compton, D.A. (2004) The KinI kinesin Kif2a is required for bipolar spindle assembly through a functional relationship with MCAK. *J. Cell Biol.* 166, 473–478

33 Murray, A.W. and Mitchison, T.J. (1994) Mitosis. Kinetochores pass the IQ test. *Curr. Biol.* 4, 38–41

34 Garcia, M.A. *et al.* (2002) Two kinesin-like Kin I family proteins in fission yeast regulate the establishment of metaphase and the onset of anaphase A. *Curr. Biol.* 12, 610–621

35 Kline-Smith, S.L. *et al.* (2004) Depletion of centromeric MCAK leads to chromosome congression and segregation defects due to improper kinetochore attachments. *Mol. Biol. Cell* 15, 1146–1159

36 Cassimeris, L. and Morabito, J. (2004) TOGp, the human homolog of XMAP215/Dis1, is required for centrosome integrity, spindle pole organization, and bipolar spindle assembly. *Mol. Biol. Cell* 15, 1580–1590

37 Holmfeldt, P. *et al.* (2004) Differential functional interplay of TOGp/XMAP215 and the KinI kinesin MCAK during interphase and mitosis. *EMBO J.* 23, 627–637

38 Homma, N. *et al.* (2003) Kinesin superfamily protein 2A (KIF2A) functions in suppression of collateral branch extension. *Cell* 114, 229–239

39 Santama, N. *et al.* (1998) KIF2β, a new kinesin superfamily protein in non-neuronal cells, is associated with lysosomes and may be implicated in their centrifugal translocation. *EMBO J.* 17, 5855–5867

40 Cheng, L.J. *et al.* (2002) Expression of a novel HsMCAK mRNA splice variant, tsMCAK gene, in human testis. *Life Sci.* 71, 2741–2757

41 Mitchison, T.J. (1989) Polewards microtubule flux in the mitotic spindle: evidence from photoactivation of fluorescence. *J. Cell Biol.* 109, 637–652

42 Endow, S.A. *et al.* (1994) Yeast Kar3 is a minus-end microtubule motor protein that destabilizes microtubules preferentially at the minus ends. *EMBO J.* 13, 2708–2713

43 Hildebrandt, E.R. and Hoyt, M.A. (2000) Mitotic motors in *Saccharomyces cerevisiae*. *Biochim. Biophys. Acta* 1496, 99–116

44 Andrews, P.D. *et al.* (2004) Aurora B regulates MCAK at the mitotic centromere. *Dev. Cell* 6, 253–268

45 Lan, W. *et al.* (2004) Aurora B phosphorylates centromeric MCAK and regulates its localization and microtubule depolymerization activity. *Curr. Biol.* 14, 273–286

46 Ohi, R. *et al.* (2004) Differentiation of cytoplasmic and meiotic spindle assembly MCAK functions by Aurora B-dependent phosphorylation. *Mol. Biol. Cell* 15, 2895–2906

47 Trinkle-Mulcahy, L. *et al.* (2001) Dynamic targeting of protein phosphatase 1 within the nuclei of living mammalian cells. *J. Cell Sci.* 114, 4219–4228

48 Murata-Hori, M. *et al.* (2002) Probing the dynamics and functions of aurora B kinase in living cells during mitosis and cytokinesis. *Mol. Biol. Cell* 13, 1099–1108

49 Murata-Hori, M. and Wang, Y.L. (2002) The kinase activity of aurora B is required for kinetochore–microtubule interactions during mitosis. *Curr. Biol.* 12, 894–899

50 Crane, R. *et al.* (2004) Aurora A, meiosis and mitosis. *Biol. Cell.* 96, 215–229

51 Wordeman, L. *et al.* (1999) Mutations in the ATP-binding domain affect the subcellular distribution of mitotic centromere-associated kinesin (MCAK). *Cell Biol. Int.* 23, 275–286

52 Ohi, R. *et al.* (2003) An inner centromere protein that stimulates the microtubule depolymerizing activity of a KinI kinesin. *Dev. Cell* 5, 309–321

53 Whitfield, M.L. *et al.* (2002) Identification of genes periodically expressed in the human cell cycle and their expression in tumors. *Mol. Biol. Cell* 13, 1977–2000

54 Perou, C.M. *et al.* (1999) Distinctive gene expression patterns in human mammary epithelial cells and breast cancers. *Proc. Natl. Acad. Sci. U. S. A.* 96, 9212–9217

55 Adams, R.R. *et al.* (2001) Chromosomal passengers and the (aurora) ABCs of mitosis. *Trends Cell Biol.* 11, 49–54

56 Kline-Smith, S.L. and Walczak, C.E. (2002) The microtubule-destabilizing kinesin XKCM1 regulates microtubule dynamic instability in cells. *Mol. Biol. Cell* 13, 2718–2731

57 Bhalla, K.N. (2003) Microtubule-targeted anticancer agents and apoptosis. *Oncogene* 22, 9075–9086

58 Jordan, M.A. (2002) Mechanism of action of antitumor drugs that interact with microtubules and tubulin. *Curr. Med. Chem. Anti-Canc. Agents* 2, 1–17

59 Lawrence, C.J. *et al.* (2002) Maximum likelihood methods reveal conservation of function among closely related kinesin families. *J. Mol. Evol.* 54, 42–53

60 Dagenbach, E.M. and Endow, S.A. (2004) A new kinesin tree. *J. Cell Sci.* 117, 3–7

61 Mitchison, T. and Kirschner, M. (1984) Dynamic instability of microtubule growth. *Nature* 312, 237–242

62 Alberts, B. *et al.* (2002) *Molecular Biology Of The Cell*, Garland Science

63 Scliwa, M. and Honer, B. (1993) Microtubules, centrosomes and intermediate filaments in directed cell movement. *Trends Cell Biol.* 3, 377–380

64 Sato, M. and Toda, T. (2004) Reconstruction of microtubules; entry into interphase. *Dev. Cell* 6, 456–458

65 Stukenberg, P.T. (2003) Mitosis: long-range signals guide microtubules. *Curr. Biol.* 13, R848–R850

66 Garrett, S. and Kapoor, T.M. (2003) Microtubule assembly: catastrophe factors to the rescue. *Curr. Biol.* 13, R810–R812

67 Sawin, K.E. and Scholey, J.M. (1991) Motor proteins in cell division. *Trends Cell Biol.* 1, 122–129

68 Aist, J.R. (2002) Mitosis and motor proteins in the filamentous ascomycete, *Nectria haematococca*, and some related fungi. *Int. Rev. Cytol.* 212, 239–263

69 Mandelkow, E. and Mandelkow, E.M. (2002) Kinesin motors and disease. *Trends Cell Biol.* 12, 585–591

70 Sharp, D.J. *et al.* (2000) Microtubule motors in mitosis. *Nature* 407, 41–47

71 Pihan, G. and Doxsey, S.J. (2003) Mutations and aneuploidy: co-conspirators in cancer? *Cancer Cell* 4, 89–94

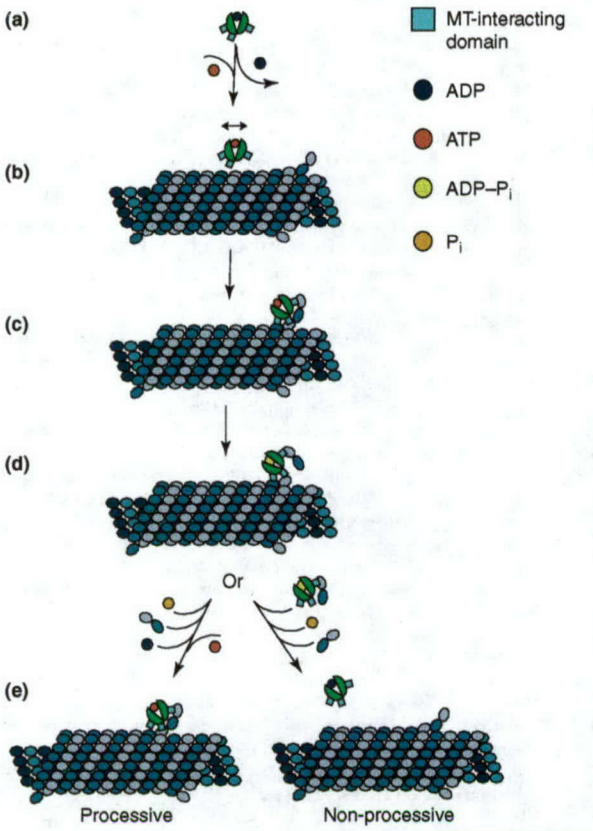

Figure 1. Proposed mechanism of mitotic centromere-associated kinesin (MCAK)-mediated depolymerization. **(a)** Crystal structures of *Murine* Kif2C (MCAK) show that the motor domain has several distinct regions that confer a convex conformation to the protein. **(b)** In this conformation, the motor is unable to lie flat on the surface of the microtubule (MT) and might diffuse along the lattice until it reaches an MT end. **(c)** The conformationally distinct curvature of the MT end might conform to the concave shape of the motor and promote tight coupling and ATP hydrolysis. **(d)** MCAK binds tightly to the MT end in the presence of ATP. ATP hydrolysis might then promote active dissociation of the terminal tubulin dimer from the MT or its release from the motor. **(e)** Processive and non-processive models show how, subsequently, MCAK might be recycled to perform several rounds of depolymerization. This model is consistent for both plus (+)- and minus (–)-end depolymerization because both ends exhibit curved terminal tubulin dimers.

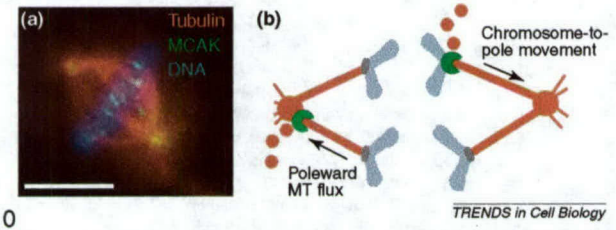

Figure 2. Localization of mitotic centromere-associated kinesin (MCAK) during mitosis and the role of microtubule (MT) depolymerizers. **(a)** A human primary fibroblast cell in metaphase, labeled with antibodies for MCAK (green) and tubulin (red), and stained for DNA (blue). MCAK is localized to centromeres and centrosomes. Scale bar, 5 μm. **(b)** Model showing how depolymerizing motors might function at the centromere and centrosome. Motors at the centromere might 'chew' away at MTs and move the chromatids poleward as they shorten the MTs. Motors at the centrosomes or spindle poles might chew away at MTs and reel the chromatids in towards the pole (analogous to reeling in with a fishing rod). This process is termed 'poleward MT flux'.

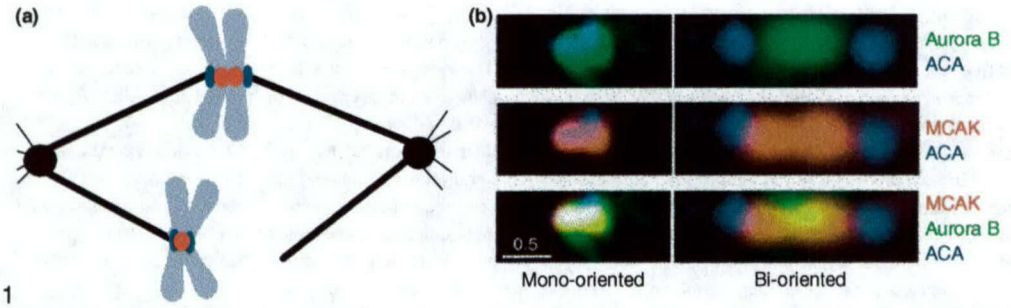

Figure 3. Centromere and kinetochore morphology of mono-oriented and bi-oriented chromosomes. **(a)** Distinct morphology of the centromere and the mitotic kinetochore during periods of high (bi-orientation) and low (mono-orientation) tension. During high tension, kinetochores (blue) are markedly further apart and the centromeric region (red) is stretched. **(b)** Apparent differences in protein localization during microtubule attachment and stretch across the kinetochores. Two chromosomes, one mono-oriented and the other bi-oriented, were imaged from the same prometaphase cell. Colocalization of mitotic centromere-associated kinesin (MCAK; red) and Aurora B (green) seems to change with respect to tension across sister kinetochores, as judged by ACA (CREST) staining for kinetochores (blue). This suggests that the localization of MCAK might be dynamic across the centromere. Reproduced, with permission, from Ref. [44].

Box 1. Microtubule dynamics and microtubule-associated proteins

Microtubules (MTs) are dynamic polymers [61] that comprise a major portion of the cytoskeleton. Composed of tubulin heterodimers (α- and β-tubulin), they assemble first longitudinally to form protofilaments and then cylindrically to form a 13-filament tube. MTs have an inherent polarity: the exposed β-tubulin end is called the 'plus end' and the exposed α-tubulin end is called the 'minus end' [62] (Figure I). During periods of MT growth, the tubulin heterodimers are bound to GTP and straight. During periods of shrinkage, they use the energy derived from GTP hydrolysis to assume a bent conformation that destabilizes MTs from their ends [27,28]. The minus ends of most cellular MTs are anchored to a structure called the centrosome. The surface (or 'lattice') of the MT is negatively charged, which supports electrostatic interactions with associated proteins [7,19].

MTs markedly reorder throughout the life of the cell to support cellular functions such as modulation of cell shape, cell motility [63] and cell division [64–66]. One such major reorganization takes place during mitosis when MTs form a bipolar structure termed the 'spindle' to support the accurate division of duplicated chromosomes (Figure I). The organization of this structure is mediated by numerous motor proteins such as those of the kinesin family [11,66,67]. Some of these motors generate force and position the mitotic spindle, including KlpA/ncd [43,68], BimC [68], Eg5 [69] and CHO1 [70]; some position chromosomes such as CENP-E [11,70], chromokinesin [11,70] and Xkid [11]; and some depolymerize MTs, for example, mitotic centromere-associated kinesin (MCAK) [11], Kip3p [43], Klp10A [8] and Klp59C [8], to name a few.

The motility of these kinesins is predicted by the position of their motor domain. Amino-terminally located motor domains (Kin-N) tend to indicate motility directed to the plus end. Carboxy-terminally located motor domains (Kin-C) tend to indicate motility directed to the minus end. Internally located motor domains (Kin-I) tend to possess depolymerizing capabilities. MT depolymerizers such as MCAK rapidly destabilize MTs from their ends (Figure I). Cooperation between numerous members of the kinesin motor family, as well other proteins, enables the MT cytoskeleton to reconfigure in response to various cellular needs.

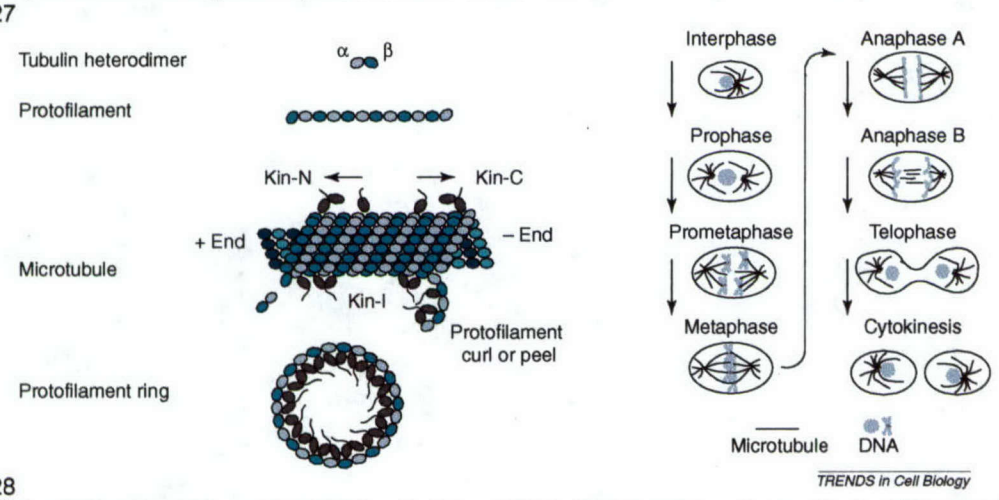

Figure I. Microtubule (MT) assembly and MT dynamics during cell division. The left panel shows the assembly of an MT, from its individual tubulin heterodimers to its cylindrical structure. Some kinesin motors travel along the MT surface in the plus (+)- or minus (–)-end direction, whereas others depolymerize MTs from their ends. This is dictated largely by the position of their motor domains. The right panel shows how MTs are drastically re-ordered during mitosis to support the accurate segregation of genetic material.

Box 2. An in-depth look at the kinetochore and centromere of a mitotic cell

The kinetochore is the site of microtubule (MT) attachment to the chromosomes (Figure I). Once the chromosomes establish connections to MTs, they oscillate back and forth, creating and breaking MT attachments until they are correctly bi-oriented. Paired sister chromatids must

capture MTs emanating from their respective poles and maintain a bi-orientation [62]. This process is error prone and misconnections are often made during early stages of mitosis. Merotelic attachments arise when one sister chromatid is attached to both poles, whereas syntelic attachments occur when both sister chromatids are connected to one pole (Figure I). These erroneous attachments can be detrimental to the cell because they can cause the loss or gain of chromosomes in one or both daughter cells in a process known as 'aneuploidy', which is one of the principal causes of tumorigenesis [71]. Fortunately, the cell has many safeguards against aneuploidy.

The kinetochore consists of three distinct 'plates' and a fibrous outer region called the 'corona' (Figure I). This complex assemblage coordinates MT attachment with movement and MT dynamics [62]. Numerous motors and other MT-binding proteins have been identified on the centromere and kinetochore, and their function is to ensure that chromosomes are correctly bi-oriented and segregated into daughter cells [10,11,67]. The kinetochore also associates with 'checkpoint' proteins that translate biophysical measures of bi-orientation such as MT attachment and tension into a biochemical signal that the cell can read to determine when to enter anaphase. Disturbances in the activity, distribution or expression of these proteins can cause detrimental or lethal consequences to cells and the organism.

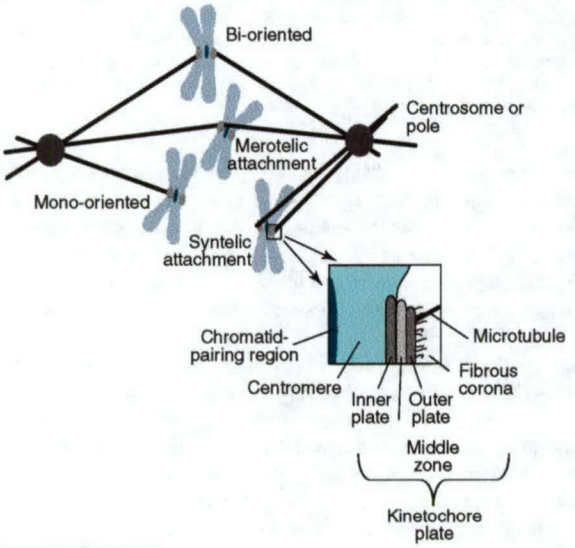

TRENDS in Cell Biology

Figure I. The kinetochore, the centromere and microtubule (MT) attachment. Many erroneous MT attachments can arise as chromosomes seek bi-orientation and alignment at the metaphase plate. These attachments include merotelic (one sister chromatid attached to both poles) and syntelic (both sister chromatids attached to one pole) attachments. Fortunately, many motors are distributed throughout the centromere and kinetochore to correct these mal-attachments and promote the accurate segregation of genetic material during mitosis.

Table 1. MT-depolymerizing motors: localization, knockout phenotype and proposed mechanism[a]

Depolymerizing kinesins	Localization during mitosis	Knockdown and dominant-negative phenotypes	Presumed role during mitosis	References
Vertebrate MCAK (*Cg*MCAK, *Mm*Kif2C, *Xl*XKCM1)	Centromeres; spindle poles; midbodies; cytoplasm	Lagging chromosomes; merotelic and syntelic connections; increased chromatid oscillations at anaphase; long spindles; partially separated spindle poles	Correct merotelic connections during prometaphase; anaphase depolymerase; suppresses anaphase oscillations; mitotic spindle assembly and maintenance	[8,29–31,35–37]
*Dm*Klp10A	Centromeres until anaphase; spindle poles	Monopolar spindles; long bipolar spindles; unaligned metaphase plate; slow anaphase poleward movement	Minus-end depolymerase; promotes poleward chromatid movement via MT flux	[8]
*Dm*Klp59C	Centromeres	Unaligned metaphase plate; abnormal anaphase segregation; slow chromatid to pole movement during anaphase	Plus-end MT depolymerase; promotes poleward chromatid motility via the 'Pac-Man™' method	[8]
*Mm*Kif2Aβ, *Hs*Kif2Aβ	Centrosomes, spindle MTs at spindle pole	Monopolar spindles	Bipolar spindle assembly	[32]
[b]Kip3 family (*Sc*Kip3p, *Sp*Klp5, *Sp*Klp6)	Cytoplasmic MTs; spindle MTs; spindle midzone in late anaphase	Cytoplasmic MTs do not enter bud; long metaphase and telophase spindles; stable cytoplasmic MTs; delay in anaphase exit	Spindle assembly and maintenance; destabilization of cytoplasmic and nuclear MTs	[6,11,34,43]
[b]*Sc*Kar3p	Spindle pole bodies; nucleus, spindle	Longer cytoplasmic MTs	Crosslinking antiparallel MTs; spindle assembly and maintenance; spindle positioning; destabilization of cytoplasmic and nuclear MTs	[6,11,43]
[b]*Dm*Klp67A		Long MTs; enlarged spindle; curved spindles	Centrosomes separation; chromosome segregation; central spindle assembly; MT disassembly	[9]
[c]*Pf*Kin-I				[7,20]
[c]*Mm*Kif2B				[4]
[c]*Dm*Klp59D				[8]

[a]Abbreviations: *Cg*, *Cricetulus griseus*; *Dm*, *Drosophila melanogaster*; *Hs*, *Homo sapiens*; MCAK, mitotic centromere-associated kinesin; *Mm*, *Mus musculus*; MT, microtubule; *Pf*, *Plasmodium falciparum*; *Sc*, *Saccharomyces cerevisiae*; *Sp*, *Schizosaccharomyces pombe*; *Xl*, *Xenopus laevis*.

[b]These kinesin motors show some sequence homology and/or functional activity that resembles that of well-characterized depolymerizing Kin-I kinesins; so far, however, data to determine whether they affect MT depolymerization directly or indirectly are still preliminary.

[c]So far, these Kin-I kinesins have not been implicated in mitotic activity.

MCAK associates with the Tips of Polymerizing Microtubules.

Ayana T. Moore*, George von Dassow#, Michael Wagenbach*, Yulia Ovechkina*, Leticia Peris**, Annie Andrieux**, Didier Job** and Linda Wordeman*

*Dept. of Physiology and Biophysics, Univ. of Washington,
#Center for Cell Dynamics, Friday Harbor Labs, Univ. of Washington
**Laboratoire du Cytosquelette, INSERM, Grenoble France

To whom correspondence should be sent:
Linda Wordeman, Box 357290, Dept. of Physiology and Biophysics, University of Washington, Seattle, WA 98195. Phone: 206-543-4135, FAX: 206-685-0619, Email: worde@u.washington.edu

Condensed Title: MCAK tracks on Microtubule Tips.

Keywords: MCAK, EB1, CLIP-170, microtubules, kinesin

Introduction

MCAK is a member of the KinI/MCAK/kinesin-13 (Lawrence, 2004) family of depolymerizing kinesins. Previous studies have implicated MCAK in the regulation of microtubule (MT) dynamics during interphase and mitosis and in ensuring proper chromosome segregation during mitosis. MCAK is a potent depolymerase of stabilized MTs (Desai et al., 1999; Hunter et al., 2003) and strongly increases the catastrophe frequency of dynamic MTs in vitro (Newton et al., 2004). MCAK is the most potent MT depolymerizer that has yet been identified (Ogawa et al., 2004; Tournebize et al., 2000). MCAK displays extremely high affinity for MT ends, yet its localization to ends in fixed cells is intermittent at best. For, these reasons we imaged live cells transfected with levels of GFP or RFP-MCAK that do not appreciably disturb the overall MT polymer level. When imaged in this manner, MCAK is observed to track with polymerizing MT tips.

A number of proteins exhibit the unusual property of targeting and treadmilling (tracking) along polymerizing microtubule (MT) ends. The two most well characterized of these are members of the Clip-170 and Eb1 families (reviewed in (Carvalho et al., 2003)). Thus far, all known treadmilling tip proteins exhibit microtubule stabilizing activity. For this reason, it is remarkable that the potent microtubule depolymerase, MCAK, tracks the tips of polymerizing microtubules. MCAK strongly co-localizes with EB1 suggesting that EB1 (and possibly other tip tracking proteins) opposes MCAK activity at the tip until preferentially lost. MCAK's tip tracking is dependent on phosphorylation which may regulate the association of MCAK with free tubulin dimers and thus the ability to localize to polymerizing MT ends.

Results and Discussion

When fluorescent MCAK is expressed in live cultured cells at levels that do not significantly alter microtubule polymer levels, MCAK can be detected on microtubule lattice and in obvious densities on microtubule tips (Figure 1). Time-lapse imaging shows tips polymerizing toward the cell edge (tracking) in a manner identical to that seen with GFP-EB1 (Figure 1, arrows). In fact the MCAK tip densities are perfectly coincident with GFP-EB1 in living cells (Figure 2A, A'). Surfing of MCAK on microtubule tips is not dependent on a functional motor domain as it can be seen clearly in cells transfected with GFP-ML-MCAK (Figure 2B), a construct in which the 350kD motor domain has been removed and the N-terminal domain of MCAK fused directly to the C-terminal domain (Maney et al., 1998). A mutant of MCAK that contains three point mutations in the motor domain rendering the protein inactive with respect to depolymerizing activity (GFP-hypir-MCAK) also exhibits tip surfing. Tip localization and surfing is seen in either interphase or mitotic cells (Figure 2C). To summarize, MCAK is found on the tips of polymerizing microtubules in both interphase and mitotic cells and this localization is not dependent on a functional motor domain. This is a striking observation because MCAK has been previously shown to be a potent depolymerizer of microtubules (Desai et al., 1999; Hunter et al., 2003). Therefore, to see MCAK on the tips of polymerizing microtubules suggests that MCAK's depolymerizing activity is inhibited on tips.

We were interested to determine whether other known microtubule depolymerizing proteins are present on microtubule tips. Because the localization of proteins to microtubules is variable when fixed, we assayed a number of proteins fused to GFP in living HeLa cells. The results of those experiments are summarized in Table I. GFP-proteins were assayed for association with the microtubule lattice, with tips and assayed in living cells by time-lapse imaging for tip tracking. As described above, GFP-MCAK, GFP-ML-MCAK and GFP-hypir MCAK associated with tips and also exhibited tip tracking. Both GFP-ML-MCAK and GFP-hypir-MCAK exhibited less interaction with microtubule lattice despite a strong interaction with tips. This is consistent with our previous results suggesting that MCAK hydrolyzes ATP on the lattice and this increases the dwell time of active motor on the lattice (Moore and Wordeman, 2004). An active phospho-mutant of MCAK (GFP-AAAAA-MCAK) also exhibited robust tip tracking. In this mutant all of the sites known to be phosphorylated by Aurora B kinase have been mutated to alanine (Andrews et al., 2004). Significantly, a phospho-mimic mutant of MCAK (GFP-EEEEE-MCAK) showed no tip tracking even though this protein is capable of weak interactions with the microtubule lattice (Table I, Figure 3A). This result is counterintuitive because previously phosphorylation has been demonstrated as a mechanism for inactivating MCAK's depolymerizing activity (Andrews et al., 2004; Lan et al., 2004; Ohi et al., 2004). The fact that GFP-EEEEE-MCAK does not decorate the tips of polymerizing microtubules and GFP-AAAAA-MCAK does suggests that phosphorylation is not the means by which MCAK is inhibited on tips of polymerizing microtubules.

GFP-EB1 showed robust tip tracking as described in Figure 2. We also tested two other Kin I/kinesin-13 kinesins: Kif2Aα and Kif2Aβ. Both proteins exhibited significant depolymerizing activity when overexpressed. However, these proteins were not found tracking on microtubule tips. Because MCAK and Kif2Aα/βshare high amino acid identity within the neck+motor domain we tested whether MCAK's minimal full strength depolymerization domain (neck+motor (Maney et al., 2001; Ovechkina et al., 2002)) was capable of tip tracking. As can be seen in Table I, neither the core motor domain or the motor+neck domain were capable of tip tracking. This suggests that tip tracking may depend on more divergent domains outside of the neck+motor domain. It is interesting that although the Aurora B consensus phosphorylation sites appear to be conserved between all the KinI/kinesin-13 family members (Andrews et al., 2004), the protein sequence surrounding the conserved phosphorylation sites are quite divergent between MCAK and Kif2Aα/β. This implicates the N-terminus of MCAK, particularly the region surrounding the Aurora B/Ipl1 phosphorylation sites in associating with tubulin in a phosphorylation-dependent manner.

We tested several other phosphorylation-dependent regulators of microtubule dynamics. Neither GFP-stathmin (Marklund et al., 1996), GFP-ch-TOG (Charrasse et al., 1998) or GFP-ICIS (Ohi et al., 2003) was found to be tracking on microtubule tips. This suggests that MCAK is the only microtubule depolymerizer that tracks on the tips of polymerizing microtubules. GFP-APC decorated microtubule tips did not exhibit the same distribution or dynamics as those decorated with MCAK or EB1. Instead tips exhibited aperiodic bending previously described in (Dayanandan et al., 2003).

Because the tip tracking behavior of MCAK was dependent on phosphorylation we observed the behavior of endogenous MCAK in the presence of the kinase inhibitor Roscovitine. CHO cells were incubated in either DMSO or 10 mM Roscovitine in DMSO for five hours and then fixed and labeled for endogenous MCAK and microtubules (Figure 3B top and bottom, respectively). After five hours of Roscovitine treatment endogenous MCAK exhibited significantly greater association with microtubule tips. The total amount of microtubule polymer was not affected. This was not surprising as the levels of Roscovitine used are capable of inhibiting a number of kinases (Meijer et al., 1997) and it would be impossible to predict the overall effect on all microtubule modulators. Nevertheless, the redistribution of endogenous MCAK was striking (Figure 3B, bottom). We performed time-lapse imaging of GFP-MCAK transfected cells in order to confirm that MCAK was tracking with tips in the presence of Roscovitine (Figure 3C).

Tip tracking has not proved to be amenable to study with purified proteins in vitro as it is not seen in stabilized microtubules and it is difficult to assay using living microtubules in vitro. Therefore, to explore the mechanism of phosphorylation-dependent tip tracking of MCAK we assayed the ability of tubulin to compete with MCAK's weak association with microtubule lattice in the absence of ATP. Previously we have found that free tubulin dimer can compete MCAK off of the microtubule lattice in the absence of ATP (Moore and Wordeman, 2004). Furthermore, (Newton et al., 2004) have hypothesized that MCAK is capable of sequestering tubulin in the absence of ATP hydrolysis. We mixed purified MCAK protein with paclitaxel-stabilized microtubules in the absence of ATP. Both unphosphorylated MCAK and MCAK which has been phosphorylated using Ipl1/Sli15 associate preferentially with microtubule lattice (Figure 4A, lanes 3 and 5). However, in the presence of free tubulin, unphosphorylated MCAK is partially competed off of stabilized microtubules and remains in the supernatant after the microtubules are pelleted (Figure 4A, lane 4). Phosphorylated MCAK cannot be competed off of microtubule lattice with free tubulin (Figure 4A, lane 6). This demonstrates that MCAK's interaction with free tubulin is dependent upon the phosphorylation state of the protein. How this relates to the mechanism of tip tracking and regulation of microtubule dynamics by MCAK is illustrated in Figure 4B. Phosphorylated MCAK is unable to interact with free tubulin and is also unable to track on microtubule tips. This suggests a model for tip tracking of EB1 and MCAK in which the microtubule is insensitive to the effects of MCAK as long as sufficient EB1 is associated with the tip. Although both EB1 and MCAK are lost slowly from the lattice, MCAK remains loosely associated with the lattice but capable of initiating microtubule depolymerization via lattice priming (Moore and Wordeman, 2004) or diffusional motility to the terminal dimers at the tip (Hunter et al., 2003). Although MCAK is the only depolymerizer assayed that we have found to track to tips, other treadmilling tip tracking proteins such as CLIP-170 may also contribute to the balance of catastrophe and rescue at the microtubule tip.

MCAK is the sole identified microtubule depolymerizer that tracks on microtubule tips. Neither stathmin or either splice variant of Kif2A were able to track on microtubule tips. It is interesting that Kif2Aα/β is both unable to track on tips and is also a weaker MT depolymerizer in vivo (KE Rankin and L Wordeman, unpublished, (Ogawa et al., 2004)).

It is unlikely that MCAK and Kif2A differ markedly in their mechanism of MT depolymerization. Therefore, we predict that MCAK has a second, non motor-dependent tubulin binding site. This site may weakly anchor MCAK to the lattice and increase its MT depolymerization rate via "lattice priming"(Moore and Wordeman, 2004). Kif2Aα/β may lack this binding site or may interact with different proteins in a phosphorylation-dependent manner via this region.

Previously, it has been shown that MCAK's activity and sub-centromeric distribution is regulated by phosphorylation by Aurora kinase (Andrews et al., 2004). Phosphorylated MCAK is preferentially localized to the inner centromere while de-phosphorylated MCAK is preferentially localized to the distal face of the centromere. Phosphorylation significantly inhibits MCAKs activity and we show here that phosphorylation also eliminates the tip tracking behavior of MCAK. Furthermore, tip tracking of endogenous MCAK is enhanced by short incubations in the kinase inhibitor Roscovitine. Although the motor domain of MCAK has been shown to preferentially associate with microtubule ends (Desai et al., 1999; Hunter et al., 2003), tip tracking is not dependent on the presence or activity of the motor domain. Instead, the N-terminal conserved phosphorylation sites which inhibit MCAK's MT depolymerization activity and targeting to the outer face of the kinetochore when phosphorylated (Andrews et al., 2004). Tip tracking along kinetochore microtubules by de-phosphorylated MCAK may be the mechanism by which active de-P MCAK localizes to the outer centromere during mitosis.

Materials and Methods

Constructs

EGFP-cgMCAK (pYOY152) was prepared by pasting a BspeI-HindIII fragment of pYOY71 (Ovechkina et al., 2002) into pEGFPC1 (Clontech). EGFP-ML-cgMCAK (pYOY154) was prepared originally from GFP-ML-MCAK (Maney et al., 1998). A BspeI-HindIII fragment was subcloned into pEGFPC1 (Clontech). EGFP-hypir-cgMCAK (pYOY153) consists of a H530A, R534A, K537A mutations engineered by overlapping pcr (pYOY146) and cloned into pEGFPC1.
EGFP-mmStathmin (pMX666) was
EGFP-hsch-TOG (pMX114) was pasted from ch-TOGp, a kind gift of Dr. Christian Larroque (INSERM, France) into EGFP-C1.
Kif2aα (GenBank D12644) and Kif2aβ (GenBank Y15894) cDNA plasmids were a gift of N. Santama. The coding regions were amplified by PCR, and cloned into pEGFP-C1 to generate pMX155 and pMX156, which were sequenced to confirm expected structures. EGFP-APC was a kind gift of Dr. Rina Arbesfeld (Tel Aviv University). EGFP-EEEEE-MCAK (pYOY177) and EGFP-AAAAA-MCAK (pYOY178) were prepared as described in (Andrews et al., 2004). The ECFP gene was deleted from pECFP-N1 (Clontech) by digestion with BamHI and NotI, blunt end with T4 DNA polymerase and replaced with a MluI linker to generate pCMV-M1. RFP was copied from pRSETB-mRFP1 (a kind gift of Roger Tsien) by PCR and digested and cloned into EcoR1 (5') and BamHI (3') sites of pYOY152. RFP+MCAK were ligated into pCMV-

M1 to generate RFP-MCAK (pMX188). EGFP-EB1 was a kind gift of Lynne Cassimeris (Lehigh Univeristy). The 3' end of ICIS was copied from IMAGE clone 4240274 by PCR to give Xho (5') and BamHI (3') ends and cloned into pEGFP-C1 to generate pMX144. The 5' end of ICIS was amplified by PCR from mouse brain cDNA with forward primer CACACTCGAGCTATGAATGATGATAATTCAGATAGGACA and reverse primer CCTGTTACCTGAGGGTTGGGTGTGTCCTTCATTA. The PCR product and pMX144 were digested with XhoI and ApaLI and ligated to generate EGFP-ICIS (pMX152).

Cell transfection and immunofluorescence

HeLa cells or CHO cells were cultured as described in (Ovechkina et al., 2002). One day before transfection cells were plated onto either glass bottomed Petri dishes (MatTek Corp.) for live filming or 12-mm round coverslips for fixed imaging. Cells were transfected using Lipofectamine (Invitrogen) for 4 hours. HeLa cells were imaged 48 hours after transfection whereas CHO cells were imaged 24 hours post-transfection. Fixation was performed as described in (Maney et al., 1998) and immunofluorescence staining using DM1α (Sigma-Aldrich) and sheep-anti-MCAK antibodies was completed at room temp for 1 hour. Purified cgMCAK protein was prepared as described in (Maney et al., 1998) and used to immunize sheep (Pocono). Serum was affinity purified using cgMCAK protein linked to affi-gel (Bio-Rad). Secondary antibodies Texas-Red donkey anti-sheep and Fluorescein donkey anti-mouse were used at a dilution of 1:40 (Jackson Immunoresearch).

Live Imaging

Transfected cells were imaged using a Nikon inverted microscope with a cooled CCD camera (Photometrics) controlled by Metamorph (Universal Imaging) imaging software. Cells were maintained in CO2-independent media (Gibco) with 10% FBS during imaging. Temperature was maintained at 36°C using a piezoelectric control system (). Interphase cells were imaged at 1 frame per 5 sec. And mitotic cells were imaged at 1 frame per 20s. Subsequent analysis was performed with Image J.

Expression and purification of recombinant MCAK, Ipl1p and Sli15p

MCAK expression and purification were performed as previously described (Maney et al., 1998). Ipl1p and Sli15p GST fusion plasmids were kind gifts of Dr. Sue Biggins (Fred Hutchinson Cancer Research Center). Bacteria containing plasmids were grown in 2XTY media with 0.125 mg/ml ampicilin at 37° C until midlog phase. 0.1mM IPTG was used to induce protein expression at 23° C for 3 hours. Cells were pelleted and resuspended in cold PBS. Cell lysis was performed with PBS plus 1mM EGTA, 1mM EDTA, 1mM PMSP, 1X LPC, and 200μg/ml lysozyme. Upon lysis, KCl was added to a final concentration of 0.25M and DTT to a final concentration of 15mM. Supernatant was recovered after centrifugation and added to GST-agarose. GST conjugated protein was eluted with 50mM Tris pH 8.0, 0.25M KCL, and 5mM reduced glutathione. Pooled fractions were then dialyzed overnight at 4° C against PBS with 30% glycerol.

In vitro phosphorylation and pelleting assays

Bovine brain tubulin was acquired from Cytoskeleton (Denver, CO). 50μM of tubulin was added to BRB80 (80mM Pipes, pH 6.8, 1mM EGTA, 1mM $MgCl_2$) with 4mM $MgCl_2$, 1mM GTP, and 5% DMSO and incubated for 20 minutes at 37° C. Following the incubation, MTs were diluted 1:25 in 37° C BRB80 plus 1mM DTT and 10μM paclitaxel (Sigma-Aldrich). Phosphorylation of MCAK was performed by incubating 50nM of active MCAK with 5μl of Ipl1p and 1μl Sli15p in kinase buffer (50mM Tris-Hcl pH 7.5, 0.1mM EGTA, 5mM $MgCl_2$) with 1mM DTT, 0.2mM ATP, 1μM Microcystin-LR and 0.3% TritonX-100 for 1 hour at room temperature (25±1° C). Sixteen microliters of the phosphorylation reaction was incubated with 80ul of MTs at room temperature for 5 minutes and centrifuged in an airfuge at 149,000 x g for 10 minutes. Supernatants and pellets were assayed for the presence of tubulin and motor on Coomassie stained SDS-polyacrylamide gels (Invitrogen, Carlsbad, CA). Bands were quantified using NIH Image 1.62.

Acknowledgements

We are indebted to Greg Martin (Keck Center for Neural Imaging) and Paulette Brunner (Center for Cell Dynamics, Friday Harbor Laboratories) for invaluable assistance with live imaging. This work is supported by a National Institutes of Health Predoctoral Fellowship 1 F31 GM65061 (to A.T. Moore) and Dept. of Defense grant DAMD 17-01-1-0450 and National Institutes of Health Grant (GM69429) to L.Wordeman.

References

Andrews, P.D., Y. Ovechkina, N. Morrice, M. Wagenbach, K. Duncan, L. Wordeman, and J.R. Swedlow. 2004. Aurora B regulates MCAK at the mitotic centromere. *Dev Cell.* 6:253-68.

Carvalho, P., J.S. Tirnauer, and D. Pellman. 2003. Surfing on microtubule ends. *Trends Cell Biol.* 13:229-37.

Charrasse, S., M. Schroeder, C. Gauthier-Rouviere, F. Ango, L. Cassimeris, D.L. Gard, and C. Larroque. 1998. The TOGp protein is a new human microtubule-associated protein homologous to the Xenopus XMAP215. *J Cell Sci.* 111 (Pt 10):1371-83.

Dayanandan, R., R. Butler, P.R. Gordon-Weeks, A. Matus, S. Kaech, S. Lovestone, B.H. Anderton, and J.M. Gallo. 2003. Dynamic properties of APC-decorated microtubules in living cells. *Cell Motil Cytoskeleton.* 54:237-47.

Desai, A., S. Verma, T.J. Mitchison, and C.E. Walczak. 1999. Kin I kinesins are microtubule-destabilizing enzymes. *Cell.* 96:69-78.

Hunter, A.W., M. Caplow, D.L. Coy, W.O. Hancock, S. Diez, L. Wordeman, and J. Howard. 2003. The kinesin-related protein MCAK is a microtubule depolymerase that forms an ATP-hydrolyzing complex at microtubule ends. *Mol Cell.* 11:445-57.

Lan, W., X. Zhang, S.L. Kline-Smith, S.E. Rosasco, G.A. Barrett-Wilt, J. Shabanowitz, D.F. Hunt, C.E. Walczak, and P.T. Stukenberg. 2004. Aurora B phosphorylates centromeric MCAK and regulates its localization and microtubule depolymerization activity. *Curr Biol.* 14:273-86.

Lawrence, C.J. 2004. A standardized kinesin nomenclature. *J Cell Biol.* In press.

Maney, T., A.W. Hunter, M. Wagenbach, and L. Wordeman. 1998. Mitotic centromere-associated kinesin is important for anaphase chromosome segregation. *J Cell Biol.* 142:787-801.

Maney, T., M. Wagenbach, and L. Wordeman. 2001. Molecular dissection of the microtubule depolymerizing activity of mitotic centromere-associated kinesin. *J Biol Chem.* 276:34753-8.

Marklund, U., N. Larsson, H.M. Gradin, G. Brattsand, and M. Gullberg. 1996. Oncoprotein 18 is a phosphorylation-responsive regulator of microtubule dynamics. *Embo J.* 15:5290-8.

Meijer, L., A. Borgne, O. Mulner, J.P. Chong, J.J. Blow, N. Inagaki, M. Inagaki, J.G. Delcros, and J.P. Moulinoux. 1997. Biochemical and cellular effects of roscovitine, a potent and selective inhibitor of the cyclin-dependent kinases cdc2, cdk2 and cdk5. *Eur J Biochem.* 243:527-36.

Moore, A.T., and L. Wordeman. 2004. The carboxyl-terminus of mitotic centromere-associated kinesin (MCAK) inhibits its lattice stimulated ATPase activity. *Biochem J.* Pt.

Newton, C.N., M. Wagenbach, Y. Ovechkina, L. Wordeman, and L. Wilson. 2004. MCAK, a Kin I kinesin, increases the catastrophe frequency of steady-state HeLa cell microtubules in an ATP-dependent manner in vitro. *FEBS Lett.* 572:80-4.

Ogawa, T., R. Nitta, Y. Okada, and N. Hirokawa. 2004. A common mechanism for microtubule destabilizers-M type kinesins stabilize curling of the protofilament using the class-specific neck and loops. *Cell.* 116:591-602.

Ohi, R., M.L. Coughlin, W.S. Lane, and T.J. Mitchison. 2003. An inner centromere protein that stimulates the microtubule depolymerizing activity of a KinI kinesin. *Dev Cell.* 5:309-21.

Ohi, R., T. Sapra, J. Howard, and T.J. Mitchison. 2004. Differentiation of cytoplasmic and meiotic spindle assembly MCAK functions by Aurora B-dependent phosphorylation. *Mol Biol Cell.* 15:2895-906.

Ovechkina, Y., M. Wagenbach, and L. Wordeman. 2002. K-loop insertion restores microtubule depolymerizing activity of a "neckless" MCAK mutant. *J Cell Biol.* 159:557-62.

Tournebize, R., A. Popov, K. Kinoshita, A.J. Ashford, S. Rybina, A. Pozniakovsky, T.U. Mayer, C.E. Walczak, E. Karsenti, and A.A. Hyman. 2000. Control of microtubule dynamics by the antagonistic activities of XMAP215 and XKCM1 in Xenopus egg extracts. *Nat Cell Biol.* 2:13-9.

Table I: Tip Tracking of Microtubule Proteins in Living Cells			
Construct	**Lattice**	**Tips**	**Tip tracking**
GFP-MCAK, RFP-MCAK	Yes	Yes	Yes
GFP-ML-MCAK	Decreased	Yes	Yes
GFP-hypir-MCAK	Decreased	Yes	Yes
GFP-AAAAA-MCAK	Yes	Yes	Yes
GFP-EEEEE-MCAK	Yes	No	No
GFP-Motor+Neck	Yes	No	No
GFP-Motor	No	No	No
GFP-Kif2Aα	Yes	No	No
GFP-Kif2Aβ	Yes	No	No
GFP-EB1	No*	Yes	Yes
GFP-APC	No	Yes	No
GFP-Stathmin	No	No	No
GFP-ch-Tog	No	No	No
GFP-ICIS	Yes**	No	No

*Unless highly over-expressed

**Very strong association with MT lattice

Figure Legends

Figure 1. MCAK exhibits tip tracking behavior in living cells. The edge of an interphase HeLa cell cotransfected with RFP-MCAK (right) and GFP-tubulin (left). Dual images of successive 5 seccond time points are shown. Densities of MCAK protein travel distally toward the edge of the cell with time. (arrows).

Figure 2. MCAK is part of the tip complex of polymerizing microtubules. (A) GFP-EB1 colocalizes with (A') RFP-MCAK in living cells (arrows). RFP-MCAK is also found on microtubule lattice in addition to tips (arrowhead). (B) Inactive GFP-ML-MCAK also exhibits tip tracking in living cells (small arrows). Three successive 5 second time points are shown.(C) Inactive GFP-hypir-MCAK tracks on tips of astral microtubules in a living mitotic cell (small arrows). Two successive 20 second timepoints are shown.

Figure 3. Tip tracking of MCAK protein is dependent on phosphorylation. (A) GFP-AAAAA-MCAK binds to microtubule tips (left) whereas GFP-EEEEE-MCAK is not found on tips (right). (B) Two fields of CHO cells labeled for endogenous MCAK (B) and microtubules (B'). The top field of CHO cells are control cells. The bottom field of CHO cells were cultured for five hours in 10 μM Roscovitine and then fixed. Increased association of endogenous MCAK with distal ends of microtubules is evident (B, lower; arrows). (C) The edge of a HeLa cell transfected with RFP-MCAK and cultured subsequently in 10 μM Roscovitine. The accumulated MCAK protein tracks on tips in Roscovitine (arrows).

Figure 4. Phosphorylation inhibits the association of MCAK with tubulin dimers. (A) A coomassie gel showing the distribution of phosphorylated or unphosphorylated MCAK protein into pellets (P) or supernatants (S) of assembled microtubules in the absence of ATP. MCAK was phosphorylated with S. cerevesiae Ipl1/sli15. Both species of MCAK associated preferentially with assembled microtubules in the absence of ATP (lanes 3-6). Only unphosphorylated MCAK is capable of being partially competed off of polymerized microtubules by the addition of excess tubulin dimer (lane 4). (B) A model for the regulation of MT dynamics by MCAK and EB1. Co-assembly of EB1 and MCAK with tubulin dimers onto the tip inhibits MCAK's depolymerization activity. As EB1 leaves the microtubule lattice, MCAK can prime the microtubule for depolymerization. Tip tracking may depend on the phosphorylation-dependent ability of MCAK (and EB1) to associate with tubulin dimers as well as a preference for the structural conformation of the microtubule tip over the lattice.

Figure 1: Moore et al.

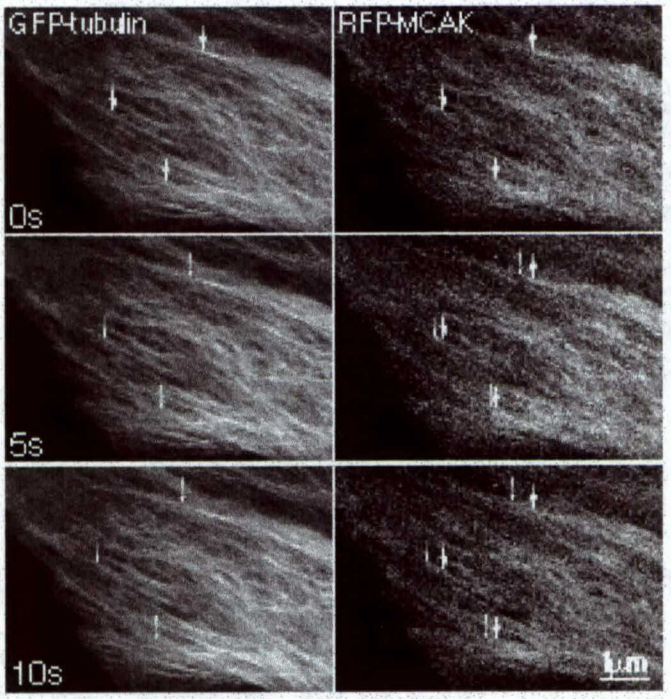

Figure 2: Moore et al.

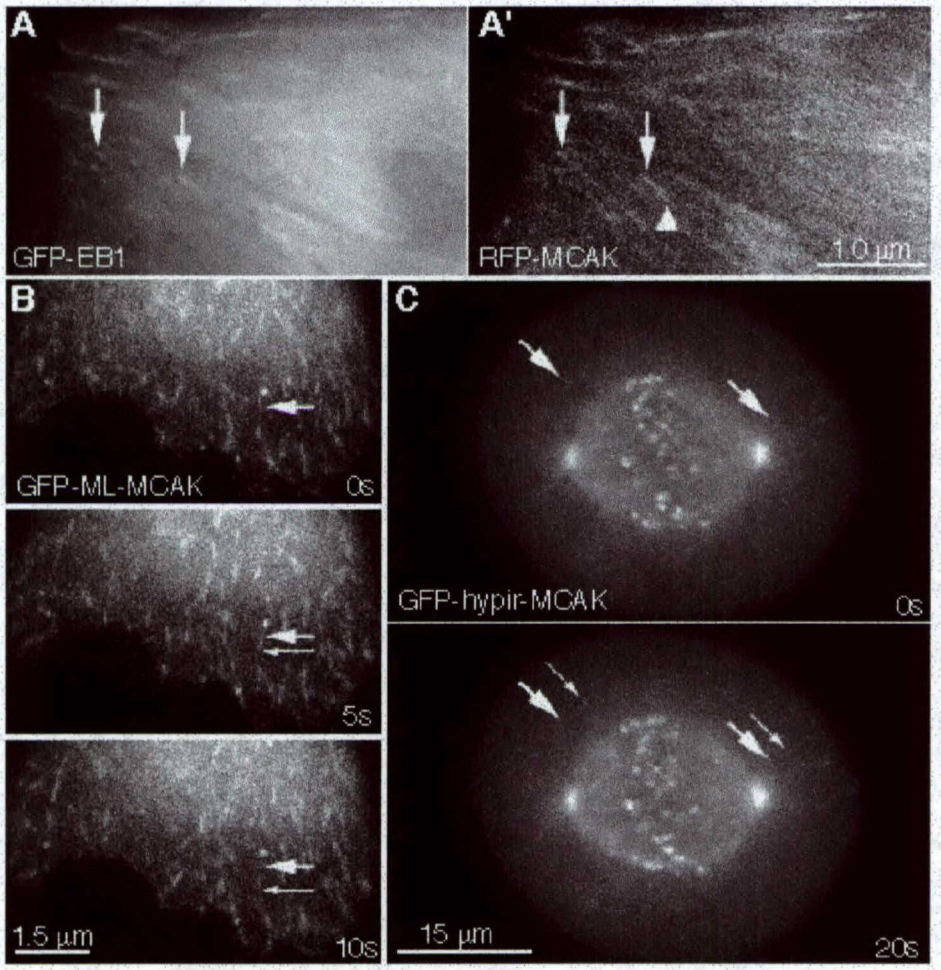

Figure 3: Moore et al.

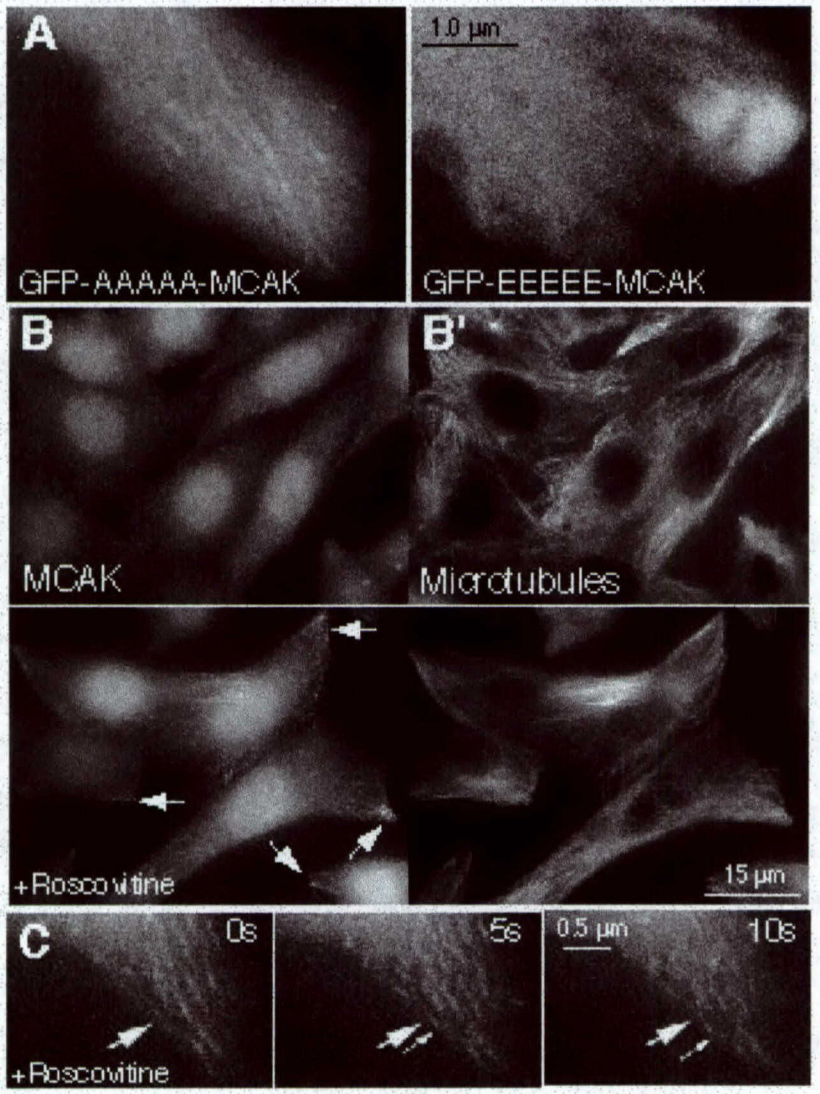

Figure 4: Moore et al

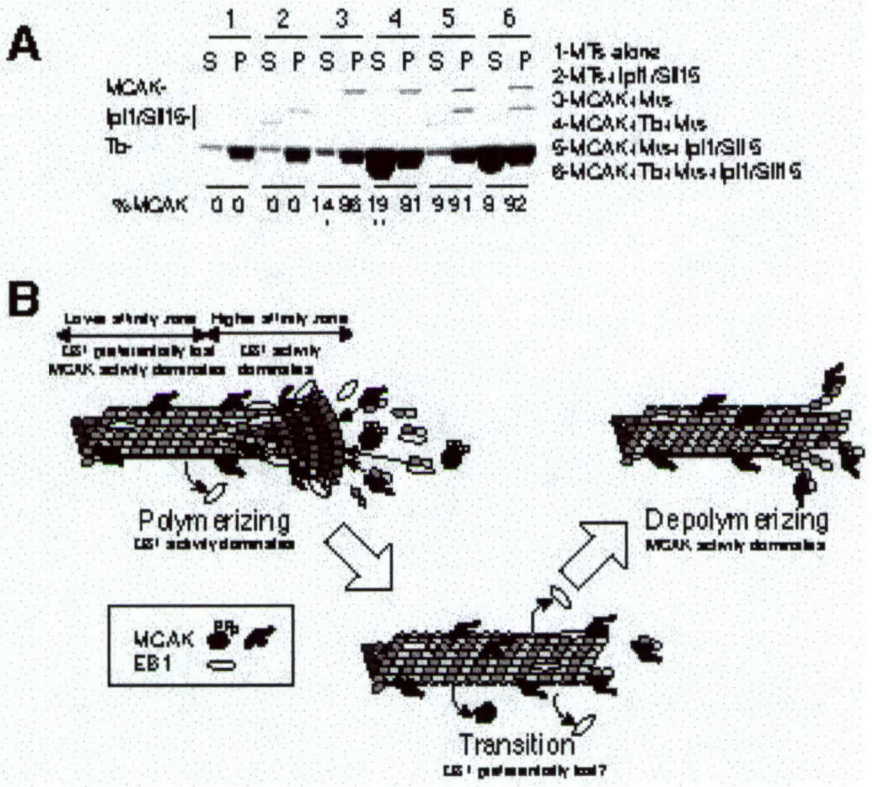

From: Linda Wordeman <worde@u.washington.edu>
Subject: **Re: Aneuploidy in Cortona**
Date: July 14, 2004 3:44:51 PM PDT
To: Maurizio Gatti <maurizio.gatti@uniroma1.it>

Dear Dr. Gatti,

Below is pasted my abstract for the Aneuploidy meeting in Cortona. If you have any difficulty or confusion or any questions please let me know. I apologize for the tardiness of this abstract.

Cheers,
Linda Wordeman

****

The Influence of Aurora B-regulated MCAK on Oscillatory Chromosome Movement.
Linda Wordeman, Yulia Ovechkina and Mike Wagenbach. Dept. of Phsiology and Biophysics, University of Washington, Seattle, WA 98195.

Mitotic Centromere-associated Kinesin (MCAK) is a kinesin-related protein that depolymerizes microtubules (MTs) from both ends. MCAK is a substrate of Aurora B kinase. Phosphorylation by Aurora B inhibits MCAK's MT-depolymerizing activity and also influences targeting of MCAK within the kinetochore and to the tips of interphase microtubules. We have used phospho-mimic and phospho-mutant versions of MCAK to target the enzyme to specific regions of the kinetochore of mitotic HeLa cells. We have combined these mutants with a novel mutation within the HYPIR domain of MCAK's motor that inactivates the MT-depolymerizing activity. In this way we can target inactive MCAK to specific regions within the kinetochore and more precisely define its role in chromosome movement. We have found that an inactive phospho-mutant of MCAK that preferentially associates with the outer face of the kinetochore influences pre-anaphase oscillatory behavior and tension within the centromere. The presence of this mutant slows the speed of chromosome movement. We present evidence that this is due to loss of coordination between sister-centromeres during oscillatory movement. This argues against a Pac-man model for MCAK function prior to anaphase (although Pac-man may still operate during anaphase). Instead our data suggests that MCAK facilitates directional switching during oscillatory chromosome movement.
****

On Jul 12, 2004, at 4:10 AM, Maurizio Gatti wrote:

> Dear colleague,
>
> We need to finalize the Cortona meeting and would really appreciate if you could send me your abstract. Please, send me your abstract no later than July 16.
>
> Thank you very much